# Le larynx artificiel : de l'in vitro à la première implantation clinique

Agnès Dupret Dupret Bories

# UNIVERSITÉ DE STRASBOURG

*École Doctorale des SCIENCES de la Vie et de la Santé*

**INSERM UMR 1121, Biomaterials and Bioengineering**

# THÈSE

présentée par :

**Agnès Dupret-Bories**

soutenue le 30.09.2013

pour obtenir le grade de : **Docteur de l'université de Strasbourg**

Spécialité : Sciences médicales

## Le larynx artificiel : de l'*in vitro* à la première implantation clinique

**THÈSE dirigée par :**

| | |
|---|---|
| **M. LAVALLE Philippe** | Docteur, Inserm 1121, Strasbourg |
| **M. DEBRY Christian** | Professeur des Universités, Strasbourg |

**RAPPORTEURS :**

| | |
|---|---|
| **M. CHEVALIER Dominique** | Professeur des Universités, Lille |
| **M. MAKEIEFF Marc** | Professeur des Universités, Reims |

**AUTRES MEMBRES DU JURY :**

| | |
|---|---|
| **M. MASSARD Gilbert** | Professeur des Universités, Strasbourg |
| **M. VERGEZ Sébastien** | Professeur des Universités, Toulouse |

A ma fille Mona, qui est devenue ma principale raison d'exister

A Pierre, mon amour, mari et papa idéal

# Remerciements

Je tiens à exprimer ma profonde gratitude à mes 2 directeurs de thèse.

Au Docteur Philippe Lavalle,

Pour ton encadrement depuis le master 2, durant ces 4 années de travail. Tu as toujours été disponible pour répondre à la moindre question et pour les relectures rapides. Je te remercie pour tes multiples conseils, pour tes qualités humaines d'écoute et de compréhension. Sois assuré de ma profonde reconnaissance.

Au Professeur Christian Debry,

Tu m'as permis de bénéficier de ton enseignement et de ton soutien depuis 8 années, depuis le début de mon internat. Tu as été à l'initiative du projet ambitieux du larynx artificiel et créé ce partenariat fort entre notre service hospitalier et l'équipe Inserm 1121. Tu m'as permis de mener à bien ce travail de thèse en m'intégrant dans cette équipe dynamique et en m'encadrant dans l'ensemble de nos recherches. Sans toi, rien n'aurait été possible. Ces quelques lignes me permettent de t'exprimer ma profonde reconnaissance.

Au Professeur Dominique Chevalier,

Vous me faîtes l'honneur d'avoir accepté de juger ce travail. Je vous remercie pour vos conseils, que j'espère avoir suivi, lors de la présentation de nos travaux à mi-parcours. Veuillez croire en ma profonde estime.

Au Professeur Marc Makeieff,

Vous me faites l'honneur de juger de ce travail. Vous avez réalisé de nombreux travaux sur la pathologie laryngée. J'espère que ce travail de thèse aura su susciter votre intérêt. Veuillez croire à mon profond respect.

Au Professeur Gilbert Massard,

Après la thèse du Pr Philippe Schultz, vous me faîtes l'honneur d'avoir accepté de juger de l'avancée de nos travaux sur le thème du larynx artificiel. Vos connaissances sur les reconstructions de trachée font de vous un juge essentiel. Veuillez trouver ici le témoignage de mon profond respect.

Au Professeur Sébastien Vergez,

Tu as accepté de me faire l'honneur de juger ce travail de thèse. Je tiens à te remercier pour ton enseignement lors de mon semestre toulousain. Tu as plus que contribué à rendre mon séjour dans votre équipe inoubliable. J'espère que nous allons poursuivre notre association « de malfaiteurs », jusqu'ici fructueuse. « Brindille » à la fin de la soutenance…

Au Docteur Nihal Engin Vrana,

Sans toi et ton dynamisme, ton acharnement au travail, ton intelligence, ce travail aurait été bien différent. Je tiens à te remercier pour ces 4 années de collaboration. Tu as mené à bien tous les projets. Nous nous sommes compris dans notre volonté de respecter en permanence les règles d'éthique en matière d'expérimentation animale. Nous allons encore poursuivre cette collaboration pour l'amélioration du larynx artificiel tout en développant d'autres projets complémentaires. Je te souhaite tout le bonheur possible à toi et Alix avec la venue de votre petite fille.

Au docteur Dominique Vautier,

Tu as été l'aide opératoire rêvé lors de nos reconstructions de trachée sur le modèle lapin. Je te remercie pour ton accueil au sein du laboratoire, ton aide de tous les jours, ton humour.

Au Professeur Philippe Schultz,

Je te remercie pour tes conseils et ton aide précieuse dans ce travail et tout au long de ma formation hospitalière. Tu m'as permis de prendre la suite de tes recherches, tu m'as accompagné. Tu m'as montré mes premières manipulations des rats, même si depuis, j'ai quelque peu modifié les protocoles. Sois assuré de ma profonde estime et de mon amitié.

Au Docteur Jean-Claude Voegel, directeur de l'unité Inserm 977, et au Docteur Pierre Schaaf, directeur de l'unité Inserm 1121,

Pour m'avoir accueillie au sein du laboratoire et pour votre soutien.

Au Docteur Patrick Hémar,

Pour avoir participé à nos discussions sur le concept de la prothèse de larynx, pour nous avoir aidé par tes conseils éclairés. Ces lignes me permettent de te remercier une nouvelle fois pour la formation que tu m'as apportée durant toutes ces dernières années et pour ton amitié.

Au Professeur André Gentine,

Je vous remercie pour ces années passées à vos côtés, votre enseignement, votre gentillesse. Soyez assuré de mon profond respect pour toute votre carrière.

Au Professeur Anne Charpiot,

Pour ton encadrement et ton amitié.

A l’équipe PROTiP ; Audrey Maniette, Nicolas Perrin, Maurice Béranger, Jean-Marc Fressard, et André Walder.

A l’ensemble de l’équipe Inserm 1121 dont Christiane, Morgan, Damien et Bernard

Au service d’ORL de Strasbourg avec un remerciement spécial à mes supers co-chefs Lila et Nicolas

A mes parents

A mes frères

A ma belle-famille

# Table des matières

# Liste des figures

# Liste des tableaux

# Partie 1

# Introduction

# Partie 1 : Introduction

# 1.1. La pathologie laryngo-trachéale

La laryngectomie totale réalise l'exérèse complète du larynx, du cricoïde, à l'os hyoïde (figure 1). Une fois le pharynx refermé par plusieurs plans muqueux et musculaires, le conduit digestif devient totalement séparé du conduit aérien. L'extrémité proximale de la trachée est amarrée à la peau via un trachéostome définitif. La laryngectomie totale (figure 2) est indiquée lorsque l'extension locale de la tumeur primitive contre-indique la réalisation d'une laryngectomie partielle fonctionnelle et lorsqu'un protocole de conservation d'organe (chimio-radiothérapie) est impossible ou en situation d'échec. La première laryngectomie totale a été réalisée en 1873 par Christian Billroth. Le patient est décédé dans le mois suivant l'intervention. Plus de 100 ans après, la survie à cinq ans des sujets laryngectomisés, tous stades confondus, dépasse 43% (Akduman et al., 2010). Si cette intervention chirurgicale accorde une espérance de vie satisfaisante, elle entraine des difficultés majeures dans la vie quotidienne des patients.

Figure 1 : le larynx, schéma d'une coupe sagittale (issu de "Anatomy of larynx" University of Pittsburgh Medical Center)

Figure 2 : schéma avant (à gauche) et après (à droite) laryngectomie totale (InHealth Technologies, Carpinteria, CA)

Les conséquences d'une laryngectomie totale sont :

· séparation du système respiratoire et digestif,

· trachéostomie définitive,

· perte de la phonation laryngée,

· perte de la respiration bucconasale,

· perte totale de l'odorat,

· perte de l'étanchéité cutanée au niveau du trachéostome (au contact de l'eau).

· perturbation de l'image corporelle,

· perte des efforts à glotte fermée (ayant des conséquences sur la défécation, l'acte sexuel chez l'homme).

Chaque année en France 1800 laryngectomies totales sont pratiquées (Haute Autorité de Santé, 2007). Actuellement, seule la réhabilitation vocale est possible et ce par des mesures palliatives, à savoir la voix oesophagienne, la fistule trachéo-oesophagienne avec prothèse phonatoire, les fistules chirurgicales et l'électrolarynx. Le handicap, créé par la perte du larynx, aboutit à des difficultés importantes de réinsertion sociale et constitue un problème de santé publique (Babin et al., 2008). Le patient laryngectomisé présente une modification de l'image de soi conduisant à une altération de sa relation aux autres et un isolement social. De plus, la présence d'une trachéotomie définitive aurait un impact plus négatif sur la qualité de vie que ne l'est la perte de la voix (Boscolo-Rizzo et al., 2008).

# 1.2. Etat de l'art dans la reconstruction du larynx

La très grande majorité des travaux de recherche dans le monde s'est axée sur la réhabilitation vocale (Hobson and Carney, 2011 ; Singer et al., 2012), mais peu d'études s'intéressent à la suppression de l'orifice de trachéostomie, imposant de rétablir un passage commun entre les voies respiratoires et digestives.

Il reste un important champ de recherche pour la réhabilitation du patient laryngectomisé.

Le larynx, carrefour entre les voies aériennes et digestives, est un organe complexe nécessitant pour sa reconstruction soit une greffe complète de larynx, soit la création d'un larynx artificiel comprenant 2 structures associées : 1) une structure rétablissant la fonction de sphincter laryngé ; 2) une structure prolongeant la trachée restante après laryngectomie totale.

La reconstruction de trachée est un préambule à la reconstruction d'un larynx artificiel et fait l'objet de nombreux travaux de recherche.

## 1.2.1. Voies de recherches actuelles dans la reconstruction trachéale

La recherche d'un substitut trachéal idéal fait l'objet de nombreuses études, et ce depuis plus de 50 ans. Avec un objectif différent de celui du larynx artificiel, mais avec une problématique identique, d'autres équipes travaillent sur le remplacement trachéal. Pour les cas de lésions trachéales tumorales ou traumatiques étendues à plus de la moitié de la trachée chez l'adulte ou du tiers chez l'enfant, l'anastomose directe est impossible à effectuer, même sous couvert d'une mobilisation trachéale maximale. Les résections trachéales étendues demeurent un problème chirurgical non résolu en termes de reconstruction. De nombreux matériaux de remplacement ont été testés (Grillo, 2002, 2003a, b) sur les modèles animaux. Ces matériaux incluent les prothèses synthétiques (Dodge-Khatami et al., 2003), les homo et allogreffes trachéales (Neville et al., 1976; Tojo et al., 1998), les autos et allo-transplantations tissulaires (Davidson et al., 2009; Kim et al., 2012; Martinod, 2012; Martinod et al., 2001b; Seguin et al., 2009b; Wurtz, 2010), et l'ingénierie tissulaire (Delaere and Hermans, 2009; Macchiarini et al., 2008; Yang et al., 2012; Zhang et al., 2009). L'équipe du Professeur

Martinod (Martinod, 2012; Martinod et al., 2001a; Martinod et al., 2005; Seguin et al., 2009a) a utilisé une allogreffe aortique, associée à une prothèse en silicone, comme substitut trachéal. Les résultats d'abord obtenus chez la brebis ont été spectaculaires avec l'ablation du tube de silicone au bout de 6 mois et la transformation de l'aorte en une véritable trachée comportant des cartilages organisés en anneaux et recouverts d'un épithélium mucociliaire. Les résultats préliminaires rapportés chez l'homme sont contradictoires. Sur 6 patients opérés, avec un suivi moyen de 34 mois, 4 sont en vie et aucun n'a pu bénéficier de l'ablation du tube de silicone (Wurtz et al., 2010). Par ailleurs les phénomènes de régénération du tissu aortique en structure cartilagineuse semblent retardés chez l'homme, puisqu'ils ne sont que partiels à 34 mois.

Malgré l'indéniable portée de ces résultats, l'utilisation de ce greffon aortique semble difficile à proposer dans le cadre d'une reconstruction laryngo-trachéale. En raison de sa flaccidité initiale et l'impossibilité chez l'homme de retirer la prothèse en silicone, il ne peut supporter l'association d'une valve supérieure qui remplacerait la fonction du sphincter laryngé.

### 1.2.2. Voies de recherche actuelles dans la greffe de larynx

Deux allogreffes de larynx ont précédemment été décrites (Birchall et al., 2006; Strome et al., 2001; UC Newsroom, 2011). La première greffe de larynx a été réalisée en 1998 par l'équipe du Dr Marshall Strome (Strome et al., 2001). En 2001 les auteurs ont publiés la procédure chirurgicale et les résultats cliniques avec un suivi de 40 mois. Le patient, âgé de 40 ans, présentait un larynx non fonctionnel avec nécessité de trachéotomie suite à un accident à l'âge de 20 ans. 4 ans après l'implantation, le larynx était objectivement réinnervé (validée par électromygraphie laryngée), mais la trachéotomie n'a pas pu être fermée (Lorenz et al., 2004). De plus, les procédures nécessitaient le recours à un traitement immunosuppresseur. Les indications retenues de cette intervention étaient les laryngectomies pour traumatisme ou tumeurs bénignes et les laryngectomies pour cancer 5 ans après une survie sans récidive. La laryngectomie totale est pratiquée dans la majorité des cas pour le traitement des carcinomes épidermoïdes pharyngo-laryngés. Il est admis qu'un patient sous traitement immunosuppresseur pour une allogreffe a trois à quatre fois plus de risque de

développer une tumeur maligne que la population générale (Leon et al., 2008). Il existe de plus une évidence indirecte d'effet synergique entre un traitement immunosuppresseur au long cours et des antécédents de consommation d'alcool et de tabac dans le développement de cancers de la tête et du cou (Saigal et al., 2002). De plus, après de tels cancers, l'incidence du risque de développer un second cancer est élevé, estimé entre 9,1% (Jones et al., 1995) et 23% (Cooper et al., 1989). Dans ces conditions il semble difficile de proposer un traitement immunosupresseur, même à 5 ans d'une chirurgie, à un patient présentant un antécédent de carcinome épidermoïde de la tête et du cou (Hall and Narula, 2012).

Grâce aux techniques de bioingénierie tissulaire, un transplant de larynx obtenu a partir d'un larynx humain décellularisé a fait l'objet d'une publication récente (Baiguera et al., 2011). L'innovation technique est l'absence de recours à un traitement immunosupresseur lors de l'implantation. Cependant il reste à déterminer les modalités de réinnervation d'un tel transplant afin de le rendre fonctionnel.

# 1.3. Développement du larynx artificiel

Notre équipe s'intéresse depuis une décennie à la conception d'une prothèse laryngée implantable remplaçant les fonctions du larynx (Debry et al., 2003; Dupret-Bories et al., 2011; Schultz et al. 2004, 2007, 2010; Vrana et al. 2011). Elle associe une structure rigide inamovible et une structure amovible biofonctionnelle. Deux types d'études ont été menées en parallèle : 1) la recherche d'un substitut trachéal idéal, composée d'une structure inamovible, qui vise à prolonger la trachée proximale restant après laryngectomie totale; 2) le développement d'une valve supérieure, composée d'une structure amovible, synchronisant les fonctions respiratoire et digestives.

La structure rigide inamovible, visant à remplacer un segment trachéal, doit représenter un support suffisamment rigide pour y insérer en proximal la valve, néo-fonction sphinctérienne s'ouvrant à la respiration, se fermant lors du passage du bol alimentaire et incluant au mieux une capacité phonatoire (figure 3). Le larynx possédant des tissus comparables à la trachée à l'exception des cordes vocales (enveloppe externe constituée de périchondre et de tissu conjonctif, cartilage en dedans recouvert d'un épithélium squameux cilié pseudostratifié), les reconstructions trachéales constituent un préambule aux reconstructions laryngées.

La restauration de la fonction laryngée devrait se faire en plusieurs étapes. La première étape consisterait à prolonger le segment trachéal proximal restant après laryngectomie totale, par un biomatériau totalement intégré. La deuxième étape comprendrait l'ajout d'une valve supérieure remplissant la fonction de sphincter.

Figure 3 : Schéma de la prothèse trachéale inamovible avec valve supérieure : larynx artificiel (schéma de la trachée issue de The McGrow-Hill compagnies, Inc)

## 1.3.1. Développement d'une prothèse trachéale en titane poreux

Les travaux antérieurs de notre équipe (Schultz et al., 2004, 2007) ont permis la mise au point d'un biomatériau constitué d'un assemblage de microbilles de titane. Notre choix s'est porté sur le titane puisqu'il est couramment employé pour des applications en chirurgie orthopédique et maxillofaciale en raison de ses propriétés biomécaniques et de sa stabilité électrochimique. Le titane est par ailleurs un métal inerte et non toxique. Il est considéré comme étant peu sensible aux bactéries et aux moisissures. Sa rigidité lui permettrait de jouer un rôle de soutien en remplacement de plusieurs anneaux trachéaux. Notre équipe a conçu il y a quelques années un biomatériau poreux constitué d'un assemblage de microbilles de titane. Les porosités entre les microbilles sont destinées à favoriser l'intégration du biomatériau par une colonisation cellulaire provenant des tissus environnants. Un tube creux destiné à prolonger ou remplacer une portion de trachée a donc été réalisé. Après sa mise en place par résections sutures trachée-prothèse, les tissus entourant la prothèse doivent combler les porosités et fournir un réseau vasculaire destiné à nourrir et à oxygéner un épithélium de repousse endoluminal provenant des extrémités trachéales.

## 1.3.2. Etudes antérieures sur le remplacement trachéal par prothèse en titane poreux

L'implantation de prothèses trachéales en titane poreux chez le rat a montré une intégration rapide de la prothèse par un tissu de colonisation vascularisé puis épithélialisé en endoluminal avec des survies supérieures à 1 an (Schultz et al., 2002; 2004) (figure 4). Ces données ont encouragé notre équipe à poursuivre l'expérimentation chez la brebis dont le diamètre trachéal est très proche de celui de l'homme (ten Hallers et al., 2004). Une étude à court terme (6 mois) portant sur 6 animaux a été menée avec une bonne intégration du matériel, mais un faible taux de survie (Schultz et al., 2007). L'implantation des prothèses en un temps et sans tube de silicone endoluminal (même protocole opératoire que celui précédemment mené chez le rat) conduit à une sténose des anastomoses trachée-prothèse

(Figure 5) avec une épithélialisation endoprothétique faible. Les décès précoces observés chez la brebis et chez le rat étaient majoritairement provoqués par une obstruction de la lumière endoprothétique suite à une prolifération de tissu fibroblastique et inflammatoire aux zones de jonction prothèse-extrémités trachéales.

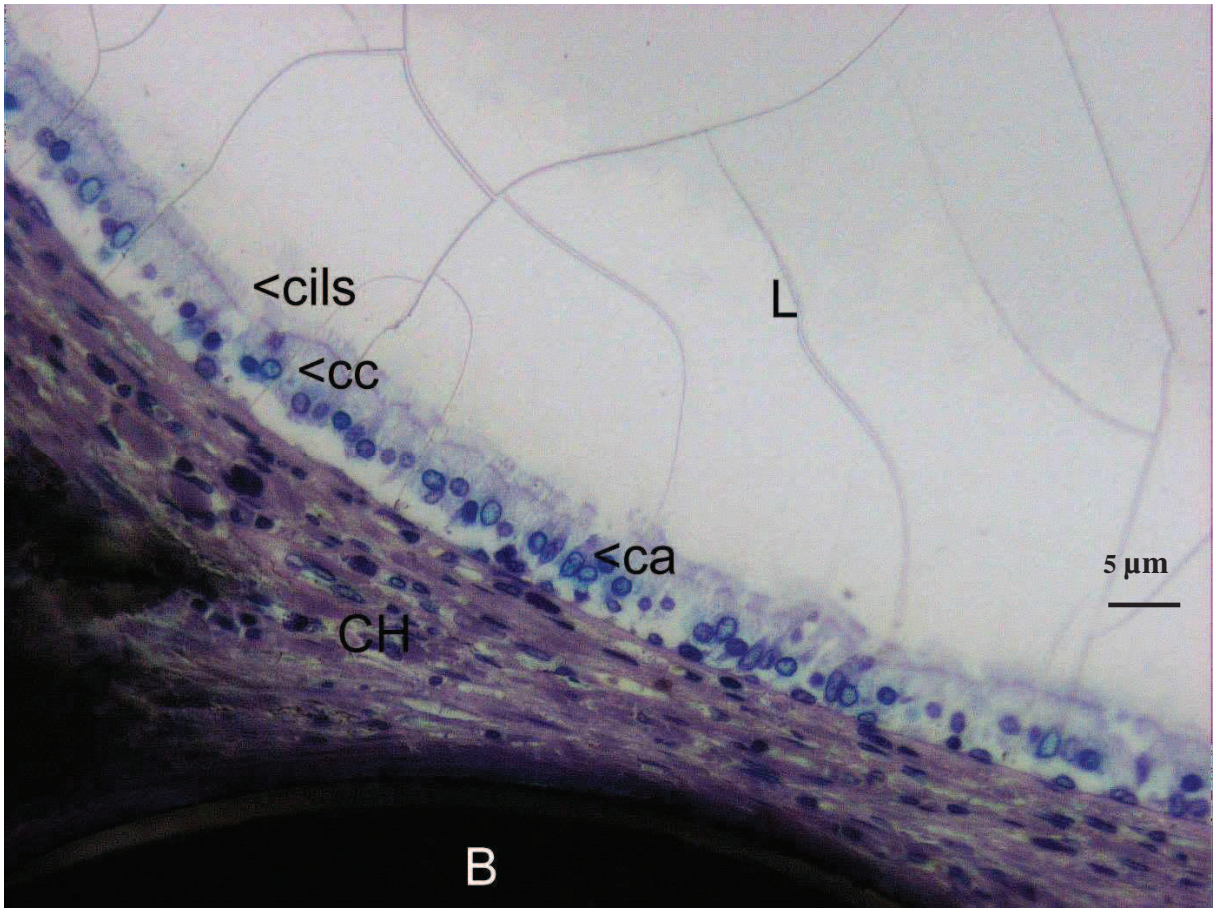


Figure 4 : analyse histologique de la face endoluminale d'une prothèse trachéale en titane poreux observée en microscopie optique après coloration.
B : bille de titane, cc : cellules ciliées, ca : cellule calciforme, L : lumière endoprothétique

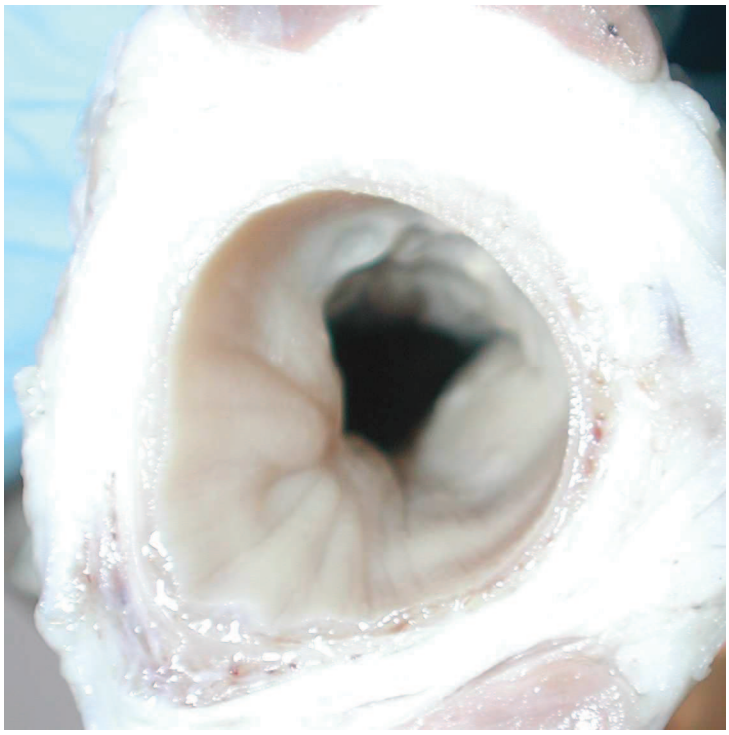

Figure 5 : analyse macroscopique d'un bloc cervical (brebis, étude précédente)

Visualisation d'une sténose au niveau de la jonction extrémité trachéale-prothèse en titane poreux. Les sténoses des zones de jonction représentent la principale cause de décès au cours de l'étude précédente réalisée chez la brebis (mode d'implantation en 1 temps de la prothèse trachéale en titane poreux sans tube de silicone endoprothétique)

## 1.3.3. Du remplacement d'un segment trachéal par prothèse en titane poreux au larynx artificiel

Le travail présenté dans ce mémoire s'articule autour de six publications.
Ayant pour objectif de réduire les sténoses endoluminales des prothèses de trachée en titane poreux et ainsi d'améliorer la survie des animaux, nous avons testés, sur la brebis 5 techniques chirurgicales différentes d'implantation dans une même unité de temps. Les résultats de ces implantation sont analysés dans le premier article (Dupret-Bories et al., 2011).
Pour améliorer la colonisation des prothèses en titane poreux, un polymère biodégradable à base de PLLA (poly(acide l,-lactique)), comblant les pores des prothèses en titane, a été utilisé. Le deuxième article (Vrana et al., 2013) est à considérer comme le chapitre

« Matériels et méthodes » des 2 deux articles suivants. Nous décrivons des procédures des expérimentations *in vivo* et *in vitro* menées sur les prothèses en titane poreux associant le polymère PLLA. Le troisième article (Vrana et al., 2011) décrit essentiellement la technique de préparation et de mise en place du polymère et les résultats *in vitro* de son comportement sur la prolifération cellulaire.
Le quatrième article (Vrana et al., 2012) détaille les résultats des tests *in vivo* d'implantation de ce système hybride en remplacement trachéal chez le lapin.

En parallèle, nous nous sommes intéressés à l'intégration des prothèses en titane poreux en fonction de la taille des billes. Des tests *in vitro* et *in vivo* (modèle lapin) ont été menés avec 3 types de tailles de billes : 150 µm, 300 µm et 500 µm. Les résultats sont détaillés dans le cinquième article (Vrana et al., 2013).

Suite à l'ensemble de ces résultats, nous avons réalisé la première application clinique mondiale du larynx artificiel ("Implantation of an artificial larynx after total laryngectomy", Protocol NCT01474005, http://clinicaltrials.gov/). Un premier patient, ayant subi l'ablation du larynx pour raison carcinologique, a été implanté avec une prothèse de larynx artificiel fonctionnelle en 2 étapes chirurgicales au CHU de Strasbourg. La procédure chirurgicale et les résultats de cette première implantation clinique sont détaillés dans le sixième article (Debry et al., 2013, Head and Neck, soumission).

# Partie 2 : Matériels et Méthodes

# Partie 2 : Matériels et Méthodes

# 2.1 Les prothèses de trachée

## 2.1.1 Les prothèses de trachée en titane poreux

Les prothèses destinées à être implantées en remplacement trachéal (figure 6) sont manufacturées par la société PROTiP (http://www.protipmedical.fr). Les prothèses utilisées sur les modèles animaux sont formées d'un assemblage de billes de titane de 400-500 µm de diamètre (Schultz et al., 2002). Le titane est produit selon les standards AFNOR (Association Française de NORmalisation) à partir du Ti40 utilisé par ailleurs pour certaines applications comme matériel chirurgical. Les billes sont placées dans un moule de forme finale désirée puis soudées entre elles sous l'action d'un courant de décharge. La porosité entre chaque bille est de l'ordre de 150 µm, soit une porosité d'environ 35%. Les prothèses sont constituées de couches de billes fusionnées sous la forme d'un tube. Les dimensions de chaque prothèse sont variables en fonction du modèle animal utilisé (tableau 1). 3 à 6 trous sont situés à chaque extrémité de la prothèse, pour permettre les sutures prothèse-extrémités trachéales.

Figure 6 : prothèse de trachée utilisée chez le lapin

| Animaux | Hauteur de la prothèse | Diamètre interne | Diamètre externe | Nombre de couches de billes |
|---|---|---|---|---|
| Brebis | 30 mm | 19,7 mm | 23 mm | 4 |
| Lapins | 20 mm | 7 mm | 10 mm | 3 |

Tableau 1: Dimensions des prothèses de trachée en titane poreux en fonction du modèle animal

## 2.1.2 Les tubes en silicone

Des tubes de silicone (stents) sont utilisés en calibrage endoluminal des prothèses en titane poreux implantées en remplacement d'un segment trachéal. Leur dureté est de 50 shore. Leur dimension est variable en fonction du modèle animal utilisé (tableau 2). Ils dépassent de 10 mm (modèle lapin) à 25 mm (modèle brebis) à chaque extrémité des prothèses, permettant une protection des anastomoses extrémités trachéales-prothèse.

Les prothèses et tubes de silicone sont stérilisés par autoclavage avant implantation.

| Animaux | Hauteur | Diamètre interne |
|---|---|---|
| Brebis | 80 mm | 19 mm |
| Lapins | 40 mm | 5 mm |

Tableau 2: Dimension du tube de silicone en fonction du modèle animal

# 2.2. Le larynx artificiel

Le larynx artificiel (Figure 7) est constitué d'une partie inamovible et d'une partie amovible.

Les essais cliniques du larynx artificiel ont été conduits en collaboration avec les Hopitaux Universitaires de Strasbourg.

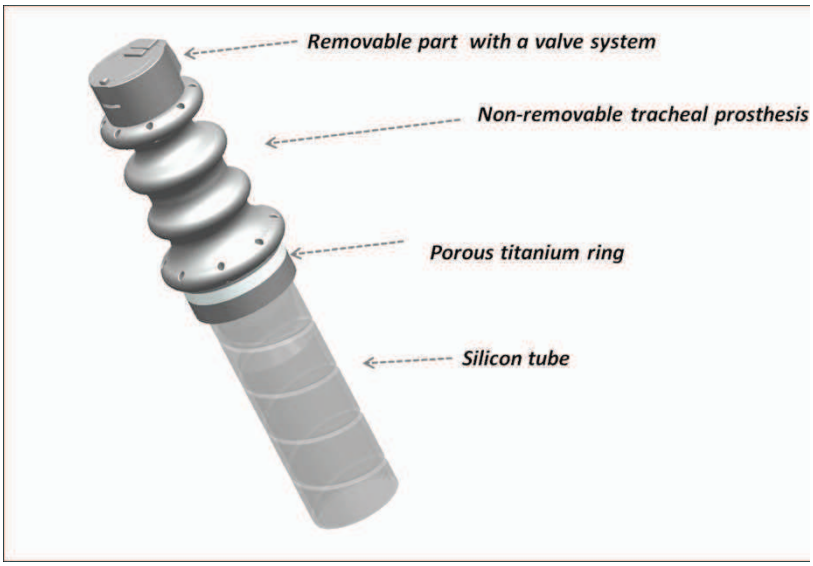


Figure 7 : Schéma du larynx artificiel.

## 2.2.1. Partie inamovible du larynx artificiel

La partie inamovible du larynx artificiel est composée de titane pur et de titane poreux. Le titane poreux est assemblé sous la forme d'une bague inférieure faisant la jonction avec la partie supérieure de la trachée.

Aux extrémités supérieure et inférieure du larynx artificiel se situent des trous permettant de rattacher par suture la prothèse à la base de langue (extrémité supérieure) et à la trachée (extrémité inférieure).

## 2.2.2. Partie amovible du larynx artificiel

La partie amovible du larynx artificiel est un conduit qui possède 2 extrémités fonctionnelles. A son extrémité inférieure, on trouve une liaison mécanique permettant son maintien sur la bague trachéale, en empêchant notamment tout mouvement de rotation. Son extrémité supérieure possède un système de double valves qui s'ouvrent et se ferment avec le passage d'air. La dépression créée par les poumons lors de la phase inspiratoire ouvre une valve dite inspiratoire (vers le bas). La surpression créée par les poumons lors de la phase expiratoire ou d'expectoration ouvre une valve dite expiratoire (vers le haut). La valve inspiratoire possède une légère résistance à l'ouverture afin d'éviter que, sous son propre poids, le bol alimentaire n'abaisse la valve et ne passe dans la trachée puis les poumons.

## 2.2.3. Le tube de silicone

Un tube de silicone est placé dans la lumière de la partie inamovible de manière transitoire afin de calibrer les zones de jonction prothèse/extrémité trachéale. Le tube est en silicone de grade médical (70 shores, diamètre 20 mm).

# 2.3. Les plaques en titane poreux

Des plaques en titane poreux de forme carrée de 10 mm de côté et 1,5 mm d'épaisseur ont été utilisées pour les expérimentations décrites dans le cinquième article.
Les plaques ont été séparées en 3 groupes en fonction du diamètre des billes utilisées à savoir 150-250 µm, 300-400 µm et 400-500 µm (Figure 8).

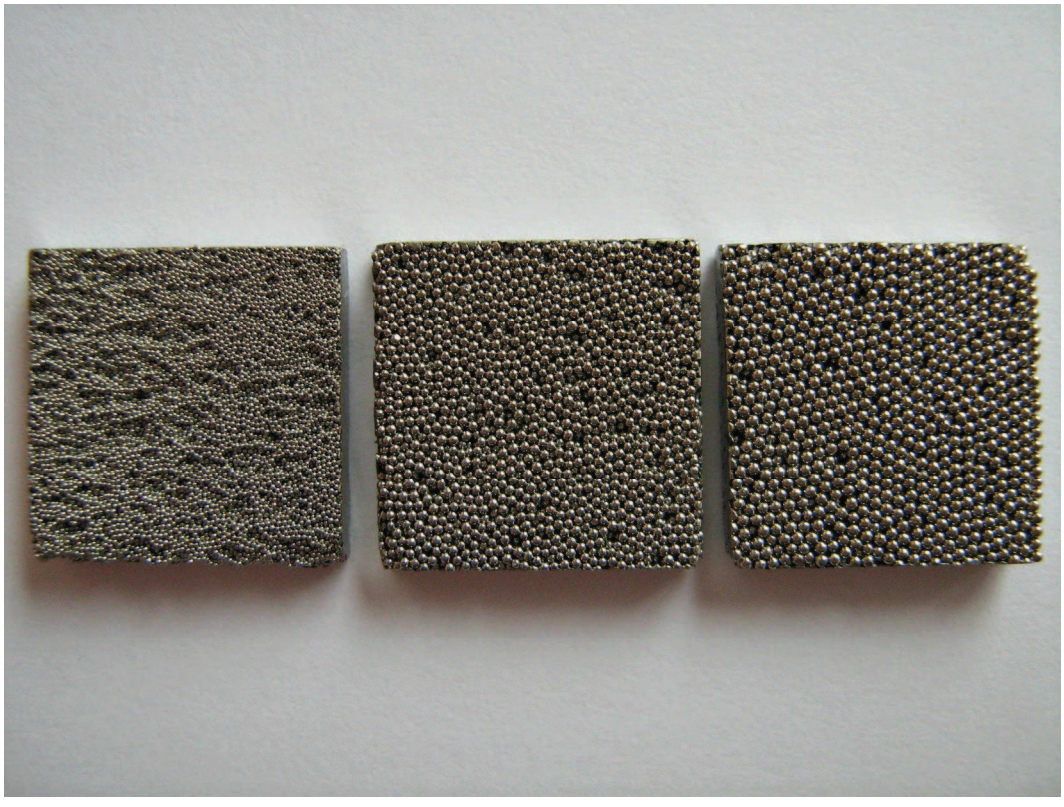

Figure 8 : Plaques en titane poreux avec 3 tailles de bille (150-250 µm à gauche, 300-400 µm au centre et 400-500 µm à droite).

# 2.4. Les modèles animaux, les procédures d'anesthésie et d'euthanasie

## 2.4.1. Le modèle brebis

Des brebis (n=11), âgées de 4 à 11 mois et pesant en moyenne 60 kg ont été utilisées pour l'étude décrite dans le premier article. Chaque animal était logé et nourri en accord avec les recommandations du Guide pour le bien-être des animaux de laboratoires (Guide for the care and use of laboratory animals, 2010). Les interventions d'implantation et d'explantation ont été réalisées à l'IMM recherche (Institut Mutualiste Monsouris, Paris, France).

Chaque procédure chirurgicale a été réalisée sous anesthésie générale. Après une prémédication par kétamine (6mg/kg) en intramusculaire, l'induction anesthésique était obtenue par une injection intraveineuse de sodium thiopenthal (10mg/kg). L'anesthésie était maintenue par ventilation après intubation endotrachéale avec de l'halothane inhalée (1-2% d'isoflurane et 100% d'oxygène). Une antibioprophylaxie par injection intraveineuse de Cefamandol (15mg/kg) couvrait l'ensemble de la chirurgie. L'analgésie post opératoire était entretenue par une injection de morphine sodique en intramusculaire (0,2 mg/kg) durant 5 jours.

Les animaux ont eu accès à l'eau et à la nourriture *ad libitum*. Leur état de santé a été contrôlé plusieurs fois par jour avec une pesée des animaux hebdomadaire.

A la fin des protocoles d'expérimentation ou lors de l'apparition de signes de souffrance de l'animal non résolus par traitement médical et avant d'atteindre le point limite, les brebis ont été euthanasiées. Le protocole d'euthanasie comprenait une induction d'anesthésie par propofol en intraveineux (2mg/kg, Diprivan® 500 mg/50 ml, AstraZeneca) suivie d'une injection intraveineuse de chlorure de potassium (120 à 250 ml, B.BRAUN 10% (0,1 g/ml)).

## 2.4.2. Le modèle lapin

Des lapins femelles néo-zélandais blancs (mieux connu des chercheurs sous le nom de New Zealand White) (n=15), âgées de plus de 4 mois et pesant en moyenne 2.5 à 3 kg ont été utilisés pour les expérimentations décrites dans le troisième, quatrième et cinquième article.
Chaque animal a été nourri en accord avec les recommandations du Guide pour le bien-être des animaux de laboratoires (Guide for the care and use of laboratory animals, 2011). Les interventions d'implantations et d'explantations ont été réalisées au laboratoire de Virologie de la Faculté de Médecine de Strasbourg.

Les procédures chirurgicales ont été réalisées sous anesthésie générale. L'induction anesthésique a été obtenue par un mélange de kétamine (30mg/kg, KETAMINE 500®, VIRBAC, France), de Xylazine (3mg/kg, Rompun® 2%, Bayer SA-NV, Belgium) et de midazolam (0.2mg/kg, Hypnovel®, 5mg/5ml, Roche Pharma, Austria) en intramusculaire en paravertébrale. ½ dose de ce mélange a été réinjectée au cours de l'intervention. Une oxygénothérapie à 2L/min était maintenue tout au long de l'intervention chirurgicale. L'analgésie post opératoire a été entretenue par l'application d'un patch de fentanyl (1/4 de patch de 12 µg de Fentanyl-Mepha®;Mepha Pharma, Austria) renouvelé à 72h.
Les animaux ont eu accès à l'eau et à la nourriture *ad libitum*. Leur état de santé a été contrôlé plusieurs fois par jour avec une pesée des animaux hebdomadaire.

A la fin des protocoles d'expérimentation ou lors de l'apparition de signes de souffrance de l'animal non résolus par traitement médical et avant d'atteindre le point limite, les lapins ont été euthanasiés. Une induction anesthésique était obtenue par un mélange de kétamine (30mg/kg, KETAMINE 500®, VIRBAC, France), de xylazine (3mg/kg, Rompun® 2%, Bayer SA-NV, Belgium) et de midazolam (0.2mg/kg, Hypnovel®, 5mg/5ml, Roche Pharma, Austria) en intramusculaire. L'euthanasie de l'animal était ensuite réalisée par une injection en intra veineux (veine marginale de l'oreille) de pentobarbital (120 mg/kg, Pentothal ®, Ceva Santé Animale, France).

## 2.4.3. Le modèle rat

Des rats mâles de la race Wistar (n=6), âgés de plus de 2 mois et pesant en moyenne 300 grammes, ont été utilisés pour les expérimentations décrites dans le quatrième article.
Chaque animal a été nourri en accord avec les recommandations du Guide pour le bien-être des animaux de laboratoires (Guide for the care and use of laboratory animals, 2011). Les interventions d'implantations et d'explantations ont été réalisées à l'animalerie de la Faculté de Médecine de Strasbourg.
Les procédures chirurgicales ont été réalisées sous anesthésie générale par injection en intra péritonéale d'un mélange de kétamine (20 mg/kg, Ketamine 500®; Virbac France) et de midazolam (10 mg/kg, Mydazolam®; Mylan, France).

Les animaux ont eu accès à l'eau et à la nourriture *ad libitum*. Leur état de santé a été contrôlé plusieurs fois par jour avec une pesée hebdomadaire des animaux.

A la fin des protocoles d'expérimentation les rats ont été euthanasiés par une injection intrapéritonéale de pentobarbital (100mg/kg, Pentothal ®, Ceva Santé Animale, France)

# 2.5. Analyses histologiques

Les explants ont été obtenus selon une résection en bloc, emportant les tissus environnants et la prothèse en titane (ou plaque en titane poreux) et ont été fixés dans du formol à 10%.
Les analyses histologiques ont été réalisées à l'Institut Biomatech (Chasse sur Rhône, France). et à l'IMM-Recherche (Paris, France).
Les préparations des explants et les modalités d'analyse histologique ont pu varier en fonction du centre sélectionné pour la réalisation technique.

## 2.5.1. Analyses histologiques à l'Institut Biomatech

Les explants préalablement fixés au formol 10 % tamponné ont été déshydratés dans des bains d'alcool de concentration croissante, clarifiés au xylène et inclus en PMMA (polyméthyleméthacrylate). Pour chaque explant, une section longitudinale centrale a été réalisée selon une technique de coupe à la scie diamantée et de microponçage adaptée de Donath (Donath and Breuner, 1982). Les sections histologiques obtenues ont été colorées au Paragon modifiée. Une évaluation qualitative et semi-quantitative a été réalisée selon la norme ISO 10993 : « Evaluation des dispositifs médicaux ». L'intégration tissulaire, la tolérance locale des implants (cellules inflammatoires, néovaisseaux, nécrose, débris particulaires) ont été analysées. Les lames ont été observées à l'aide d'un microscope optique NIKON Eclipse E600 muni des objectifs x4,x10, x20, x40 et des microphotographies ont été réalisées.

## 2.5.2. Analyses histologiques à l'IMM-Recherche

Les pièces, préalablement fixées dans 10% de formaldéhyde pour être préservées, ont été déshydratées dans des bains contenant des concentrations croissantes d'alcool puis

incluses dans de la paraffine. Des coupes de 5µm d'épaisseur (une horizontale sous l'anneau plein de titane et deux verticales au dessus et au dessous de l'anneau) ont été réalisées à l'aide d'un microtome HM 350 et colorées par hématoxyline-éosine-safran visibles par microscopie optique (Nikon Eclipse E 600). L'intégration tissulaire des explants, les réactions inflammatoires locales, la colonisation par l'épithélium ont été analysées.

# 2.6. Produits et réactifs utilisés pour l'expérimentation *in vitro* et *in vivo*

| **Nom du produit/Réactif** | **Fournisseur** | **Numéro de catalogue** | **Commentaires** |
|---|---|---|---|
| Dioxane | Sigma-Aldrich | 360481 | Produit toxique<br>Utilisation stricte sous hotte |
| PLLA<br>1)Poly(L-lactide) inherent viscosity ~0.5 dl/g<br>2)Poly(L-lactide) inherent viscosity ~2.0 dl/g | Sigma-Aldrich | 94829, 81273 | Le choix du poids moléculaire et donc de la viscosité varie en fonction de l'utilisation |
| PRONOVA UP LVG (Sodium Alginate) | Novamatrix | 4200006 | Viscosité basse (20-200 mPa.s) |
| Collagen type I (Bovine) | Symatese | CBPE2US100 | |
| Pen/Strep, Fungizone | Promocell | C42020 | |
| Genipin | Wako | 703021 | |
| Silicon nitride probes with aspring constant of 0.03 $N.m^{-1}$. | Bruker | MSCT | |
| Trifluoroacetic acid for | Sigma- | 302031 | Matière dangereuse |

| | | | |
|---|---|---|---|
| HPLC ,≥99.0% | Aldrich | | |
| Acetonitrile, for HPLC ,≥99.9% | Sigma-Aldrich | 34998 | |
| Calcein-AM | Invitrogen | C3100MP | |
| PKH26 Red Fluorescent Cell Linker Kit for General Cell Membrane Labeling | Sigma-Aldrich | PKH26GL | |
| Rabbit C-Reactive Protein (CRP) ELISA kit | Genway Bio | GWB-9BF960 | |
| DMSO, Bioreagent, ≥99.7% | Sigma-Aldrich | D2650 | |

Tableau 3: Liste des produits et réactifs

# Partie 3 : Développement d'un protocole chirurgical pour implantation de prothèse de trachée chez la brebis

# Partie 3 : Développement d'un protocole chirurgical pour implantation de prothèses de trachée chez la brebis



Development of a surgical protocol for the implantation of tracheal prostheses in sheep.

Dupret-Bories A, Shultz P, Vrana NE, Lavalle P, Vautier D, Debry C. J Rehabil Res Dev. J 2011;48(7)

Partie 3 : Développement d'un protocole chirurgical pour implantation de prothèses de trachée chez la brebis

# 3.1. Introduction à l'article 1

Nos précédents travaux réalisés sur le rat (Schultz et al., 2002) ont montré que la prothèse en titane poreux est un biomatériau capable de se substituer aux anneaux trachéaux. Notre équipe a ensuite poursuivi les expérimentations sur la brebis (Schultz et al., 2007) afin de se rapprocher du diamètre trachéal de l'homme. Le protocole opératoire était une résection d'un segment trachéal avec remplacement par la prothèse de trachée en titane poreux nue. L'étude a été menée sur 6 animaux. Après 6 semaines d'implantation, 4 animaux sont décédés suite à une obstruction de la lumière des prothèses par du tissus fibro-musculaire au niveau des jonctions trachée-prothèse en titane poreux. Les 2 autres brebis ont été sacrifiées, comme programmé, à 3 et 6 mois. Les résultats histologiques ont montré qu'une intégration tissulaire des pores de la prothèse (tissu conjonctivo-inflammatoire) était visible à partir de 6 semaines d'implantation.

La colonisation endoprothétique par un épithélium respiratoire était limitée sur quelques millimètres et ne progressait que très lentement avec la durée d'implantation. Ces implantations réalisées chez la brebis ont démontré que la prothèse de trachée ou le protocole opératoire devait être modifié.

Nous avons choisi dans un premier temps de modifier le protocole opératoire chez la brebis afin d'optimiser l'acceptation au long cours de la prothèse de trachée en titane poreux.
5 techniques chirurgicales différentes d'implantation ont été pratiquées dans une même unité de temps sur la brebis et une étude comparative basée sur la survie et les résultats histologiques a été réalisée.

# 3.2. Résumé de l'article 1

L'objectif de cette étude est de rapporter les expérimentations réalisées chez la brebis dans le but de concevoir un larynx artificiel. Celui-ci se composerait d'un tube creux poreux prolongeant la trachée, coiffé d'une valve jouant le rôle de sphincter laryngé. Grâce à un partenariat industriel, notre équipe a développé un biomatériau poreux colonisable par les tissus cervicaux, utilisé chez l'animal pour remplacer une portion de trachée mais aussi destiné à terme à se substituer aux cartilages laryngés. La prothèse est un tube cylindrique creux composé d'un assemblage de microbilles de titane. Nous avons réalisé une étude chez le gros animal avec pour objectif d'établir un protocole opératoire optimal de remplacement trachéal. L'étude porte sur 11 brebis (n=11). 5 modes d'implantation sont comparés. Un protocole opératoire optimal en 3 temps a pu être établi afin de rendre une prothèse de trachée en titane poreux fonctionnelle : 1) lumière endoprothétique large ; 2) colonisation par les tissus périphériques ; 3) épithélialisation endoprothétique. Cette étude est la première étape dans l'élaboration d'un larynx artificiel puisqu'elle a permis de définir un biomatériau susceptible de prolonger la trachée afin de s'ouvrir au niveau du carrefour des voies aérodigestives supérieures.

# 3.3. Article 1



JRRD Volume 48, Number 7, 2011
Pages 851–864
Journal of Rehabilitation Research & Development

## Development of surgical protocol for implantation of tracheal prostheses in sheep

**Agnès Dupret-Bories, MD;[1*] Philippe Schultz, MD, PhD;[1] Nihal Engin Vrana, PhD;[2] Philippe Lavalle, PhD;[2] Dominique Vautier, PhD;[2] Christian Debry, MD, PhD[1]**
*[1]Department of Otorhinolaryngology and Technical Research Team, Hôpitaux Universitaires de Strasbourg, Hôpital de Hautepierre, France; [2]Department of Research, Institut National de la Santé et de la Recherche Médicale (INSERM), INSERM Unité 977, Strasbourg, France*

**Abstract**—This article documents experiments performed in ewes to design an artificial larynx. The artificial larynx is composed of a hollow, porous tube that elongates the trachea and is capped with a valve that acts as a laryngeal sphincter. Through an industrial collaboration, our team developed a porous biomaterial that can be colonized by cervical tissues. This biomaterial has been used in animals to replace part of the trachea, but it is meant to eventually substitute for laryngeal cartilage. The tracheal prosthesis is a hollow cylindrical tube composed of titanium microbeads. We performed a study in large animals to establish an optimal surgical protocol for tracheal replacement in humans. The study included 11 sheep ($n$ = 11) and compared 5 methods of implantation. We successfully established an optimal three-step surgical protocol to make the porous-titanium tracheal prosthesis functional: (1) large lumen endoprosthetics, (2) colonization by the peripheral tissues, and (3) endoprosthetic epithelialization. This study is the first step in developing an artificial larynx because it successfully identifies a biomaterial capable of extending the trachea to allow it to open at the junction of the upper aerodigestive tracts.

**Key words:** artificial larynx, epithelium, function, laryngeal cancer, laryngectomees, outcome, porous titanium, prosthetic surgery, rehabilitation, sheep, surgical protocol, survival rate.

### INTRODUCTION

Extensive squamous cell carcinoma of the larynx and pharynx could necessitate performing a total laryngectomy. More than 57,000 laryngectomees live in the United States, according to the International Association of Laryngectomees (http://www.theial.com). The laryngectomy results in severe mutilation because it requires the anastomosis of the trachea to the skin and the complete separation of the respiratory and digestive tracts. The disability resulting from the loss of the larynx is a public health problem [1]. It leads to significant difficulties with social reintegration, because only palliative measures are available for vocal rehabilitation and the tracheostomy must be maintained for life.

For several years, our team has been interested in developing an artificial larynx. This would require creating a permanent, rigid, biointegrable structure [2–4] to replace the laryngotracheal tract. This structure, which is designed to replace a tracheal segment, must be sufficiently rigid to support the proximal insertion of a neosphincter that opens during respiration and closes

**Abbreviations:** IM = implantation method, IMM = Institut Mutualiste Monsouris, INSERM = Institut National de la Santé et de la Recherche Médicale.

[*]**Address all correspondence to Agnès Dupret-Bories, MD; Department of Otorhinolaryngology and Technical Research Team, CHU Hautepierre, avenue Molière, 67098 Strasbourg, Cedex, France; +03-88-127654; fax: +03-88-127656.**
**Email: agnes.dupret@chru-strasbourg.fr**
DOI:10.1682/JRRD.2010.10.0194

Partie 3 : Développement d'un protocole chirurgical pour implantation de prothèses de trachée chez la brebis



during the passage of a food bolus and, at best, would include phonatory capabilities. Laryngeal tissue is comparable to tracheal tissue, except for the vocal cords; the outer layer of the vocal cords consists of perichondrium and connective tissue, and the inner layer contains cartilage covered with mucosal epithelium consisting mainly of pseudostratified ciliated cells. Tracheal reconstructions are a step toward laryngeal reconstructions.

The restoration of laryngeal function would begin with the use of an entirely integrated biomaterial to extend the proximal tracheal segment remaining after a total laryngectomy. We chose titanium because it is routinely used in orthopedic and maxillofacial surgery for its biomechanical properties and electrochemical stability [5]. Moreover, titanium is an inert and nontoxic metal that is insensitive to bacteria and mold. Titanium's rigidity provides support when it is replacing multiple tracheal rings. A few years ago, our team designed a porous biomaterial composed of titanium microbeads. The pores between the microbeads promote the material's integration by allowing cellular colonization from surrounding tissues. We have thereby succeeded in developing the hollow tube needed to extend or replace part of the trachea. After the trachea is resected and the prosthesis is placed, the tissues surrounding the prosthesis must fill the pores in the biomaterial and provide a vascular network to nourish and oxygenate the regenerating endoluminal epithelium from the tracheal extremities.

In an initial study, Schultz et al. implanted tracheal prostheses made from porous titanium in rats that were rapidly integrated by vascularized colonizing tissue and later by endoluminal epithelial tissues [2]. After healing, more than 50 percent of the animals survived until scheduled euthanasia between 3 months and 1 year later [2–3]. These data encouraged us to pursue testing in sheep, whose tracheal diameter is very close to that of humans [6]. An initial short-term (6-month) study using six animals was conducted and resulted in well-integrated material but with a low survival rate [4]. Implanting the prostheses in a single step, without an endoluminal silicone tube (the same operative protocol that was used in the rat study just mentioned), led to stenosis of the tracheo-prosthetic anastomoses with little endoprosthetic epithelialization.

These findings led us to research an optimal operative protocol to improve the impermeability and endoluminal colonization of the prostheses. To this end, we implanted the prostheses in sheep using five different methods (described in the next section) and compared their survival rates and histological results. We analyzed the colonization of porous titanium prostheses with and without conditioning (placing the prosthesis in muscle for colonization before implantation) and the use of a silicone tube for endoprosthetic calibration. We also assessed the improvement in the prostheses' endoluminal epithelialization via the application of an endoprosthetic mucous graft. This study compares and analyzes the clinical and histological results of these five surgical techniques. Our aim was to determine the ideal surgical procedure for replacing a tracheal segment with a porous titanium prosthesis in large animals before the procedure is potentially translated to humans.

## METHODS

### Manufacturing Prostheses

The tracheal prostheses (**Figure 1**) were manufactured by PROTiP (Strasbourg, France). They were 400 to 500 µm in diameter and formed from a mixture of titanium beads [4]. The titanium was manufactured according to the Association française de normalisation (French Association of Normalization) standards for use of Ti40 as a surgical material. We placed the beads in a mold, then welded them together by a discharge current. The pore size between each bead was approximately 150 µm, i.e., a porosity of about 35 percent. The prostheses were composed of four layers of beads fused into the shape of a tube. The dimensions of each prosthesis were 19.7 mm internal diameter, 23 mm external diameter, and 30 mm long. A ring of solid titanium reinforced the central part of the prosthesis to confer more solidity. At each end of the prosthesis, six 1 mm-diameter holes allowed for sutures between the prosthesis and the tracheal extremities.

PROTiP also manufactures solid Ti40 titanium prostheses that act as the inner liner of the porous titanium tracheal prostheses. We used the solid prostheses to prevent the proliferation of exophytic endoluminal tissue and permit the use of mucous grafts to cover the endoluminal surface of the porous titanium prostheses. Their dimensions were 19.2 mm external diameter, 0.5 mm thick, and 50 mm long.

When we replaced a tracheal segment, we used silicone tubes (stents) for the endoluminal calibration of the porous titanium prostheses. Their hardness was 50 Shore A; they were 80 mm long with an internal diameter of 19 mm.

**Figure 1.**
Tracheal prosthesis made of porous titanium with double ring of bulk titanium.

They protruded from each end of the prosthesis by 25 mm, thus protecting the tracheo-prosthetic anastomoses. The prosthetics and silicone tubes were sterilized by autoclaving before implantation.

**Animal Model**

For this study, we used sheep ($n$ = 11) between the ages of 4 and 11 months and weighing an average of 60 kg. Each animal received care in compliance with the *Guide for the Care and Use of Laboratory Animals* [7]. The implantation and explantation operations were performed at the Institut Mutualiste Monsouris (IMM) in Paris, France.

**Anesthesia**

All surgeries were performed under general anesthesia. After providing ketamine (6 mg/kg) as intramuscular premedication, we induced anesthesia by intravenous administration of sodium thiopental (10 mg/kg). We maintained anesthesia by ventilation with inhaled halothane (1%–2% isoflurane and 100% oxygen) after endotracheal intubation. An intravenous injection of cefamandol (15 mg/kg) provided antibiotic prophylaxis for the entire surgical procedure. We maintained postoperative analgesia by intramuscular injections of morphine salt (0.2 mg/kg) for 5 days.

**Surgical Techniques**

We performed five different implantation methods: Implantation method 1 (IM1) ($n$ = 5) involved direct implantation of the porous titanium prosthesis with an endoprosthetic silicone tube in place of a tracheal segment. With the animal in the supine position after a vertical midline cervicotomy, the infrahyoid muscles were separated from the tracheal axis. After dissecting to the level of the thyroid, we resected a tracheal segment of six to seven rings (50 mm). Each tracheal extremity was then inserted into the prosthesis, which replaced the defect. A silicone tube was placed in the titanium prosthesis and sutured to the prosthesis with one proximal and one distal stitch (vicryl 2.0). For animal 1, the stent-prosthesis suture was not performed. The porous titanium prosthesis and the tracheal extremities were joined by eight proximal and distal sutures (prolene 2.0). Before closing the skin and the subcutaneous layers without drainage, we performed a myoplasty to cover the prosthesis and limit possible peritracheal leakage.

IM2 ($n$ = 2) involved Intramuscular placement of a porous titanium prosthesis and a solid titanium endoprosthesis in the quadriceps. After positioning the animal in the lateral decubitus position, we incised the skin on the lateral surface of the thigh vertically. The prosthesis and an endoprosthetic tube of solid titanium were then housed in a cavity created in the quadriceps muscles. We then sutured the skin and subcutaneous layers with separated stitches of vicryl 2.0. The goal of this technique was to study the prostheses' colonization by muscular tissue in an aseptic environment.

In IM3 ($n$ = 2), implantation was peformed in two steps:

1. Conditioning of the prosthesis with a solid titanium endoprosthetic tube under the infrahyoid muscles (day 0).
2. Implantation of the prosthesis to replace a resected tracheal segment (day 25).

Partie 3 : Développement d'un protocole chirurgical pour implantation de prothèses de trachée chez la brebis



After placing the animal in the supine position, we performed a cervicotomy with a midline vertical incision, allowing access to the infrahyoid muscles, which we separated from the tracheal axis. We placed the prosthesis between the infrahyoid muscles and the trachea and then inserted a solid titanium tube into the porous titanium prosthesis. The skin and subcutaneous layers were then closed with separated stitches of vicryl 2.0.

On day 25 after implantation, we retracted the solid titanium tube through the same incision and laterally transposed the porous titanium prosthesis, replacing a tracheal segment of 5 cm (6–7 rings), which we resected during the same surgery. We inserted the proximal and distal tracheal extremities into the titanium prosthesis and joined the junctions of the prosthesis and the tracheal extremities with 14 sutures of prolene 2.0. Before the sequential closing of the layers, we performed a myoplasty to cover the incision.

In IM4 ($n$ = 1), implantation was performed in two steps:

1. Conditioning of the prosthesis with a solid titanium endoprosthetic tube under the infrahyoid muscles (day 0).
2. Implantation of the prosthesis with a silicone tube to replace a resected tracheal segment (day 25). We repeated the surgical technique described in IM3 but with the additional insertion of a silicone tube. We placed the tube, extending beyond the ends of the prosthesis, inside the porous titanium prosthesis and sutured to it with a proximal and a distal suture (vicryl 2.0) during implantation to replace a tracheal segment.

In IM5 ($n$ = 1), Implantation was performed in three steps:

1. Conditioning of the porous titanium prosthesis with a solid titanium endoprosthetic tube under the infrahyoid muscles (day 0) for 60 days.
2. Grafting mucosal epithelium from the animal's buccal floor onto the endoluminal surface of the prosthesis. We placed a tube of solid titanium as an endoprosthetic to apply the graft (day 60). Together, the prosthesis and its graft were conditioned for 21 more days.
3. We removed the solid titanium tube, then implanted the prosthesis and the endoluminal epithelial graft with an endoprosthetic silicone calibration tube in place of a tracheal segment (day 81).

After placing the animal in the supine position, we performed a cervicotomy via a midline vertical incision to allow access to the infrahyoid muscles, which we separated from the tracheal axis. We positioned the prosthesis between the infrahyoid muscles and the trachea with a solid titanium endoprosthetic tube. We then closed the skin and subcutaneous surfaces with separated stitches of vicryl 2.0 (day 0).

After 60 days, we took a mucosal epithelium sample from the floor of the ewe's mouth. We reopened the cervical incision and used the buccal mucosa to cover the endoluminal surface of the porous titanium prosthesis (day 60) after we removed the solid titanium tube placed on day 0. We inserted another solid titanium tube (with a smaller diameter than that of the porous titanium prosthesis) into this prosthesis to secure the epithelium to the endoluminal surface. The prosthesis, covered with the epithelium on the endoluminal side, was conditioned for 21 days.

After 21 days (day 81), we reopened the cervical cutaneous incision and laterally transposed the prosthesis, with its endoluminal surface covered with buccal epithelium, to replace a 5 cm tracheal segment (6–7 rings), which we resected during the same operation. We removed the solid titanium tube and replaced it with a silicone tube (placed inside the porous titanium prosthesis) that was sutured to the prosthesis with one proximal and one distal stitch (vicryl 2.0). Before closing the skin and subcutaneous tissue, we performed a myoplasty to improve coverage and limit future leakage.

**Clinical and Endoscopic Follow-Up**

We performed a daily clinical follow-up. We recorded data regarding the general well-being of the animals and their weight throughout the experiment. We performed endoscopic follow-up (with archival films and photographs) under general anesthesia weekly during the first month after tracheal-segment prosthesis implantation, then every 2 weeks, to evaluate the endoluminal diameter of the prosthesis and the colonization tissue. Endoscopic evaluations were also performed in cases of dyspnea and before scheduled euthanasia.

**Histological Analysis**

After an observation period ranging from 1 to 14 months, the sheep were euthanized with a mixture of propofol and potassium chloride. We performed a block resection, including surrounding tissues as well as the prosthesis. The tissue was then fixed in 10 percent formaldehyde for preservation, dehydrated with an alcohol

gradient, and embedded in paraffin. We distinguished the prostheses from surrounding tissue with radiography. We obtained 5 μm-thick sections (equivalent to a horizontal section under the solid titanium ring and two vertical sections above and below the ring) with an HM 350 microtome, stained them with hematoxylin-eosin-safran, and viewed them under an optical microscope (Nikon Eclipse E 600, Nikon Instruments, Inc; Melville, New York). We analyzed the tissue integration of the prosthesis, local inflammatory reactions, the endoluminal colonization of the epithelium, and the internal diameter. We performed histological analyses at the IMM and at Biomatech (Chasse sur Rhone, France).

## RESULTS

### Clinical Results

The results are reported in the **Table**. The surgeries and the immediate postoperative care had no complications.

In IM1 ($n = 5$), the endoscopic test performed at day 6 on animal 1 showed proximal migration of the stent; it had not been fixed. We removed the silicone tube on day 13 by endoscopy. The distal anastomosis (the area not in contact with the stent) exhibited stenosis, which subsequently worsened until the animal's death on day 32. In contrast, the proximal anastomosis had been calibrated by the stent and remained nonstenotic. This finding emphasizes the importance of initial calibration, because inflammation and the formation of granular tissue are typically greatest during the first weeks.

The regular endoscopic tests performed on animal 2 showed a large endoprosthetic lumen with good application of the silicone tube (**Figure 2**). The stent was removed on day 55, with no stenosis found in later endoscopic tests. The animal was euthanized on day 119, as initially planned.

For animal 3, we removed the stent on day 143, after a surveillance period and a wait for the endoscopic tests to stop detecting stenosis. Later endoscopic follow-ups showed an endoprosthetic lumen without any narrowing. The sheep was euthanized on day 172.

For animal 4, we never removed the stent. The sheep was generally in good shape throughout the study; the endoscopic tests show no stenosis. The animal was euthanized on day 419.

Animal 5 showed a favorable clinical and endoscopic profile similar to that of animal 4. We removed the stent on day 273, and the animal was euthanized on day 362.

In IM2 ($n = 2$), we placed prostheses in both thighs of animal 6. The animal was euthanized on day 400.

We implanted a prosthesis in the right thigh of animal 7, and the animal was euthanized on day 350.

The skin conditions of the implantation zones showed no signs of infection. The two sheep were in very good general health throughout the study.

In IM3 ($n = 2$), animal 8 died on day 31, 6 days after the replacement of a tracheal segment with a prosthesis that had been previously conditioned. Animal 9 died the day after the implantation. Autopsies revealed necrotic stenosis of the tracheo-prosthetic anastomoses.

In IM4 ($n = 1$), animal 10 was in a good general state and was eupneic after we implanted the prosthesis and replaced a tracheal segment. A first endoscopic test on day 28 showed a proximal loop in the silicone tube (stent) (**Figure 3**). We removed the stent by endoscopy on day 35. After exhibiting an intense stridor, the animal was euthanized. The autopsy revealed an endoprosthetic proximal stenosis in which the stent was not inserted because of plication.

In IM5 ($n = 1$), the sheep was eupneic and in a good general state throughout the experiment. The animal was euthanized on day 102 as planned, i.e., 3 weeks after prosthesis implantation and tracheal segment replacement. The prosthesis exhibited perfect coverage by the epithelium on the endoluminal surface.

### Histological Results

Only IMs 1, 2, and 5 were subjected to histological analysis because the postsurgical survival of the animals used for IMs 3 and 4 was too brief to provide prosthetic integration results. The analysis focused on the macroscopic and histological evaluation of local tolerance, the depth of tissue integration, the degree of tissue integration at the ends of the implanted tracheal prosthesis, and endoluminal epithelialization.

The histological sections included both the prosthesis and the periprosthetic matrix. The vertical sections allowed us to determine the extent of colonization along the entire length of the prosthesis. The transverse section assessed the regularity of peri-, endo-, and transprosthetic tissue colonization over 360°.

**Table.**
Clinical and histological results.

| IM | Animal | Prosthesis Implantation in Muscle | Tracheal Implantation | Silicone Tube | Stenosis | Epithelium in Lumen of Prosthesis | Prosthesis Integration | Death (D) or Euthanization (E) |
|---|---|---|---|---|---|---|---|---|
| IM1 | 1 | No | Day 0 | Day 0, removal Day 13 | Distal | Absent | Absent | Day 32 D |
| | 2 | No | Day 0 | Day 0, removal Day 155 | No | Absent | GT | Day 119 E |
| | 3 | No | Day 0 | Day 0, removal Day 143 | No | MSE near anastomoses | GT | Day 172 E |
| | 4 | No | Day 0 | Day 0, no removal | No | RE and SE | GT | Day 419 E |
| | 5 | No | Day 0 | Day 0, removal Day 273 | No | RE near anastomoses | GT | Day 362 E |
| IM2 | 6 | Day 0 (1 each thigh) | No | Day 0 | No | No | Optimum | Day 400 E |
| | 7 | Day 0 right thigh | No | Day 0 | No | No | Optimum | Day 350 E |
| IM3 | 8 | Day 0 | Day 25 | No | Anasto-moses | Absent | Absent | Day 27 D |
| | 9 | Day 0 | Day 25 | No | Anasto-moses | Absent | Absent | Day 27 D |
| IM4 | 10 | Day 0 | Day 25 | Day 25, but proxi-mal loop, removal Day 35 | Proximal | Absent | Absent | Day 39 D |
| IM5 | 11 | Day 0 + buc-cal mucosa in endolumi-nal surface Day 60 | Day 81 | Day 81 | No | RE on 80% of lumen | Optimum | Day 102 E |

GT = granular tissue, IM = implantation method, MSE = metaplastic tracheal epithelium, RE = respiratory epithelium, SE = squamous epithelium.

*IM1: Histology of Cervical Blocks, Including Prosthesis*

Macroscopically, the tracheo-prosthetic junctions were difficult to identify; no loosening of the prosthesis was visible. None of the prostheses showed signs of fracture. The prostheses were surrounded by a tissue matrix, with the thickness of the tissue around the prostheses corresponding to about 50 percent of their diameter. A growth of newly formed fibroepithelial tissue opposite

**Figure 2.**
Endoscopic evaluation of animal 2 on day 55 showed large endoprosthetic lumen with good application of silicon tube.

the juxtaprosthetic endoluminal surface created a partial stenosis without clinical consequence for animals 2 and 3. By contrast, no sign of stenosis on any section was detected in animals 4 and 5.

Microscopically, the prostheses were encapsulated by dense adventitious fibrovascular tissue continuous with the periprosthetic tracheal tissue. The interface between the external surfaces of the prostheses and the capsule consisted of Malpighian epithelium. The prosthesis spaces defined by the microbeads were mainly filled with cellular debris and inflammatory cells. For animal 3, a metaplastic tracheal epithelium ran alongside the extremities of the endoluminal surface of the prosthesis. For animals 4 and 5, ciliated pseudostratified squamous epithelium, i.e., respiratory epithelium, was visible on the endoluminal surface of the distal third of each prosthesis (**Figure 4**). Simple squamous epithelium was present on the central third of the endoluminal surface of animal 4's prosthesis (**Figure 5**).

*IM2: Histology of Prosthesis Implanted in Muscular Tissue*

Each of the three prostheses was included in the neighboring muscle. The pores between the microbeads were infiltrated by mature connective tissue composed of fibroblasts (**Figure 6**), collagen, and microvasculature, with a very small number of multinucleated giant cells. These results confirmed the very good integration and

**Figure 3.**
Endoscopic evaluation of animal 10 on day 28 showed proximal look of silicon tube.

optimal local tolerance of the intramuscularly implanted prostheses.

*IM5: Histology of Cervical Block, Including Prosthesis*

Macroscopically, the junctions of the trachea and the porous titanium prosthesis were difficult to identify, and the prosthesis showed no signs of fracture. The endoprosthetic lumen was large, reduced by a maximum of one-third of its diameter relative to the diameter of the naked porous titanium prosthesis.

The endoprosthetic surface was covered with squamous epithelium (about 80% of the total surface) (**Figure 7**), except for some scattered fields (about 20% of the surface) devoid of epithelium and filled with inflammatory tissue (polynuclear neutrophils and macrophages).

Below this endoluminal squamous epithelium was supportive fibrous tissue with numerous capillary vessels. This vascularized fibrous tissue extended toward the


**Figure 4.**
Scanning electron microscopy view of distal third of animal 5's prosthesis. Ciliated epithelium, i.e., respiratory epithelium, is present.

periphery and filled in the pores of the titanium prosthesis (**Figure 8**). The presence of fibrovascular tissue between the titanium microbeads confirmed that the prosthesis integrated quite well.

## DISCUSSION

Total laryngectomy is routinely practiced in cases of advanced pharyngolaryngeal cancer, when partial surgery or an organ preservation protocol (radiochemotherapy) is impossible or likely to fail. Removal of the larynx, with the loss of phonatory function and the need for a permanent tracheostomy, has dramatic consequences for the patient. The majority of worldwide research in the field is focused on vocal rehabilitation, but a few studies have attempted to abolish the tracheostomy opening, which

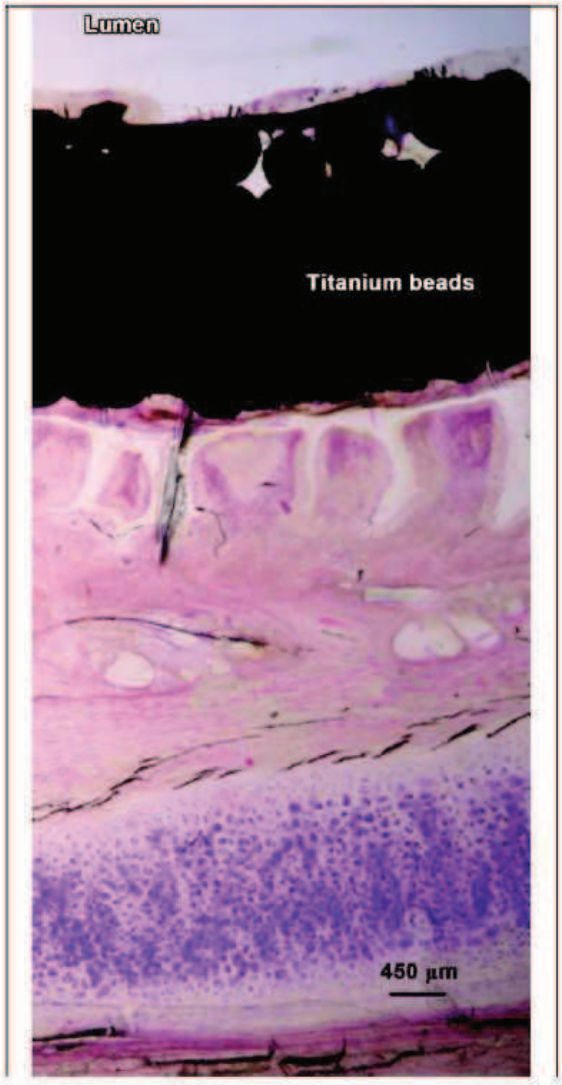


**Figure 5.**
Histological examination of central third of animal 4's tracheal prosthesis. Lumen is covered with simple squamous epithelium (hematoxylin-eosin-saffron).

would require reestablishing a common passage between the respiratory and digestive tracts. Our work focused on designing an implantable laryngeal prosthesis that would combine a rigid, immovable structure with a biofunctional,


**Figure 6.**
Microscopic view of animal 6's prosthesis after muscle implantation. Pores between beads are infiltrated by mature connective tissue composed of fibroblasts (hematoxylin-eosin-saffron).


**Figure 7.**
Histological examination of middle of animal 11's prosthesis. Squamous epithelium is present in lumen and pores are infiltrated by fibrovascular tissues (hematoxylin-eosin-saffron).

movable structure (the upper valve would synchronize the respiratory and digestive functions). The rigid structure was designed to lengthen the proximal trachea after a total laryngectomy.

The search for an ideal tracheal substitute has been the focus of many studies for more than 50 years. Several other teams have addressed the same problem of replacing a tracheal segment, but with a goal other than creating an artificial larynx. In cases of tumoral or traumatic tracheal lesions extending along more than half of the trachea in adults (or one-third in children), direct anastomosis is impossible to perform, even with maximal tracheal mobilization. Extended tracheal resections remain an unresolved surgical problem during reconstruction. Numerous replacement materials have been tested [8–10] on animal models, including synthetic prostheses [3–

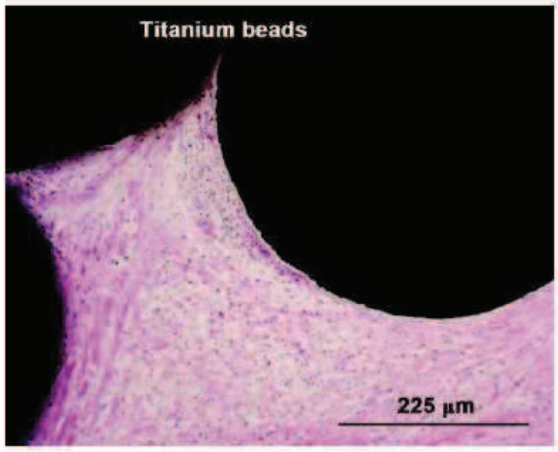


**Figure 8.**
Microscopic view of animal 11's prosthesis. Vascularized fibrous tissue filled in pores of titanium prosthesis (hematoxylin-eosin-saffron).

4,11], tracheal homo- and allografts [12–13], tissue auto- and allotransplantations [14–23], and cultured cell seeded implants [24–25]. Martinod et al. used an aortic allograft linked to a silicone prosthesis as a tracheal substitute [14–19]. The initial results, obtained in sheep, were spectacular: the silicone tube was removed after 6 months, and the aortic tissue was transformed into a real trachea composed of cartilage organized in rings and covered with a mucociliary epithelium. The preliminary results in humans were contradictory. Of six human patients, four survived after an average follow-up of 34 months and none benefited from removal of the silicone tube [26]. In addition, the process of aortic tissue reorganization into a cartilaginous structure seems delayed in humans because it was only partially complete after 34 months.

Despite the undeniable value of these results, the use of this aortic graft may not be suitable for laryngeal reconstruction. Given its initial flaccidity and the impossibility of removing the silicone prosthesis in humans, this graft cannot be attached to an upper valve that would replace the laryngeal sphincter.

The previous work of our team led to the development of a biomaterial consisting of an assembly of titanium microbeads [2–4]. This biomaterial meets several criteria: (1) being mechanically rigid, it provides support when it replaces tracheal rings; (2) being inert, it limits detrimental cellular reactions; and (3) it resists aggressive environments such as those of the upper aerodigestive

tracts. An implant meant to substitute for laryngeal or tracheal cartilages must have biofunctional properties similar to those of the respiratory tree. The implant must be perfectly integrated, i.e., perfectly colonized by the periprosthetic tissue and entirely covered by a respiratory epithelium on the endoprosthetic surface.

The implantations of uncoated titanium tracheal prostheses in rats [2–3] offered encouraging results that allowed us to proceed to implanting tracheal prostheses in sheep [4]. The first implantations performed in ewes showed good immediate tolerance; no postsurgical complications occurred. The complications and mortality occurred secondarily, after infection and prosthetic obstruction. The implants were obstructed by a thickening of the tracheal stumps via inflammatory granulation tissue. The granuloma caused bronchial stasis, which gave rise to pulmonary infections and the formation of casts or mucus plugs. Necrotic zones at the junctions of the tracheal extremities and the prosthesis were also present in some sheep. Also, the colonization of the pores of the prosthesis remained poor. The surgical protocol used in that study (the one-step implantation of a titanium prosthesis in place of a tracheal segment without a stent) was considered unsatisfactory.

Throughout our studies with porous titanium prostheses, we observed no loosening, fractures, or rejections of prostheses. These results confirm our experience with mandibular prostheses made of porous titanium in humans [27]: although the mechanical pressure was high, none of these problems occurred.

The study described here focused on the implantation of titanium prostheses in five groups of sheep. Five different surgical protocols were performed. Our goal was to establish, by comparing the results from each group, an ideal surgical technique for implanting a porous titanium tracheal prosthesis in large animals. The main criteria necessary for a biofunctional tracheal prosthesis are as follows: maintenance of a large endoprosthetic lumen, colonization of the prosthetic pores by fibrous connective tissue, and development of respiratory epithelium covering the entire endoluminal surface of the prosthesis.

In IM1 ($n$ = 5), the porous titanium prosthesis was implanted with a silicone endoprosthetic calibration tube directly in place of a tracheal segment. Long survivals were observed in this group (euthanizations occurred on days 119, 172, 362, and 419). Necrotic zones were almost nonexistent; the same was true for stenotic zones (which were completely absent from animals 4 and 5). The silicone tube calibrated the size of the airways [27] and prevented the formation of granulation tissue, which from our experience is a major cause of fatal airway stenosis [4]. Granulation tissue stents the proximal and distal anastomoses while preventing the penetration of mucus in the luminal pores toward the periphery of the prosthesis. The stent acts as a protective barrier that maintains the respiratory lumen while counterbalancing intrinsic and extrinsic pressures, thus acting as a splint. Makris and Marquette emphasized these findings when treating tracheobronchial obstructions with a stent and reported the silicone tube stent's superiority over the metallic stent for calibrating the airways [28]. An endoprosthetic epithelium was detected in IM1; it was identified in animal 3 (euthanized on day 172) in the distal extremities of the endoluminal surface of the prosthesis as a metaplastic tracheal epithelium. For animals 4 (euthanized on day 419) and 5 (euthanized on day 372), a respiratory (pseudostratified, ciliated) squamous epithelium was identified endoprosthetically. This epithelium covered the proximal and distal thirds of the endoluminal surface of the prostheses. For animal 4, the central third of the prosthesis was colonized by a simple squamous epithelium. These histological results suggest that the respiratory epithelium proliferated from the tracheal extremities that form the junction with the prosthesis; i.e., it was a continuous epithelialization. The presence of an endoprosthetic squamous epithelium in IM1 confirmed that the stent did not hinder respiratory epithelium proliferation. On the contrary, by preventing tracheal secretions from penetrating through the pores, from the lumen toward the exoluminal part of the prosthesis, the stent allowed the epithelial cells to proliferate without being subjected to the flow of mucus.

However, in IM1, the colonization of the prosthesis pores remained insufficient. A matrix composed of thick, dense granulomatous and fibrous connective tissue surrounded the prostheses and kept them aligned in the tracheal axis, allowing them to perform their functions; however, the pores of the prostheses were only filled with inflammatory cells and cellular debris and not with connective tissue, as had been expected.

To determine whether the problems of cellular colonization of the pores were linked to the premature filling of the pores with mucus, we performed IM2. The goal of IM2 ($n$ = 2) was to test only the colonization of the prosthesis pores in an aseptic environment with simple muscular contact with the periphery of the prosthesis. In

this group, the porous titanium prostheses (with an endoprosthetic tube made of solid titanium) were implanted in the quadriceps muscles. The histological analysis of these implants showed perfect integration. All the pores were filled with mature connective tissue consisting of fibroblasts that formed a bed capable of sustaining the proliferation of a viable epithelium to cover the endoprosthetic surface.

In IM3 ($n = 2$), we implanted prostheses by replacing a tracheal segment without the silicone tube after conditioning the prostheses in the infrahyoid muscles for 25 days. The animals used in this procedure died prematurely (days 27 and 29). The low survival rate of the sheep was directly linked to endoprosthetic stenosis or to necrotic junction zones. Furthermore, the bodies of the prostheses were covered with endoluminal mucus without colonization. No stenosis at the level of the prosthesis body was documented; only the tracheo-prosthetic anastomoses were involved. The prior conditioning and colonization of prostheses did not warrant bypassing the use of a stent. These results support the hypothesis that the silicone tube is necessary to protect the respiratory lumen and to stent the junction zones. The role of the silicone tube as a splint is essential, even with the improved impermeability of the conditioned prosthesis.

In accordance with these results, a sheep was implanted with a preconditioned prosthesis made of porous titanium and with a silicone tube. In IM4, we replaced a tracheal segment with a porous titanium prosthesis conditioned for 25 days and a silicone tube. The endoscopic tests demonstrated a proximal plication of the silicone tube, requiring its early removal. The animal was euthanized 4 days after the stent was removed because of inspiratory dyspnea associated with proximal endoprosthetic stenosis by granulation tissue (where the stent could not function because of plication). This finding confirmed the importance of correctly applying the stent on the endoluminal surface.

Endoluminal inflammation, likely promoting stenosis, was found in all the IMs when the stent was removed prematurely. Because the respiratory epithelium migrates very slowly (only animal 4, euthanized late at 419 days, showed total colonization of the endoprosthetic surface), accelerating its proliferation seems necessary. Performing tracheal reconstructions with a prosthesis whose endoluminal surface is pre-epithelialized (i.e., immediately functional) would eliminate the wait for the slow epithelial migration from the tracheal extremities and the classic inflammation associated with healing processes. We also performed IM5 to accelerate endoprosthetic healing by directly grafting from the oral mucosa to the lumen of the porous titanium prosthesis while using the initial technique of conditioning the prosthesis and implanting it with a silicone tube in place of a tracheal segment.

In terms of the quasitotal and immediate coverage of the endolumenal surface of the prosthesis by a squamous epithelium, as well as the absence of endoprosthetic stenosis, the results were very satisfactory. The initial conditioning provided fibrovascular supportive tissue (filling in the pores of the prosthesis) to the endoluminal epithelium, which covered more than 80 percent of the endoprosthetic surface by 21 days after the prosthesis was implanted in place of a tracheal fragment.

The method used in this last group appears to be the only truly effective one. Only one sheep was used for this technique, for only a short-term study (it was euthanized 21 days after the tracheal prosthesis was implanted). A long-term study using this method of implantation is essential for evaluating the tolerance, survival, and histological development of the endoluminal epithelial graft. Future studies should include the three following steps: (1) conditioning the prosthesis, (2) grafting an endoluminal epithelium, and (3) implanting the prosthesis with a silicone stenting tube in place of a tracheal segment.

The step of directly grafting epithelium endoprosthetically on a previously cultured prosthesis makes the tracheal prosthesis immediately functional. This graft can originate from mucosal epithelium taken endobuccally (as in IM5). Another approach, which is currently being developed, colonizes the endoluminal surface of the prosthesis in vitro with ciliated cells, thus directly creating a respiratory epithelium before the prosthesis was implanted in place of a tracheal segment (collaboration with Institut National de la Santé et de la Recherche Médicale Unit 903, Reims, France) [29–30].

## CONCLUSIONS

Our research aims to preserve a certain quality of life for laryngectomees by abolishing the mutilating consequences of the loss of the larynx, i.e., tracheostomy and complete separation of the respiratory and digestive functions. For laryngeal function to be recreated, the trachea must first be lengthened with a hollow, integrated structure that is vascularized by the surrounding tissues. Numerous

authors have considered the use of synthetic prostheses to replace a tracheal segment an inevitable failure, given the lack of graft epithelialization and/or the presence of tracheal obstruction or prosthetic migration [18,22].

Our team focused its research on replacing a tracheal segment with porous titanium Ti40 biomaterial. This sheep study has shown the prostheses' partial endoprosthetic colonization by respiratory epithelium and its functionality when replacing a tracheal segment, as authenticated by long survival of the ewes. However, the optimal integration of the prosthesis and colonization by a respiratory epithelium on the whole endoprosthetic surface remains to be achieved.

By comparing different methods of implantation, this study yields three main results that need to be considered to make a porous titanium prosthesis completely biofunctional. Stenoses in the junctions of the prosthesis and tracheal extremities, which cause premature death, were absent when an endoprosthetic silicone tube was used. The colonization of the pores of the porous titanium prosthesis was improved by the initial implantation of the prosthesis in a muscle, and the endoprosthetic epithelialization was accelerated by the grafting of amucosal tissue in the prosthetic lumen. These findings led us to establish an optimal three-step surgical protocol: (1) preconditioning the prosthesis, (2) grafting endoluminal epithelium, and (3) tracheal implantation, using a silicone tube for calibration. To reinforce the hypotheses presented in this study, a long-term study of tracheal prosthetics implanted according to this technique will be performed soon.

## ACKNOWLEDGMENTS

**Author Contributions:**
*Study concept and design:* P. Schultz, C. Debry, A. Dupret-Bories.
*Technical surgery:* P. Schultz, C. Debry, A. Dupret-Bories.
*Acquisition of data:* A. Dupret-Bories, P. Schultz, C. Debry.
*Analysis and interpretation of data:* A. Dupret-Bories, P. Schultz, C. Debry.
*Drafting and revision of manuscript:* A. Dupret-Bories, P. Schultz, C. Debry, N. E. Vrana, P. Lavalle, D. Vautier.
*Obtained funding:* C. Debry, P. Lavalle, D. Vautier.
**Financial Disclosures:** The authors have declared that no competing interests exist.
**Funding/Support:** This material was based on work supported by the Réseau National des Technologies de Santé de l'Agence Nationale de la Recherche [French National Research Agency], PROTimplant Project.
**Additional Contributions:** We thank PROTiP for providing the tracheal prostheses.
**Institutional Review:** This study was approved by the Comité d'Ethique de l'IMM Recherche [Ethics Commitee of IMM Research].

## REFERENCES

1. Babin E, Edy E, Béquignon A, Hitier M. [Personal and social identity transformations that occur over time among patients with total laryngectomy]. J Otolaryngol Head Neck Surg. 2008;37(4):495–501. French. [PMID: 19128582]
2. Schultz P, Vautier D, Chluba J, Marcellin L, Debry C. Survival analysis of rats implanted with porous titanium tracheal prosthesis. Ann Thorac Surg. 2002;73(6):1747–51. [PMID: 12078764] DOI:10.1016/S0003-4975(02)03569-5
3. Schultz P, Vautier D, Egles C, Debry C. Experimental study of a porous rat tracheal prosthesis made of T40: Long-term survival analysis. Eur Arch Otorhinolaryngol. 2004;261(9):484–88. [PMID: 14655018] DOI:10.1007/s00405-003-0717-5
4. Schultz P, Vautier D, Charpiot A, Lavalle P, Debry C. Development of tracheal prostheses made of porous titanium: A study on sheep. Eur Arch Otorhinolaryngol. 2007;264(4):433–38. [PMID: 17123095] DOI:10.1007/s00405-006-0195-7
5. Guillemot F, Porté MC, Labrugère C, Baquey Ch. Ti4+ to Ti3+ conversion of TiO2 uppermost layer by low-temperature vacuum annealing: Interest for titanium biomedical applications. J Colloid Interface Sci. 2002;255(1):75–78. [PMID: 12702370] DOI:10.1006/jcis.2002.8623
6. Ten Hallers EJ, Rakhorst G, Marres HA, Jansen JA, Van Kooten TG, Schutte HK, Van Loop JP, Van den Houwen EB, Verkerke GJ. Animals model for tracheal research. Biomaterials. 2004;25(9):1533–43. [PMID: 14697856] DOI:10.1016/S0142-9612(03)00500-3
7. Committee for the update of the guide for the care and use of laboratory animals: Institute of Laboratory Animal Resources, National Research Council. Guide for the care and use of laboratory animals. 8th rev. ed. Washington (DC): National Academies Press; 2010.
8. Grillo HC. Development of tracheal surgery: A historical review. Part 1: Techniques of tracheal surgery. Ann Thorac Surg. 2003;75(2):610–19. [PMID: 12607695] DOI:10.1016/S0003-4975(02)04108-5
9. Grillo HC. Development of tracheal surgery: A historical review. Part 2: Treatment of tracheal diseases. Ann Thorac Surg 2003;75(3):1039–47. [PMID: 12645751] DOI:10.1016/S0003-4975(02)04109-7
10. Grillo HC. Tracheal replacement: A critical review. Ann Thorac Surg. 2002;73(6):1995–2004. [PMID: 12078821] DOI:10.1016/S0003-4975(02)03564-6
11. Dodge-Khatami A, Niessen HW, Koole L, Klein MG, Van Gulik TM, De Mol BA. Tracheal replacement in rabbits

with a new composite silicone-metallic prosthesis. Asian Cardiovasc Thorac Ann. 2003;11(3):245–49. [PMID: 14514557]
12. Neville WE, Bolanowski PJ, Soltanzadeh H. Homograft replacement of the trachea using immunosuppression. J Thorac Cardiovasc Surg. 1976;72(4):596–601. [PMID: 966794]
13. Tojo T, Niwaya K, Sawabata N, Kushibe K, Nezu K, Taniguchi S, Kitamura S. Tracheal replacement with cryopreserved tracheal allograft: Experiment in dogs. Ann Thorac Surg. 1998;66(1):209–13. [PMID: 9692466] DOI:10.1016/S0003-4975(98)00270-7
14. Martinod E, Zakine G, Fornes P, Zegdi R, d'Audiffret A, Aupecle B, Goussef N, Azorin J, Chachques JC, Fabiani JN, Carpentier A. [Metaplasia of aortic tissue into tracheal tissue. Surgical perspectives]. C R Acad Sci III. 2000;323(5):455–60. French.
15. Makris D, Holder-Espinasse M, Wurtz A, Seguin A, Hubert T, Jaillard S, Copin MC, Jashari R, Duterque-Coquillaud M, Martinod E, Marquette CH. Tracheal replacement with cryopreserved allogenic aorta. Chest. 2010;137(1):60–67. [PMID: 19801581] DOI:10.1378/chest.09-1275
16. Seguin A, Radu D, Holder-Espinasse M, Bruneval P, Fialaire-Legendre A, Duterque-Coquillaud M, Carpentier A, Martinod E. Tracheal replacement with cryopreserved, decellularized, or glutaraldehyde-treated aortic allografts. Ann Thorac Surg. 2009;87(3):861–67. [PMID: 19231406] DOI:10.1016/j.athoracsur.2008.11.038
17. Azorin JF, Bertin F, Martinod E, Laskar M. Tracheal replacement with an aortic autograft. Eur J Cardiothorac Surg. 2006;29(2):261–63. [PMID: 16388953] DOI:10.1016/j.ejcts.2005.11.026
18. Martinod E, Azorin J, Carpentier A. [Tracheal replacement: New perspectives]. Rev Mal Respir. 2001;18(6 Pt 1):639–43. French. [PMID: 11924185]
19. Seguin A, Martinod E, Kambouchner M, Campo GO, Dhote P, Bruneval P, Azorin JF, Carpentier A. Carinal replacement with an aortic allograft. Ann Thorac Surg. 2006;81(3):1068–74. [PMID: 16488724]
20. Brian E, Gounant V, Fulgencio JP, Milleron B, Bazelly B. [Tracheal replacement using the abdominal aorta. Comments on a case report]. Rev Pneumol Clin. 2007;63(3):224–29. French. [PMID: 17675946] DOI:10.1016/S0761-8417(07)90127-3
21. Davidson MB, Mustafa K, Girdwood RW. Tracheal replacement with an aortic homograft. Ann Thorac Surg. 2009;88(3):1006–8. [PMID: 19699945] DOI:10.1016/j.athoracsur.2009.01.044
22. Anoosh F, Hodjati H, Dehghani S, Tanideh N, Kumar PV. Tracheal replacement by autogenous aorta. J Cardiothorac Surg. 2009;4:23. [PMID: 19508714] DOI:10.1186/1749-8090-4-23
23. Go T, Jungebluth P, Baiguero S, Asnaghi A, Martorell J, Ostertag H, Mantero S, Birchall M, Bader A, Macchiarini P. Both epithelial cells and mesenchymal stem cell-derived chondrocytes contribute to the survival of tissue-engineered airway transplants in pigs. J Thorac Cardiovasc Surg. 2010;139(2):437–43. [PMID: 19995663] DOI:10.1016/j.jtcvs.2009.10.002
24. Macchiarini P, Jungebluth P, Go T, Asnaghi MA, Rees LE, Cogan TA, Dodson A, Martorell J, Bellini S, Parnigotto PP, Dickinson SC, Hollander AP, Mantero S, Conconi MT, Birchall MA. Clinical transplantation of a tissue-engineered airway. Lancet. 2008;372(9655):2023–30. [PMID: 19022496] DOI:10.1016/S0140-6736(08)61598-6
25. Wurtz A, Porte H, Conti M, Dusson C, Desbordes J, Copin MC, Marquette CH. Surgical technique and results of tracheal and carinal replacement with aortic allografts for salivary gland-type carcinoma. J Thorac Cardiovasc Surg. 2010;140(2):387–93. [PMID: 20381819] DOI:10.1016/j.jtcvs.2010.01.043
26. Schultz P, Vautier D, Atallah I, Gentine A, Debry C. [Reconstruction of the anterior mandibule using a porous titanium implant: A case report]. Rev Laryngol Otol Rhinol (Bord). 2008;129(3):201–5. French. [PMID: 19694164]
27. Ko PJ, Liu CY, Wu YC, Chao YK, Hsieh MJ, Wu CY, Wang CJ, Liu YH, Liu HP. Granulation formation following tracheal stenosis stenting: Influence of stent position. Laryngoscope. 2009;119(12):2331–36. [PMID: 19688861] DOI:10.1002/lary.20615
28. Makris D, Marquette CH. Tracheobronchial stenting and central airway replacement. Curr Opin Pulm Med. 2007;13(4):278–83. [PMID: 17534173] DOI:10.1097/MCP.0b013e32816b5c3b
29. Kojima K, Bonassar LJ, Roy AK, Mizuno H, Cortiella J, Vacanti CA. A composite tissue-engineered trachea using sheep nasal chondrocyte and epithelial cells. FASEB J. 2003;17(8):823–28. [PMID: 12724341] DOI:10.1096/fj.02-0462com
30. Coraux C, Hajj R, Lesimple P, Puchelle E. [Repair and regeneration of the airway epithelium]. Med Sci (Paris). 2005;21(12):1063–69. French. [PMID: 16324647]

Submitted for publication October 6, 2010. Accepted January 28, 2011.

This article and any supplementary material should be cited as follows:
Dupret-Bories A, Schultz P, Vrana NE, Lavalle P, Vautier D, Debry C. Development of surgical protocol for implantation of tracheal prostheses in sheep. J Rehabil Res Dev. 2011;48(7):851–64.
DOI:10.1682/JRRD.2010.10.0194

# Partie 4 : Modification de la prothèse de trachée par ajout de structures biodégradables

# Partie 4 : Modification de la prothèse de trachée par ajout de structures biodégradables

## 4.1. Développement d'une prothèse hybride avec gradient de porosité et suivi de son intégration *in vivo,* Article 2. Chapitre Matériels et Méthodes

4.1.1. Introduction à l'article 2

4.1.2. Résumé de l'article 2

4.1.3. Article 2:

Vrana, N. E., Dupret-Bories, A., Schultz, P., Debry, C., Vautier, D. and Lavalle, P. (2013), Titanium Microbead-Based Porous Implants: Bead Size Controls Cell Response and Host Integration. Advanced Healthcare Materials. doi: 10.1002/adhm.201200369

## 4.2. Développement d'une prothèse hybride avec gradient de porosité, étude *in vitro,* Article 3

4.2.1. Introduction à l'article 3

4.2.2. Résumé de l'article 3

4.2.3. Article 3:

Hybrid Titanium/Biodegradable Polymer Implants with a Hierarchical Pore Structure as a Means to Control Selective Cell Movement.

Vrana NE, Dupret A, Coraux C, Debry C, Vautier D, Lavalle P. PLoS One. 2011;6(5):e20480

## 4.3. Etude in vivo de l'implantation d'une prothèse de trachée hybride, Article 4

4.3.1. Introduction à l'article 4

4.3.2. Résumé de l'article 4

4.3.3. Article 4:

Modification of macroporous titanium tracheal implants with biodegradable structures: Tracking in vivo integration for determination of optimal in situ epithelialization conditions.

Vrana NE, Dupret-Bories A, Bach C, Chaubaroux C, Coraux C, Vautier D, Boulmedais F, Haikel Y, Debry C, Metz-Boutigue MH, Lavalle P. Biotechnol Bioeng. 2012;109(8):2134-46

# 4.1. Développement d'une prothèse hybride avec gradient de porosité et suivi de son intégration in vivo, Article 2. Chapitre Matériels et Méthodes

## 4.1.1. Introduction à l'article 2

Avec la dernière étude réalisée chez la brebis (Dupret-Bories et al., 2011), nous avons vu que la modification du protocole opératoire pour la substitution d'un segment trachéal par une prothèse en titane poreux permettait d'améliorer la survie des animaux, mais n'était pas suffisante pour obtenir une prothèse parfaitement intégrée aux tissus.

Comme les résultats de l'article 1 nous l'ont suggéré, nous avons modifié les protocoles opératoires en utilisant un tube de silicone endoprothétique pour les expérimentations *in vivo* suivantes. A cette modification de protocole opératoire, nous avons ajouté une modification de la prothèse de trachée en titane poreux en elle-même. L'objectif était de contrôler la migration des différents types cellulaires : il s'agissait d'accélérer la prolifération d'épithélium respiratoire sur la face endoluminale tout en évitant les sténoses endoprothétiques par la prolifération excessive de tissu fibro-musculaire à travers les pores puis dans la lumière. Pour cela nous avons créé un implant en titane poreux hybride, c'est-à-dire composé d'une partie organique dégradable en polymère et d'une partie inorganique non-dégradable en titane pur. De plus, l'ensemble comportera différentes porosités adaptées au type de cellules à favoriser.

Enfin, nous avons souhaité développer une méthode alternative dans le suivi *in vivo* de l'intégration des prothèses de trachée en titane poreux sans avoir recours de manière systématique à l'analyse histologique et à l'euthanasie de l'animal.

Ce deuxième article, publié dans Journal of Visualized Experiments, est à considérer comme étant le chapitre « matériels et méthodes » des études qui seront décrites dans les articles suivants.

## 4.2. Résumé de l'article 2

Les implants métalliques, notamment les implants en titane, sont utilisés dans de nombreuses applications cliniques. Afin d'obtenir des résultats satisfaisants, l'intégration de ces implants par les tissus doit être optimale. Pour ce faire, des implants métalliques poreux, constitués de microbilles de titane, ont été élaborés. La porosité entre les billes en titane est très avantageuse car elle permet notamment leur fonctionnalisation sans compromettre les propriétés mécaniques de la structure entière. Nous décrivons ici les modifications d'implants trachéaux en titane poreux par insertion dans les porosités d'un polymère biocompatible et biodégradable.

En utilisant les propriétés physiques inhérentes telles que l'hydrophobie de titane, il a été possible d'obtenir des gradients de pores à l'intérieur des implants trachéaux en titane poreux et, en même temps, d'associer une membrane de ce même polymère dans la partie endoluminale. Ces gradients de pores à travers les parois de l'implant ont été obtenus à partir d'un polymère synthétique biocompatible et biodégradable, l'acide poly-L-lactique (PLLA), par la méthode de congélation-extraction. Ensuite, des surfaces 2D nanofibrillaires ont été formées en utilisant une association de collagène / alginate avec une étape de réticulation par un agent naturel de réticulation, la génipine. Ce film nanofibrillaire a été créé par le dépôt, couche par couche, de deux molécules de charge opposée, le collagène et l'alginate. Par ces techniques, la migration des cellules fibroblastiques à travers les pores de l'implant pouvait être contrôlée. Un tel système est décrit pour le cas spécifique du remplacement d'un segment de trachée, mais il peut être adapté à d'autres organes cibles. L'analyse des résultats sur la migration cellulaire et les méthodes permettant de créer différents gradients de pores sont décrites dans cet article.

La prochaine étape était le suivi de l'intégration de ces implants après l'implantation. L'analyse histologique des implants métalliques étant un processus long et fastidieux nous avons développé une méthode alternative pour suivre de façon régulière *in vivo* la réaction de l'hôte aux implantations. Cette méthode était basée sur l'analyse dans le sang des taux de Chromogranine A (CGA) et la mesure de la Protéine C réactive (CRP).

Les techniques, décrites dans cet article, peuvent être utilisées pour le développement d'implants pour lesquels un contrôle fin de la migration cellulaire est possible, et également pour l'analyse *in vivo* de l'intégration des implants sans recours systématique à l'analyse histologique.

## 4.1.3. Article 2

jove Journal of Visualized Experiments www.jove.com

Video Article

# Multi-Scale Modification of Metallic Implants With Pore Gradients, Polyelectrolytes and Their Indirect Monitoring *In vivo*

Nihal E. Vrana[1], Agnes Dupret-Bories[1,2], Christophe Chaubaroux[1], Elisabeth Rieger[1,2], Christian Debry[1,2], Dominique Vautier[1,3], Marie-Helene Metz-Boutigue[1,3], Philippe Lavalle[1,3]

[1]Biomatériaux et Bioingénieriee, INSERM

[2]Service Oto-Rhino-Laryngologie, Hôpitaux Universitaires de Strasbourg

[3]Faculté de Chirurgie Dentaire, Université de Strasbourg

Correspondence to: Nihal E. Vrana at evrana8@gmail.com

URL: http://www.jove.com/video/50533
DOI: doi:10.3791/50533

Keywords: Biomedical and Dental Materials, Composite Materials, Metals and Metallic Materials, Engineering (General), [Titanium, pore gradient, implant, in vivo, blood analysis, freeze-extraction, foams]

Date Published: 6/7/2013

Citation: Vrana, N.E., Dupret-Bories, A., Chaubaroux, C., Rieger, E., Debry, C., Vautier, D., Metz-Boutigue, M.H., Lavalle, P. Multi-Scale Modification of Metallic Implants With Pore Gradients, Polyelectrolytes and Their Indirect Monitoring *In vivo*. *J. Vis. Exp.* (), e50533, doi:10.3791/50533 (2013).

## Abstract

Metallic implants, especially titanium implants, are widely used in clinical applications. Tissue in-growth and integration to these implants in the tissues are important parameters for successful clinical outcomes. In order to improve tissue integration, porous metallic implants have being developed. Open porosity of metallic foams is very advantageous, since the pore areas can be functionalized without compromising the mechanical properties of the whole structure. Here we describe such modifications using porous titanium implants based on titanium microbeads. By using inherent physical properties such as hydrophobicity of titanium, it is possible to obtain hydrophobic pore gradients within microbead based metallic implants and at the same time to have a basement membrane mimic based on hydrophilic, natural polymers. 3D pore gradients are formed by synthetic polymers such as Poly-L-lactic acid (PLLA) by freeze-extraction method. 2D nanofibrillar surfaces are formed by using collagen/alginate followed by a crosslinking step with a natural crosslinker (genipin). This nanofibrillar film was built up by layer by layer (LbL) deposition method of the two oppositely charged molecules, collagen and alginate. Finally, an implant where different areas can accommodate different cell types, as this is necessary for many multicellular tissues, can be obtained. By, this way cellular movement in different directions by different cell types can be controlled. Such a system is described for the specific case of trachea regeneration, but it can be modified for other target organs. Analysis of cell migration and the possible methods for creating different pore gradients are elaborated. The next step in the analysis of such implants is their characterization after implantation. However, histological analysis of metallic implants is a long and cumbersome process, thus for monitoring host reaction to metallic implants *in vivo* an alternative method based on monitoring CGA and different blood proteins is also described. These methods can be used for developing *in vitro* custom-made migration and colonization tests and also be used for analysis of functionalized metallic implants *in vivo* without histology.

## Video Link

The video component of this article can be found at http://www.jove.com/video/50533/

## Introduction

Currently available metallic implants are suitable for load-bearing applications, but their non-degradability necessitates designs which ensure a strong interface with the tissue surrounding them [1]. By providing structures that facilitate cellular in-growth and colonization *in vivo*, the lifetime of metallic implants can be prolonged [2]. Openly porous metallic implants are promising materials for tissue interface engineering and also for ensuring good colonization of the implants. They have been actively used as orthopedic implants and also as tracheal implants [3-5]. However, there are still problems that need to be solved such as the precise control over cell movement in the pore areas. Failure to control this process might lead to incomplete colonization in one end and restenosis in the other. Also further functionalization of these implants is necessary for achieving higher functions such as, delivery of growth factors, directed vascularization and simultaneous movement of different cell types [6-8]. For tracheal implants, this is crucial as the colonization of the implant by a vascularized tissue is desirable. However, the uncontrolled tissue in-growth to the lumen of trachea is undesirable because it decreases implant patency.

One possibility to control cell movement is size exclusion. By knowing the size of the target cells and their ability to interact with a given synthetic polymer it is possible to develop gradients of pores which can effectively determine the depth of cell movement. For example by creating a pore architecture that is large enough for the entry of connective tissue cells such as fibroblasts extraluminally, but small enough (less than 10 µm) to prevent their movement intraluminally an effective control over colonization of a tubular implant can be achieved.

From available pore creation methods such as freeze-drying, particle leaching, gas foaming [9,10]; the easiest to adapt method for fast formation of pore gradients with minimal amount of necessary equipments is freeze-extraction [11]. In this method, a polymer solution is frozen in a binary

 

mixture of an organic solvent and water. Afterwards, the solvent is exchanged via extraction by a miscible pre-chilled liquid such as ethanol. Freezing and extraction conditions determine the shape and size of the pores and if the extraction is done in a way where the movement of the extraction solution can be controlled, pore size and shape can be directionally modulated.

Second step for multicellular tissues is the formation of porous barriers between different cell types to control their interaction. This is also necessary for the availability of different microenvironments for different cell types depending on their requirements [12,13]. Trachea is a tubular organ that connects larynx with bronchi. It has an inner pseudostratified ciliary epithelium lining with interdispersed goblet cells which produce mucus. The 3D structure and stability of trachea is maintained by cartilage in the shape of C-rings. Thus, in an artificial trachea there should be a defined junction between the connective tissue and the ciliary epithelial layer. While a 3D structure is necessary for the connective tissue part, the migration of epithelial cells requires a basement membrane-like surface to achieve directional movement and closure of the wound. Polyelectrolyte multilayer films (PEMs) are one possible option to obtain basement membrane mimics. Layer-by-layer method (LbL) is a versatile process to obtain thin and functional surface coatings. It is based on electrostatic interactions of two oppositely charged polyelectrolytes and their build-up in a sequential manner to obtain nanoscale surface coatings whose properties can be varied by simply changing variables such as polyelectrolyte species, pH, layer number, addition of a capping layer, crosslinking etc. One of the main advantages of the LbL method is its ability to conform to the topography of the underlying substrate. Thus, under controlled conditions this method can also be used for obtaining surface coverage of porous structures. If collagen is used as one of the polyelectrolytes it is possible to obtain nanofibrillar structures that can mimic the surface of basement membrane. The hydrophobicity of titanium enables development of such structures and fibrillarity can be preserved in thick coatings [14]. This way attachment and movement of cell on the surface can also be controlled. By using freeze-extraction and LbL film coating sequentially, a structure where cell movement can be controlled laterally, longitudinally and circumferentially can be obtained [15].

Here we describe two novel modification methods for titanium implants by using their hydrophobic behavior which can be extended to modification of various porous implants: i) formation of gradients of micropores within the macroporous titanium implants with hydrophobic, synthetic polymers ii) formation of a thick polymeric film layer on the implant surface that supports cell growth and lining formation by polyelectrolyte multilayers. These methods can be used sequentially or separately. They provide structures that ensure controlled migration and spatial organization of different cell types in multicellular tissues [16,17]. For the specific case of trachea, the desired outcome for the implant would be the colonization by fibrovascular tissue within the micropore gradients without restenosis and the formation of the inner lining of ciliated epithelial cells on the polyelectrolyte multilayers.

One way of controlling integration of implants is to do small surgical interventions during the period of their integration with the host in situ. In order to be able to decide on the timing of the interventions, it is important to have information on the systemic effects of the implant. C-Reactive Protein (CRP) has been used for monitoring of infection and inflammatory response in clinical settings. Chromogranin A (CGA) can also be used in a similar manner and might provide more accurate results to observe the level of inflammation [18]. As a possible way of observing metallic implant integration *in vivo*, we present a continuous monitoring procedure of implant systemic effects by characterization of animal blood samples with High Pressure Liquid Chromatography (HPLC) and subsequent protein sequencing. Elaboration of this method can be used to evade regular end-point histological analysis. Histological cutting of metallic implants is a long, cumbersome and expensive process and can be only undertaken at specific time points. Because of this reason, well-designed blood tests providing robust information about the implant health would be possible routes to decrease animal experiments as mandated by the recent EU rules concerning animal experiments.

The methods presented here can be used to improve the performance of metallic implants via functionalization or to have an alternative way of monitoring the existing implants.

## Protocol

### 1. Preparation of Micropore Gradients in Macroporous Metallic Implants

1. Clean the implants (such as implants made of medical grade titanium beads with a size range of 400-500 µm, Neyco SAS, France) with ethanol and then sonicate in acetone for 15 min.
2. Design and manufacture Teflon molds according to the implant size and shape (For standard experiments, cylindrical molds of 1.5 cm diameter with a height of 2 cm are used). Molds should be modular, so that the certain parts can be removed during extraction. Such a mold design ensures the control over the extraction process by forcing the movement of the extraction fluid in a directed manner.
3. For tubular implants designed to replace trachea, the structure should be composed of three pieces: i) a bottom part to determine the size of the implant, ii) a mandrel and iii) an outer core which is removable. This way, the pore size gradient can be formed from outside towards inside.
4. Prepare the synthetic polymer (PLLA) solution: For freeze/extraction PLLA solution needs to be prepared in a binary mixture of dioxane and water (87:13%, v:v).
5. Heat the mixture to 60 °C in order to obtain a homogenous solution. 60 °C selected as it is the higher limit of the temperature resistance for the precision glass syringes that has to be used for the introduction of the solution into the implants.
6. If high concentration (≥6%), high molecular weight PLLA solutions are used, introduce the solution into the implant after heating immediately. Otherwise gelation of the solution occurs without full immersion.
7. Calculate the volume of the necessary polymer solution with respect to the porosity of the implant, for accuracy change in the volume of the frozen solution can be taken into account.
8. Introduce the solution into the implants with precision glass syringes with 0.1 µl accuracy. The lower limit for the polymer concentration is 3% for reproducible pore gradient formation whereas it becomes hard to obtain homogenous distribution in the thick samples above 6%. However, for specific applications other concentrations can be used.
9. Freeze the samples either directly at -80 °C or with a prior incubation period of 30 min at room temperature. Freezing conditions determine partially the pore formation, thus the freezing conditions can be adjusted according to the porosity aimed. Keep the samples overnight at -80 °C.

 

10. Extraction: Immerse the implants in 80% pre-chilled EtOH. Carry out the extraction at -20 °C overnight. To obtain porosity gradients, remove all the mold parts except the mandrel for the tubular implants and all the parts except the bottom part for disk shaped implants. Use a pre-chilled scalpel for easier separation of the mold.
11. After extraction at -20 °C overnight [19], remove the remaining mold parts and air dry the implants. For characterization of the overall porosity of the structure mercury porosimeter analysis is necessary. Mercury Porosimeter measurements showed distinct peaks that correspond to the pores on the both sides of the implant and the smaller interdispersed pores. However the more crucial data is the difference between the porosities of intraluminal and extraluminal surfaces, which can be analyzed by Image J for pore size distribution with a scanning electron microscope (SEM) [20]. For verification of the pore gradient, freeze-fracture the samples and observe the cross-section with SEM.
12. Due to the open porous nature of the implants used, and the light reflecting capacity of Titanium, it is possible to do z-stacks of labeled cells within the porous implants. Label the cells with PKH26 or Calcein-AM and visualize the implants with confocal laser microscopy.

## 2. Surface coating of Porous Metallic Implants with Collagen/Alginate multilayers

1. For build-up of multilayers, highest reproducibility is obtained with dipping robots. However, if a dipping robot is not available these steps can be done manually.
2. Use medical grade collagen type I and sodium alginate. The optimized concentrations are 0.5 g/L for each in 150 mM NaCl in citrate buffer at pH 3.8.
3. Dissolve the collagen solution overnight to ensure the homogeneity of the solution. Acidic pH of 3.8 is necessary for stable build-up of the layers as the structure is unstable before crosslinking in neutral pH.
4. Deposit the layers by a dipping robot system by immersing the implants into collagen and alginate solutions alternatively. Deposition time is 15 min for each subsequent layer. Rinse the structure in between deposition steps with 150 mM NaCl at pH 3.8 for 5 min.
5. Design specific holder for utilization of the implants with dipping robots used in polyelectrolyte multilayer production. Deposit the layers on the surface of either titanium only implants or implants modified as described in section 1.
6. Stabilization of the basement membrane mimic with genipin: Prepare the crosslinking solution in a Dimethylsulfoxide (DMSO)/citrate buffer (150 mM NaCl, pH 3.8) at 1:4 v:v ratio. A wide range of concentrations can be used and 100 mM is adequate for crosslinking. Dissolve genipin first in the DMSO component and add the water component later to avoid clumping.
7. Crosslink the samples by the immersion in the crosslinking solution between 12-24 hr. Afterwards rinse with copious amount of citrate buffer (pH 3.8).
8. After washing steps, sterilize the samples either with UV treatment (30 min) or an antibiotic/antifungal bath (Penicillin/Streptomycin, Fungizone).
9. The main parameters that determine the quality of the basement membrane mimic are its thickness and the diameter of the fibers. Calculate the fiber diameters using Atomic Force Microscopy (AFM) images obtained in contact mode. Dry the samples with a nitrogen flow before imaging. Quantify the thickness of at least 10 fibers per image to determine the average fibril thickness with Image J software.
10. The thickness of the films can be determined by scratch tests using AFM. Dry $(COL/ALG)_{24}$ / COL multilayer films. Use a syringe needle to scratch the film. After localization of the scratch with a light microscope, obtain images with AFM on 10 x 10 $\mu m^2$ surfaces at the boundary of the scratch. Calculate the heights from the profiles obtained with the AFM software, which provides the thickness of the film layer.

## 3. Indirect Monitoring of Implant Integration In Vivo By Analysis of Blood Plasma

1. All the necessary committee approvals should be taken for animal experimentation according to the governing rules for each country [21]. In our case the Guide for the Care and Use of Laboratory Animals (National Research Council, 2010) is followed and the approval of the University of Strasbourg ethic committee is obtained.
2. Carry out the implantation at the target site. The blood monitoring protocol given here was used for tracheal replacement in New Zealand white rabbits of a 15 mm tracheal resection.
3. Following implantation a daily follow-up is necessary such as montioring the general well-being of the animals (healing around the surgical sites, rate of breathing) and recording of their weight.
4. To validate the blood test, use a well-established method such as ELISA tests for blood CRP levels. CRP tests for many animals are available and the specific test used for rabbits is listed in Table 1. Similarly, use western blotting for the determination of CGA levels. Monoclonal anti-CGA antibodies (anti-$CGA_{47-68}$) were used in this protocol.
5. For plasma characterization, obtain blood samples from the auricular veins of the rabbits. Centrifuge at 5,000 rpm for 20 min at 4 °C. Use the supernatant obtained for analysis. In our procedure, these tests are done on a weekly basis, but more frequent tests are also possible.
6. Reverse phase HPLC purification of the Plasma protein content: Extract the rabbit plasma with 0.1% of trifluoroacetic acid (1:1; v:v). Purify the extract by using a Dionex HPLC system (Ultimate 3000; Sunnyvale, CA USA) on a nucleosil reverse-phase 300-5C18-column (4 x 250 mm; particle size 5 µm; porosity, 300 Å).
7. Record the absorbance at 214 and 280 nm. The solvent system used is i)Solvent A: 0.1% (v/v) Trifluoroacetic acid (TFA) in water and ii) Solvent B: 0.09% (v/v) TFA in 70% (v/v) acetonitrile-water.
8. Use a flow rate of 700 µl/min using gradients for elutions. Collect the peak fractions. Concentrate the fractions by evaporation by speed-vacuum application. It is important to stop the speed-vacuum before complete dryness.
9. Correlate the peaks obtained at different time-points over the course of the implantation period. Use the purified peptides that are showing consistent trends during the course of implantation for identification by automatic Edman sequencing.
10. Automatic Edman sequencing of the peptides: Determine the N-terminal sequence of the purified peptides by automatic Edman degradation using a Procise microsequencer. Load the sample to polybrene-treated glass-fibre filters. Next step is the identification of Phenylthiohydantoin-amino acids (Pth-Xaa) by chromatography on a $C_{18}$ column (PTH C-18, 2.1 x 200 mm) [22]. After the sequence is obtained, it can be identified by Blast software using SWISS-Prot database.

 

## Representative Results

### Formation of pore gradients

By changing the concentration of the PLLA solution, it is possible to control the size of the pores on the extraluminal side of the implants. Pore size and shape was significantly affected by the presence of titanium implants (**Figure 1a, b**). Pore sizes ranged from 40-100 µm and utilization of lower concentrations resulted in smaller pores. Whereas, in the intraluminal side pore size was governed by the restricted extraction and was around 9 µm [23], less than the average size of fibroblasts. By adding an incubation step at room temperature a double porous structure, where the pore walls of the bigger pores have their own porosity can be obtained. This feature is important for thick implants, as it would facilitate the gas and nutrient movement (**Figure 1c**).

### Nanofibrillar basement membrane-mimic formation

After the pore gradient was formed, it is possible to add the Collagen/Alginate film layer on top of the structure (**Figure 2**). This film layer is stable on top of the PLLA foam and it can also be maintained on the surface in the absence of the foam (**Figure 3a, b**). Nanoscale collagen fibers form as the film layer grows (**Figure 3c**). The growth of the film is exponential, thus a thick film of several hundred nanometers can be obtained (**Figure 3d**).

### Analysis of blood plasma with HPLC and subsequent sequencing after implantation

Porous titanium implants integrate with the host tissue and are completely filled between 4-6 weeks in vivo (**Figure 4**). However, continuation of this process can lead to restenosis and in the presence of the pore gradient due to the PLLA structure, no fibroblast presence was observed after 6 weeks of implantation [20]. During this period HPLC analysis showed distinct peaks that fluctuate during the time course of implantation. The peak fractions of interest are sequenced and determined to be alpha and beta haemoglobin ½ chains (**Figure 5**), which had shown a similar trend with CRP readings.

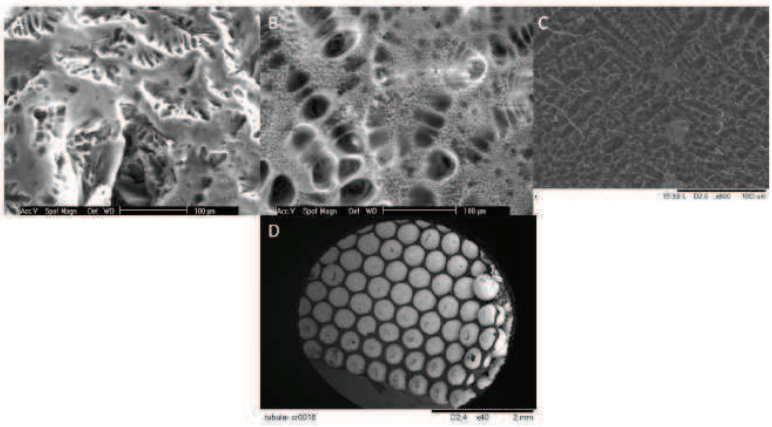


**Figure 1. Method of pore gradient formation.** Preparation ofporous PLLA foams via freeze-extraction method. SEM micrographs **(A)** without macroporous titanium implants (outer) **(B)** with macroporous titanium implants (outer) **(C)** with macroporous titanium implants (inner) . Presence of the implants changed the pore morphology. **(C, D)** Same process can be applied to tubular structures to obtain pore gradients in tubular implants. Click here to view larger figure.

 

jove Journal of Visualized Experiments www.jove.com

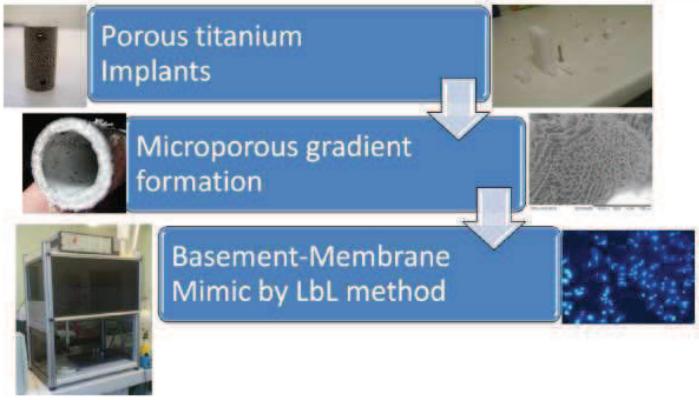


**Figure 2. Scheme of the Multifunctional implant development.** Starting from microbead based porous implants, by addition of a synthetic polymer based foam a pore size gradient can be obtained. Shape of the pore gradient is partially controlled by the structure of the molds. On top of this structure a basement membrane-like structure can be added, which would provide a suitable surface for cell attachment and lining formation in 2D.

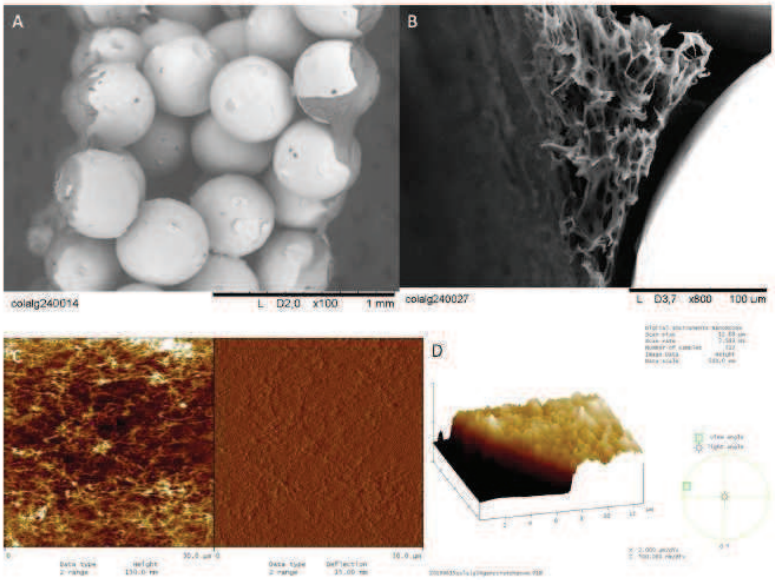


**Figure 3. Nanofibrillar Multilayer formation on titanium implants as a basement membrane mimick**. Thick Collagen/Alginate multilayers can be formed specifically on the surface of **(A)** Titanium only implants (with an average bead size of 400-500 µm) **(B)** Titanium/PLLA foam hybrids. This surface (~1 µm thick) provides a substrate for the attachment and proliferation of the endothelial cells **(C)** The nanofibrillar nature of the multilayers is characterized by AFM analysis (Scan area: 30 µm x 30 µm) **(D)** thickness of the multilayers is determined by scratch test. Click here to view larger figure.

 

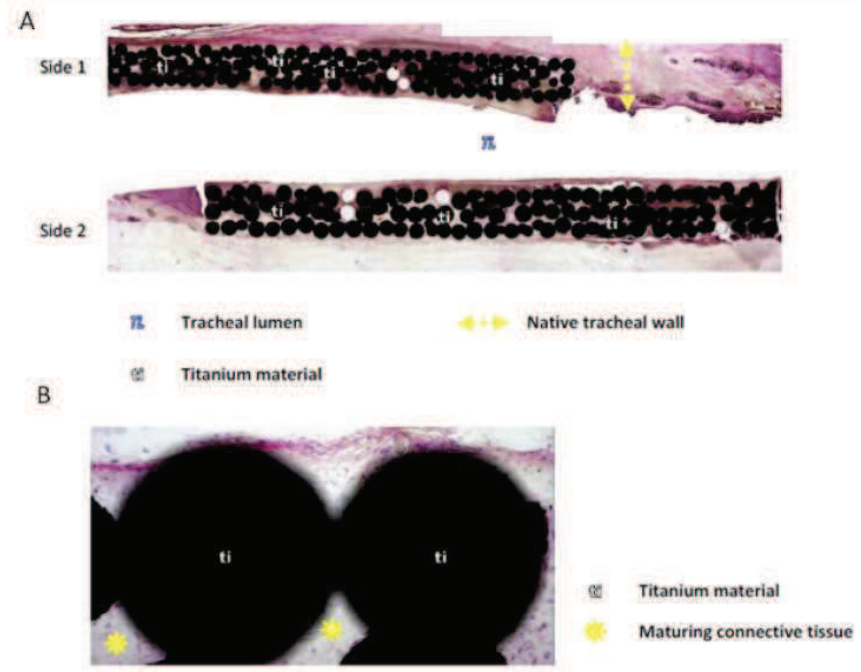


**Figure 4. Integration of porous titanium implants in-vivo in rabbits**. Haemotoxylin & Eosin staining of the explanted implant cross-sections **(A)** The porous areas can be completely filled within a period of 4-6 weeks in vivo **(B)** The tissue within the pores is a mature connective tissue with a good level of vascularization.

 

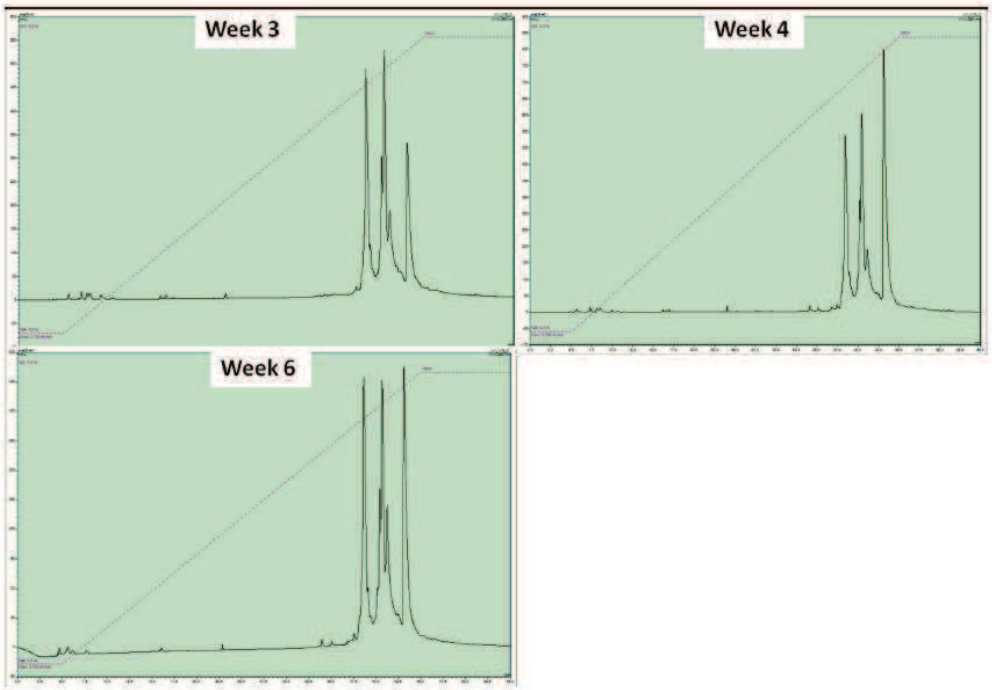


**Figure 5. Monitoring of protein content of plasma over the course of an implantation by HPLC and subsequent sequencing.** The representative HPLC curves show the peaks obtained from blood samples of animals after 3, 4 and 6 weeks of implantation respectively (top left, top right, bottom left). Each peak corresponds to a specific protein. The differences in the peak correspond to relative abundance of a given protein, which can be determined by sequencing (such as α and ß-hemoglobin ½ chains). Click here to view larger figure.

## Discussion

Pore gradients are important tools in interface tissue engineering and the system described here can be used alone or in conjunction with metallic implants to form pore gradient to study cell migration. The system does not necessitate any extra setting or extra equipment except a chemical fume hood to handle organic solvents, thus it can be applied in biology laboratories. Similar polymers such as Poly(glycolic acid) (PGA), Poly(lactic-co-glycolic) acid (PLGA) and Poly(caprolactone) (PCL) can be used with slight modifications. Other macroporous structures that would not dissolve in organic solvents can also be used. For obtaining smaller pore sizes (at nanoscale) on one surface, an additional thin nanoporous film layer formation is also possible. This can be obtained by first putting a dilute solution (1%) of the polymer on the top of the structure in a highly volatile solvent (such as chloroform) and then immediately causing phase separation by immersing in a pure ethanol solution. This way a co-culture system which is based only one material can be obtained.

The teflon mold design is crucial for the control of the pore size as the movement of the extraction fluid is determined by this. The movement of the extraction fluid and the rate of exchange between the extraction fluid and the solvent affect the formation of pores. The control can be further improved by application of laminar flow of the extraction fluid through the implant. The amount of extraction liquid is an important parameter and it should be arranged with respect to the amount of polymer used and also with respect to the size of the implant. For cylindrical implants with 2mm thickness and 11 mm diameter formed of 500 µm medical grade titanium beads an extraction bath of 200 ml is necessary. For studying cell migration, PKH26 is a better option for long term migration studies whereas Calcein-AM provides a better observation of cell morphology. Quantification of cell movement in z-direction is an indirect *in vitro* measurement of the control over cellular movement. Also this system can be used with endothelial cells for quantification of *in vitro* vascularization of the implants, either by direct seeding or using standard angiogenesis assays using gel encapsulation [24].

There are several available nanofiber formation methods such as electrospinning or phase separation, but electrospinning of collagen is generally considered to denature collagen fibrils. Utilization of a polyelectrolyte based structure ensures the prevention of denaturation while providing the necessary fibrillar structure with high level of precision. Also LbL methods are easier to adapt for complex implant shapes. Film layers on porous structures are simple methods to develop transwell-like assays with more control over the interactions between the cellular components. It is possible to observe with confocal microscopy the top layer on the implant. This can be used to observe the interaction of relevant primary cells with the multilayers in contact with the implant such as epithelial cells or endothelial cells. Either isolated [25] or commercially

 

available cells can be used. This film layer provides a surface where an inner lining for a tubular organ can be developed. For example, in this specific case the aim was to develop an artificial membrane for trachea, and this structure was shown to be suitable for respiratory epithelium [23].

Thickness of the layer is set at a level where the film is thick enough to act as a barrier (24 bi-layers). In both titanium only and titanium/PLLA implants, due to the hydrophobicity of the substrate a relatively flat film layer can be formed on the implants, where the pores contribute to the stability of the interface between the structure and the newly formed film layer. Among the available crosslinking methods, genipin crosslinking is the most suitable for animal experimentations. Other crosslinking methods such as glutaraldehyde, EDC/NHS can also be used, but they generally result in less cell attachment. Another possibility is to use photocrosslinkable collagen [26].

Protein sequencing is a promising method for implant monitoring, as it might provide more in-depth understanding. According to the nature of the proteins obtained, it is possible to infer the systemic effects of the implantation and also closely monitor possible infections which are especially important for cases where the implant is not in a sealed area, such as in the case of tracheal implants. Early detection of infections can lead to prevention of infection-related complications in a timely manner. The HPLC profile can provide more information compared to single characterization of a given protein such as CRP or CGA as several peaks with several proteins of interest can be obtained with this method. For example, alpha and beta haemoglobin ½ chains for rabbits with tracheal implants have shown similar trends with CRP readings in our full tracheal replacement model. Such versatility would provide a venue for determination of minute systemic effect with great accuracy with the improvement of the techniques described.

## Disclosures

NE Vrana is an employee of Protip SAS.

## Acknowledgements

Authors would like to thank Dr. Andre Walder and Nicolas Perrin for manufacturing titanium implants, K. Benmlih for the build-up of the Teflon molds and Dr. G. Prevost for his help with animal experiments. We also acknowledge the Region Alsace and PMNA (Pole Materiaux et Nanosciences d'Alsace) for financial contribution.

## References

1. Hollister, S.J. Porous scaffold design for tissue engineering. *Nat Mater.* **4**, 518-524, doi:10.1038/nmat1421 (2005).
2. Ryan, G., Pandit, A., & Apatsidis, D.P. Fabrication methods of porous metals for use in orthopaedic applications. *Biomaterials.* **27**, 2651-2670, doi:10.1016/j.biomaterials.2005.12.002 (2006).
3. Schultz, P., Vautier, D., Charpiot, A., Lavalle, P., & Debry, C. Development of tracheal prostheses made of porous titanium: a study on sheep. *European Archives of Oto-Rhino-Laryngology.* **264**, 433-438, doi:10.1007/s00405-006-0195-7 (2007).
4. Janssen, L.M., *et al.* Laryngotracheal reconstruction with porous titanium in rabbits: are vascular carriers and mucosal grafts really necessary? *Journal of Tissue Engineering and Regenerative Medicine.* **4**, 395-403, doi:10.1002/term.254 (2010).
5. Li, J.P., *et al.* Bone ingrowth in porous titanium implants produced by 3D fiber deposition. *Biomaterials.* **28**, 2810-2820, doi:10.1016/j.biomaterials.2007.02.020 (2007).
6. Schultz, P., *et al.* Polyelectrolyte multilayers functionalized by a synthetic analogue of an anti-inflammatory peptide, alpha-MSH, for coating a tracheal prosthesis. *Biomaterials.* **26**, 2621-2630, doi:10.1016/j.biomaterials.2004.06.049 (2005).
7. Müller, S., *et al.* VEGF-Functionalized Polyelectrolyte Multilayers as Proangiogenic Prosthetic Coatings. *Advanced Functional Materials.* **18**, 1767-1775, doi:10.1002/adfm.200701233 (2008).
8. Mills, R.J., Frith, J.E., Hudson, J.E., & Cooper-White, J.J. Effect of Geometric Challenges on Cell Migration. *Tissue Engineering Part C-Methods.* **17**, 999-1010, doi:10.1089/ten.tec.2011.0138 (2011).
9. O'Brien, F.J., Harley, B.A., Yannas, I.V., & Gibson, L.J. The effect of pore size on cell adhesion in collagen-GAG scaffolds. *Biomaterials.* **26**, 433-441, doi:10.1016/j.biomaterials.2004.02.052 (2005).
10. Karageorgiou, V. & Kaplan, D. Porosity of 3D biomaterial scaffolds and osteogenesis. *Biomaterials.* **26**, 5474-5491, doi:10.1016/j.biomaterials.2005.02.002 (2005).
11. Budyanto, L., Goh, Y.Q., & Ooi, C.P. Fabrication of porous poly(L-lactide) (PLLA) scaffolds for tissue engineering using liquid - liquid phase separation and freeze extraction. *J Mater Sci: Mater Med.* **20**, 105-111, doi:10.1007/s10856-008-3545-8 (2009).
12. Kim, H.J., Huh, D., Hamilton, G., & Ingber, D.E. Human gut-on-a-chip inhabited by microbial flora that experiences intestinal peristalsis-like motions and flow. *Lab Chip.* **12**, 2165-2174, doi:10.1039/c2lc40074j (2012).
13. Huh, D., *et al.* Reconstituting Organ-Level Lung Functions on a Chip. *Science.* **328**, 1662-1668, doi:10.1126/science.1188302 (2010).
14. Chaubaroux, C., *et al.* Collagen-Based Fibrillar Multilayer Films Cross-Linked by a Natural Agent. *Biomacromolecules.* **13**, 2128-2135, doi:10.1021/bm300529a (2012).
15. Huang, Y., Siewe, M., & Madihally, S.V. Effect of spatial architecture on cellular colonization. *Biotechnology and Bioengineering.* **93**, 64-75, doi:10.1002/bit.20703 (2006).
16. Kirkpatrick, C.J., Fuchs, S., & Unger, R.E. Co-culture systems for vascularization - Learning from nature. *Advanced Drug Delivery Reviews.* **63**, 291-299, doi:10.1016/j.addr.2011.01.009 (2011).
17. Lavalle, P., *et al.* Dynamic Aspects of Films Prepared by a Sequential Deposition of Species: Perspectives for Smart and Responsive Materials. *Advanced Materials.* **23**, 1191-1221, doi:10.1002/adma.201003309 (2011).
18. Zhang, D., *et al.* Serum concentration of chromogranin A at admission: An early biomarker of severity in critically ill patients. *Annals of Medicine.* **41**, 38-44, doi:10.1080/07853890802199791 (2009).
19. Goh, Y. & Ooi, C. Fabrication and characterization of porous poly(l -lactide) scaffolds using solid - liquid phase separation. *Journal of Materials Science: Materials in Medicine.* **19**, 2445-2452 (2008).

 

20. Vrana, N.E., *et al.* Modification of macroporous titanium tracheal implants with biodegradable structures: Tracking in vivo integration for determination of optimal in situ epithelialization conditions. *Biotechnology and Bioengineering.* **109**, 2134-2146, doi:10.1002/bit.24456 (2012).
21. Dupret-Bories, A., *et al.* Development of surgical protocol for implantation of tracheal prostheses in sheep. *J Rehabil Res Dev.* **48**, 851-864 (2011).
22. Gasnier, C., *et al.* Characterization and location of post-translational modifications on chromogranin B from bovine adrenal medullary chromaffin granules. *Proteomics.* **4**, 1789-1801 (2004).
23. Vrana, N.E., *et al.* Hybrid Titanium/Biodegradable Polymer Implants with an Hierarchical Pore Structure as a Means to Control Selective Cell Movement. *PLoS ONE.* **6**, e20480, doi:10.1371/journal.pone.0020480 (2011).
24. Nakatsu, M.N., Davis, J., & Hughes, C.C.W. Optimized Fibrin Gel Bead Assay for the Study of Angiogenesis. *J Vis Exp.* e186, doi:doi:10.3791/186 (2007).
25. Ganguly, A., Zhang, H., Sharma, R., Parsons, S., & Patel, K.D. Isolation of Human Umbilical Vein Endothelial Cells and Their Use in the Study of Neutrophil Transmigration Under Flow Conditions. *J Vis Exp.* e4032, doi:doi:10.3791/4032 (2012).
26. Dong, C.-M., *et al.* Photomediated crosslinking of C6-cinnamate derivatized type I collagen. *Biomaterials.* **26**, 4041-4049, doi:10.1016/j.biomaterials.2004.10.017 (2005).

 

# 4.2. Développement d'une prothèse hybride avec gradient de porosité, étude *in vitro*, Article 3

## 4.2.1. Introduction à l'article 3

Nous avons vu dans le chapitre précédent que nos recherches se sont axées sur la modification de la prothèse de trachée en titane poreux afin d'améliorer l'intégration aux tissus. Notre équipe a développé un système hybride composé de la prothèse de trachée en titane macroporeux associée à un polymère microporeux biodégradable. Cette matrice de polymère doit avoir un gradient distinct de porosité en accord avec la croissance et la migration de différents types cellulaires. Elle constitue un environnement adapté à l'activité cellulaire. Comme nous avons pu le constater lors des expérimentations animales précédemment décrites (Dupret-Bories et al., 2011; Schultz et al., 2007; Schultz et al., 2002), pour qu'un implant trachéal soit fonctionnel, il faut un épithélium respiratoire contigu dans la lumière de l'implant (tapis de monocouche cellulaire). Une porosité inférieure au micromètre au niveau de la lumière permettrait la colonisation la face endoprothétique par des cellules épithéliales ensemencées, le diamètre d'une cellule ciliée humaine étant de 4 à 5 µm. Ainsi, la compétition entre différents tissus peut être contrôlée. Avec ce gradient de porosité on obtient une surface optimale pour la croissance d'un épithélium linéaire, crucial pour la fonctionnalité de la prothèse.

La porosité de la prothèse en titane nue permet la migration des fibroblastes de l'extérieur vers la lumière, mais ne les stoppe pas au niveau endoluminal. La cellule fibroblastique humaine possède une longueur de 20 à 100 µm avec une largeur de 5 à 10 µm, alors que la taille des pores des prothèses en titane poreux est constante et de l'ordre de 150 µm. Ceci peut conduire à une prolifération exophytique endoprothétique de fibroblastes avec obstruction de la lumière (phénomène observé chez les rats et les brebis implantée sans tube de silicone).

Le but est d'obtenir, avec l'ajout du polymère, un gradient de porosité qui permettrait de contrôler la migration des fibroblastes et notamment de bloquer leur migration et prolifération vers la lumière.

L'article 3 décrit la technique utilisée pour la création de l'implant hybride titane poreux/polymère PLLA et les résultats sur la colonisation cellulaire *in vitro*.

## 4.2.2. Résumé de l'article 3

Afin d'améliorer le taux de réussite d'implantation des biomatériaux, il est important d'améliorer leurs réactions face aux tissus environnants. *In vivo,* la prolifération incontrôlée de cellules inflammatoires et de fibroblastes est un facteur majeur de risque d'échec que l'on peut améliorer en modifiant la porosité des implants. Nous décrivons dans cet article un système hybride composé d'une structure de titane macroporeux remplie d'un polymère biodégradable microporeux. Cette matrice de polymère a la capacité de présenter un gradient de porosité adapté à la migration et prolifération de différents types cellulaires (fibroblastes et cellules épithéliales). La principale application clinique de cette prothèse hybride sera la prévention de la sténose due à la migration et prolifération excessive de fibroblastes dans la lumière des prothèses de trachée en titane macroporeux.

**Méthodologie et principaux résultats** : Les pores d'une prothèse en titane poreux composée de microbilles de titane ont été remplis d'une solution obtenue à partir de poly(acide L-lactique) (PLLA) selon la technique de congélation-extraction. Des gammes de porosité distinctes ont été obtenues entre la surface interne et la surface externe de la prothèse, caractérisées par une analyse des images acquises en microscopie électronique et par mesure de porosimètrie au mercure (valeurs moyennes de pores de 9.8 microns pour la face interne, 36.7 pour la face externe). A la surface, une fine couche de PLLA a été ajoutée afin d'optimiser la prolifération de cellules épithéliales, ce qui a été confirmé par l'utilisation de cellules respiratoires humaines. Pour tester l'hypothèse que l'addition de PLLA à l'implant en titane permet un contrôle de la migration cellulaire des fibroblastes, des fibroblastes marqués par la sonde fluorescente rouge PKH26 ont été ensemencés sur les implants en titane poreux nu et sur implants hybrides (titane poreux/PLLA). La migration cellulaire a été observée en microscopie confocale : en une semaine les cellules avaient migré rapidement et plus en profondeur dans l'implant en titane poreux nu comparé à l'implant hybride.

**Conclusions :** Ces expérimentations réalisées *in vitro* ont mis en évidence la capacité de l'implant hybride à guider la migration des différents types de cellules, notamment celles

qui seront en contact lors des implantations ultérieures. Globalement ce système est capable de nous permettre un contrôle dans l'espace et dans le temps de la migration des cellules grâce à un gradient de porosité allant du macroporeux au nanoporeux à travers la paroi de l'implant. Les propriétés mécaniques de la prothèse restent inchangées puisqu'elles sont essentiellement conférées par la structure en titane de l'implant. Cela rend possible le design d'une structure polymérique indépendamment des caractéristiques mécaniques liées à la structure polymère. Ce type d'implant hybride peut être utile pour d'autres domaines d'application comme en orthopédie par exemple.

## 4.2.3. Article 3

OPEN ACCESS Freely available online

PLoS one

# Hybrid Titanium/Biodegradable Polymer Implants with an Hierarchical Pore Structure as a Means to Control Selective Cell Movement

**Nihal Engin Vrana[1], Agnès Dupret[1,3], Christelle Coraux[4], Dominique Vautier[1,2], Christian Debry[1,3], Philippe Lavalle[1,2]***

**1** Institut National de la Santé et de la Recherche Médicale, INSERM Unité 977, Strasbourg, France, **2** Faculté de Chirurgie Dentaire, Université Louis Pasteur, Strasbourg, France, **3** Hôpitaux Universitaires de Strasbourg, Hôpital de Hautepierre, Service Otorhinolaryngologie & Chirurgie Cervicofaciale, Strasbourg, France, **4** Institut National de la Santé et de la Recherche Médicale, INSERM Unité 903, Reims, France

## Abstract

In order to improve implant success rate, it is important to enhance their responsiveness to the prevailing conditions following implantation. Uncontrolled movement of inflammatory cells and fibroblasts is one of these in vivo problems and the porosity properties of the implant have a strong effect on these. Here, we describe a hybrid system composed of a macroporous titanium structure filled with a microporous biodegradable polymer. This polymer matrix has a distinct porosity gradient to accommodate different cell types (fibroblasts and epithelial cells). The main clinical application of this system will be the prevention of restenosis due to excessive fibroblast migration and proliferation in the case of tracheal implants.

*Methodology/Principal Findings:* A microbead-based titanium template was filled with a porous Poly (L-lactic acid) (PLLA) body by freeze-extraction method. A distinct porosity difference was obtained between the inner and outer surfaces of the implant as characterized by image analysis and Mercury porosimetry (9.8±2.2 μm vs. 36.7±11.4 μm, $p \leq 0.05$). On top, a thin PLLA film was added to optimize the growth of epithelial cells, which was confirmed by using human respiratory epithelial cells. To check the control of fibroblast movement, PKH26 labeled fibroblasts were seeded onto Titanium and Titanium/PLLA implants. The cell movement was quantified by confocal microscopy: in one week cells moved deeper in Ti samples compared to Ti/PLLA.

*Conclusions:* In vitro experiments showed that this new implant is effective for guiding different kind of cells it will contact upon implantation. Overall, this system would enable spatial and temporal control over cell migration by a gradient ranging from macroporosity to nanoporosity within a tracheal implant. Moreover, mechanical properties will be dependent mainly on the titanium frame. This will make it possible to create a polymeric environment which is suitable for cells without the need to meet mechanical requirements with the polymeric structure.

**Citation:** Vrana NE, Dupret A, Coraux C, Vautier D, Debry C, et al. (2011) Hybrid Titanium/Biodegradable Polymer Implants with an Hierarchical Pore Structure as a Means to Control Selective Cell Movement. PLoS ONE 6(5): e20480. doi:10.1371/journal.pone.0020480

**Editor:** Christophe Egles, Université de Technologie de Compiègne, France

**Received** March 12, 2011; **Accepted** April 27, 2011; **Published** May 26, 2011



**Funding:** The study was funded by Région Alsace and Pôle Matériaux et Nanosciences d'Alsace (PMNA). The funders had no role in study design, data collection and analysis, decision to publish, or preparation of the manuscript.

**Competing Interests:** The authors have declared that no competing interests exist.

* E-mail: philippe.lavalle@inserm.fr

## Introduction

Cell containing biomedical devices such as biosensors, tissue engineering products or cellularized implants must be able to segregate cells they enclose and control their behaviour [1,2]. This is especially important when the target area's functionality depends on two or more types of cells which are present in a certain orientation. For example, for proper functioning of a tracheal implant, a respiratory epithelium lining on its lumen is essential. This necessitates a smooth implant surface with a porosity smaller than cell size that would allow the migration of epithelial cells from anastomosis sites [3,4]. On the other hand, if a biodegradable material is used, the bulk of the implant should be populated with connective tissue via migration before extensive degradation, to prevent the mechanical failure or collapse of airway upon implantation. Incorporation of the necessary properties for accommodating these two requirements is challenging.

The primary design concern for implants is their responsiveness to the cell types which are necessary for the functionality of the target tissue. However, inflammation process and movement of fibroblasts during the healing process, which are common themes of mammalian response to foreign bodies, must also be taken into account [5]. Implant designs which would direct and control these body reactions would provide the functional parts of the implant with a better environment for healing.

Microbead based porous titanium technology allows to create open macroporous structures by using medical grade titanium microbeads. This system is in clinical trial stage in several implant related technologies. Our current efforts are concentrated on development of tracheal, dental, and bone implants by using this

technology [6,7,8]. The open pore structure of the porous titanium together with its mechanical properties and biocompatibility makes it an ideal implant material for tracheal replacement. The previous efforts in tissue engineering of trachea generally faced up difficulties due to inferior mechanical properties and inflammatory reactions. Moreover most surfaces such as silicone are not good for epithelial cell growth and also prevent vascularization which decreases the functionality of the overall implant [9,10]. Our previous in vivo experiments with rats and sheep [7,11] gave promising results but the recurring problem of restenosis, which is the overgrowth of connective tissue, needs to be solved to ensure long-term success of the implant (Figure 1). Extensive restenosis within the lumen must be prevented since it decreases the size of the lumen leading to airway obstruction. For this aim we propose development of a new titanium/biodegradable polymer hybrid material, which can be described as a tissue engineering scaffold within a mechanically stable titanium template. By this method the formation of new diverse tissue can be limited to certain areas of the implant. Such strategy is more appropriate than a total renewal that would compromise mechanical stability since degradation can outpace tissue formation. Moreover, competition for a certain area of the implant such as the lumen between different growing tissues, that results most of the time in population by only one invasive cell type such as fibroblasts, will be controlled [12].

Freeze-Extraction is a suitable, easy to scale-up method for developing porous polymer structures without residual solvent problem [13]. It is a thermally induced phase separation technique, in which open, interconnected pores are formed via extraction of the frozen solvent (such as dioxane) from frozen polymer solution via a non-solvent (such as ethanol) for the polymer. However, the scaffolds prepared by this method did not have suitable mechanical properties for use in load bearing tissues [14]. But in our case, use of a robust titanium template would ensure the mechanical stability of a full hybrid implant. Also presence of the titanium template allows adjustment of the procedure in a way to obtain porosity gradients without the need to compensate for the associated strength loss.

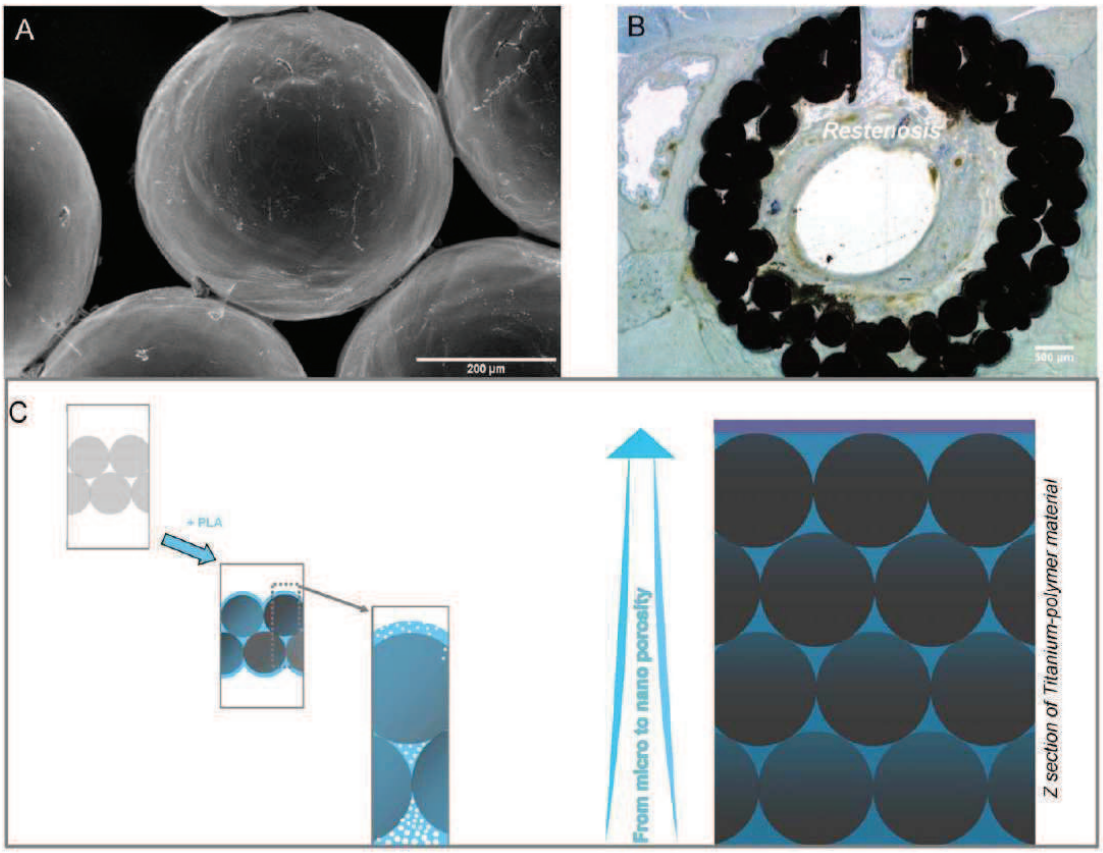


**Figure 1. Occurrence of restenosis and proposed solution.** a) SEM observation displaying microscopic structure of macroporous titanium implants. b) When implanted(with a slice of native trachea left in place, as seen as a hole), tubular macroporous titanium implants are prone to development of restenosis in rats after 1 month of implantation and subsequent decrease in lumen diameter due to the fact that the open porous structure permits excessive movement of fibroblasts and inflammatory cells as observed by histological sections. c) The scheme of proposed hybrid material to control cell movement in both radial (fibroblasts) and longitidunal (epithelial cells) directions.
doi:10.1371/journal.pone.0020480.g001

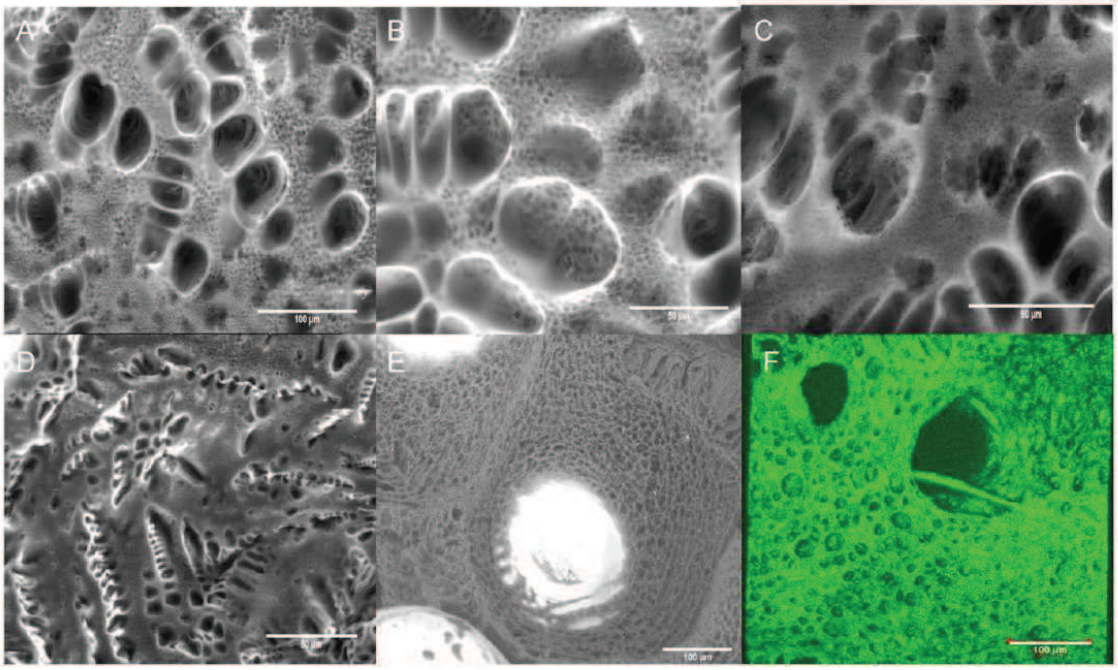


**Figure 2. Pore structure of the hybrid implants.** a–c) ESEM images of the back surface of the Titanium/PLLA hybrid prepared by 6% PLLA solution with a pre-gelling step at room temperature; distribution of small pores in between big pores due to the pregelling step is visible. d) Pore structure of the constructs when only PLLA was used. e) Coverage of the titanium beads with porous polymer filling f) 3D reconstruction of the back surface of the Titanium/PLLA hybrid obtained by confocal laser scanning microscopy.
doi:10.1371/journal.pone.0020480.g002

Four main areas can be classified where it is beneficial to have pore gradients : 1) When there is a need to have different cell types which are in contact but yet spatially separated; [15,16] 2) When the two parts of an organ or a junction (such as osteochondral junction) necessitates different properties; [17,18] 3) When there is a need to control the migration rate of cells in a given direction; [19] 4) When it is important to retain cells in a spatial organization, for example to prevent restenosis related to smooth muscle cell movement in blood vessels while keeping the scaffold connected with the rest of the system for fluid and nutrient flow [20].

Here, we define production of an inter-connective, porous biodegradable polymer filling of the macroporous titanium tracheal implants for developing a system that enables fine control of different modes of cell movement in different areas of the implant. The final aim is to prevent fibroblast movement into the lumen for short term and at the same time to provide a suitable surface for the growth and migration of epithelial cells in vivo which are crucial for the functionality of composite tissues. By hindering the movement of the fibroblast, formation of epithelial layer will be promoted. Porous polymer filling was produced by successive use of thermally induced phase separation techniques within molds that directs the process hence permitting formation of pore gradients. A porosity gradient starting at the bottom of the material with macro open pores and turning into micropores that are large enough for cell infiltration was achieved. Then, in the upper part of the materials, these pores turns into lower microlevel ones which would obstruct cellular movement. This would permit fibroblasts to move within the scaffold but it would impede their migration to the upper surface since the average pore size on that face is lower than their size. On top of this structure a thin layer of polymer film either smooth or with nanolevel pores to induce 2D epithelial cell migration was also added.

## Results

The procedure to produce the pore gradient based on two steps. First, the pore gradient between the back and front surfaces was established by porous PLLA formation via freeze-extraction within a confining Teflon mold. The back surface is in direct contact with the extraction medium whereas the front surface is in contact with the Teflon mold which directs the movement of the extraction fluid. At the back, freeze-extraction process produced pores that are big enough to allow cell movement (Figure 2). The shape and the distribution of the pores were dependent on the polymer concentration and the cooling regime. For example a conventional open, interconnected pore structure can be achieved with lower concentrations (4%) and with a faster cooling regime. On the other hand, a high concentration of PLLA (6%) with a pre-gelation (incubation at room temperature) treatment produced a double-porous structure due to the phase separation within the gel body in which smaller pores are interspersed within the walls of bigger pores (Figure 2a–c; 2e). The morphology of the pores were quite similar to those obtained in the absence of Titanium and the Titanium body was totally engulfed by the polymer network (Figure 2e,f).

Analysis of the cross-sections of the PLLA impregnated titanium showed the decrease in the pore size along the cross-section, in

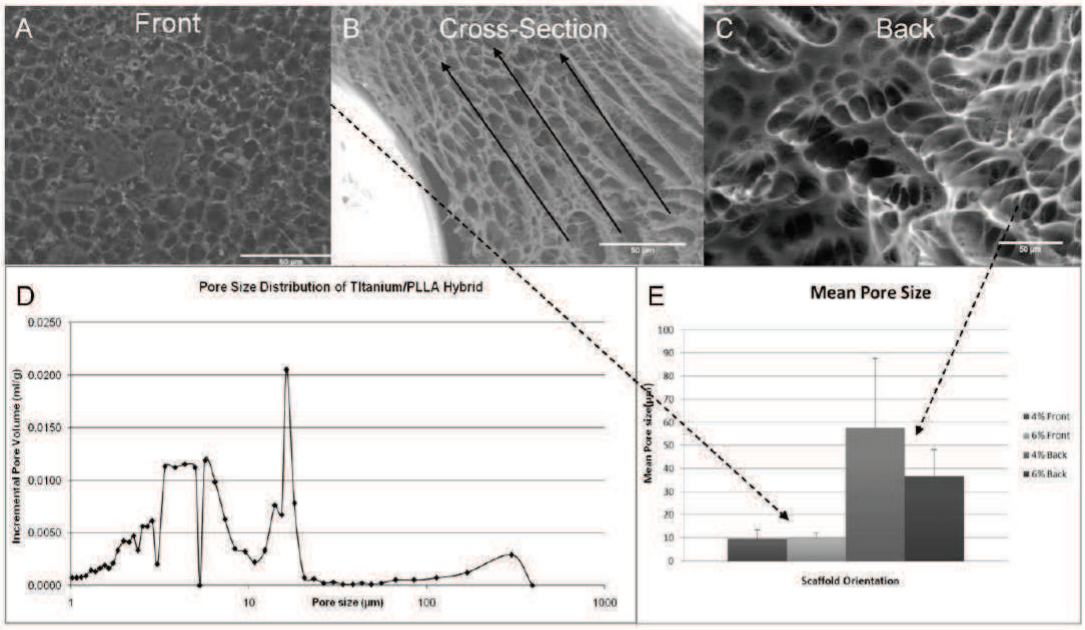


**Figure 3. Pore gradient.** a) Front surface of the hybrid implant with smaller pores. b) Cross-section of the hybrid implant shows the decrease in the pore size in the direction of ethanol in-flow which causes the pore gradient formation c) Back surface of the hybrid implant with bigger pores. d) Pore size distribution for the Titanium/PLLA hybrid; the distribution demonstrated the hierarchical gradient(6% PLLA). e) Difference in mean pore size between two surfaces was consistent in different PLLA concentrations where the front surface is less porous in both cases.
doi:10.1371/journal.pone.0020480.g003

which the pores are interconnected. Fluid movement can be observed in the shape of the pores (Figure 3b). Pore size distribution analysis of the filling shows a multi modal structure due to the preparation conditions (Figure 3 a,c). The difference in the porosity of the both side of the implant was significant which was determined by mercury porosimetry and image analysis (Figure 3 d–e). Mercury porosimetry results showed a 43% porosity for the hybrid system after PLLA impregnation with a primary average porosity of 5.5 µm and a secondary average of 16.4 µm. Moreover there was a distinct peak in the pore size distribution close to the values measured from SEM images which accounts for the highly porous area in the back side.

In the second step, to improve the range of the gradient even further for reasons such as designing a surface with a pore size less than that of epithelial cells (less than 5 µm) and of suitable roughness (<1 µm) [21] for their successful culture, a film formation process on the surface is devised. Films are either formed by conventional solvent casting (non-porous) on the Titanium/PLLA hybrids or by an additional pore formation step to induce surface porosity. A dilute solution of PLLA (1%) in chloroform is applied on to the top surface of the structure for solvent-casting (Figure 4a, b) and in the second case, to induce pore formation, the hybrid is then immersed into ethanol. This step was done immediately after the addition of the PLLA solution and it would cause local precipitation of PLLA and thus pore formation in the film body (Figure 4 c, d). AFM images showed that the obtained surface had a surface average pore size of 836 nm with a wide range of pore size distribution (lower 110 nm, upper 2.9 µm). This porous surface had a higher roughness (Ra = 54.9± 26.5 nm) compared to the solvent cast PLLA (Ra = 4.6±2.8 nm) films but still its surface roughness was below the limit of 1 µm necessary for epithelial cell culture. When the implant was only filled with polymer (no pore forming steps) formed layer followed the contours of the titanium beads (Figure 4e).

Our tests with human respiratory epithelial cells also showed that nanoporous surface was suitable for their culture. The respiratory epithelial cells were able to proliferate and form cell to cell contacts on the hybrid system (Figure 5 a, b). Cellular proliferation on the porous film layers was comparable to that of the transwell membrane, which is the established culturing substrate for these cells (Figure 6a). However presence of the film layer helped the definition of the growth surface for the epithelial cells (Figure 6b), i.e cells stayed on the film layer. On the other hand, when seeded to scaffolds without any film layer the epithelial cells attach to the inplant but cannot form a layer and were observed dissipated into the depth of the scaffold (Figure 6c). It was possible to observe the confluent layers via the macropores between the titanium beads by phase contrast microscopy (Figure S1).

To test the hypothesis that the addition of the PLLA filling can impede cell movement, an aggressive fibroblastic cell line (NIH-3T3) [22] was seeded both on empty titanium and titanium/PLLA hybrids after cell surface was labeled with a non-toxic fluorescent marker (PKH26). The hybrids were placed on culture inserts face-down and the cells were seeded from the back. After 1 week of culture, cell migration was observed with confocal microscopy and the depth of the cell movement was determined (Figure 7). Cells moved considerably deeper into the titanium only implants (350 µm compared to 200 µm in titanium/PLLA hybrids) and

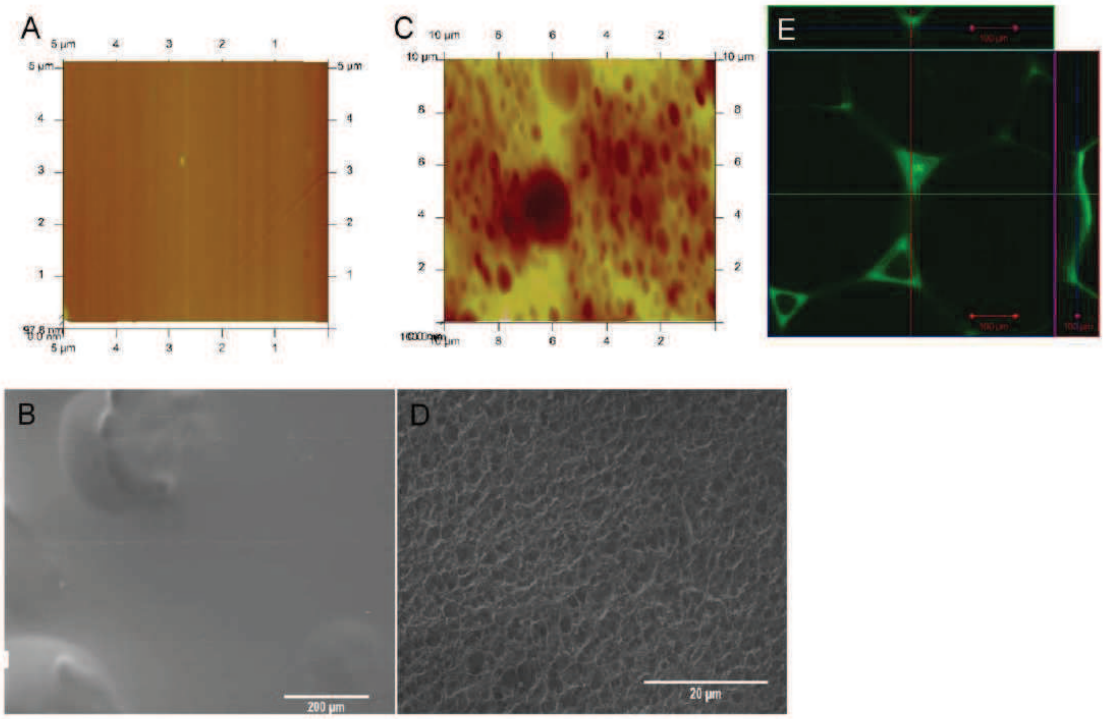


**Figure 4. Surface nanoporous film layer.** AFM and SEM images of a–b) solvent cast PLLA film and c–d) nanoporous top layer. A defined surface was obtained with both methods on top of Titanium/PLLA hybrid system. e) Confocal images of PLLA solvent casted on empty Titanium scaffolds. Solvent casting results in uniform PLLA distribution between the bead while the top layer follows the contour of the beads, whereas after freeze-extraction and film formation; a thin layer of polymer (~4 µm) was on top of a body of porous PLLA covering the titanium beads.
doi:10.1371/journal.pone.0020480.g004

the depth where the highest number of cells was present was also deeper (~150 µm compared to ~100 µm) (Figure 8a). The proliferation assays showed that cells grew more on PLLA/titanium hybrid compared to pure titanium, (Figure 8b). Moreover, the number of cells at the bottom layer of the implant was significantly less on Titanium/PLLA hybrids compared to pure titanium which showed that even though movement of the cells through PLLA is possible, it is slower compared to empty titanium (Figure 8 c,d).

## Discussion

In the area of trachea tissue engineering, there are two main challenges that needs to be overcome. First one is to obtain a collapse-resistant tubular structure tube that would enable the passage of air and the second one is the coverage of the inner surface of this tube with functional respiratory epithelium. In the body, the collapse resistance was provided by c-shaped cartilage rings, thus a considerable part of tracheal replacement efforts is focused on regeneration of this cartilaginous part [23]. However, the only function of these rings is the prevention of the tube's collapse, so the main requirements of the replacement are purely mechanical. But, the necessity of the epithelial layer inside imposes a vascular support beneath, thus the integration of the implant with the vasculature of the body becomes an important determinant [24]. The open porous structure of titanium is excellent for tissue ingrowth, but it lacks the ability to control the extent of the ingrowth. The design presented in this study provides the means to control the incoming fibroblast and inflammatory cell movement with a biodegradable scaffold, which would provide the necessary time for the migration of the epithelial cells from the anastomosis sites [25]. For obtaining a defined porosity gradient in the polymer body, the extraction process has been controlled by directing the inflow of the ethanol with a Teflon mold which resulted in a more porous back surface and a less porous front surface. This structure was clearly apparent in SEM images and results in slowing down of fibroblast movement. Moreover, in the double porous structure obtained the smaller pores would retard the movement of fibroblastic cells but provide large scale fluid flow thus enabling the nurturing of the cells while they are moving.

The ability of epithelial cells to migrate and to form a pseudostratified epithelium on the surface of the implant is limited and generally full epithelialization is never observed [26]. Cognizant of the necessity of seeding epithelial cells prior or after implantation, the current design contains a nanoporous structure providing a feasible surface for epithelial cell migration and culture. The nanoporosity would not hinder the movement of the epithelial cells, but can improve the degradation and finally would provide the route for vascularization of the top layer. Epithelial cells were able to grow on this surface and form cell-cell contacts on their way to forming an epithelial barrier.

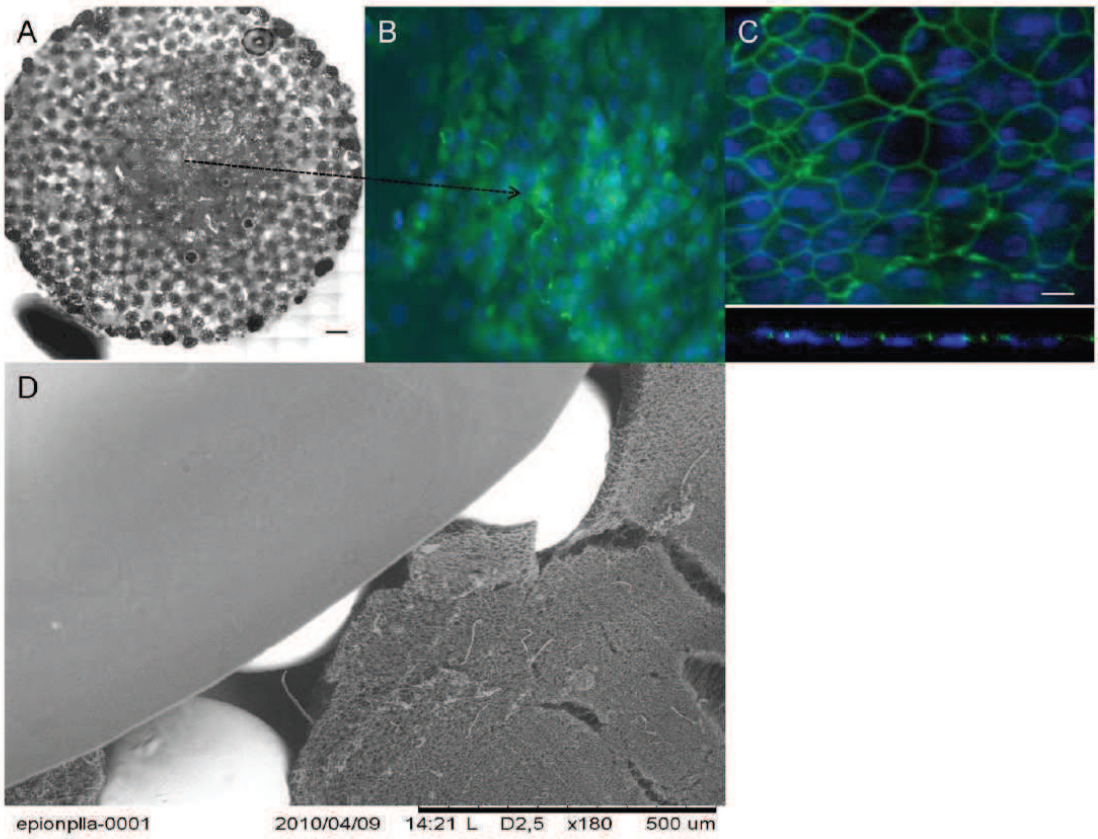


**Figure 5. Overall structure of the hybrid implant and epithelialization.** a) Collation of a full surface of a circular PLLA/Ti hybrid implant, seeded with freshly isolated Human respiratory epithelial cells isolated from nasal polyps(Scale bar: 500 μm). c) DAPI and anti-ZO1 stainings showed monolayer formation on the hybrid implant surface (Day 19). c) Confocal images on x–y plane and Z-section confirms the development of strong cell-cell contacts. d) SEM image of the overall hybrid structure, showing the titanium beads, the micropous body and the top film layer.
doi:10.1371/journal.pone.0020480.g005

The next step in this aspect of the study is to differentiate the epithelial cells by air/liquid interface culture [27].

Change of the pore structure not only affected the cell movement but also had a slight effect on the proliferation: cells in the hybrid scaffold proliferated more. This might be due to the fact that the slowing down of cell movement had triggered proliferation or due to the increased amount of accessible surface area due to the presence of polymer. The open pores of the empty titanium are too large for cells to cover immediately, which would also explain the difference.

The next step would be testing the current system under in vivo conditions, to see whether it will hinder the movement of fibroblasts and decrease restenosis while providing enough time for slower epithelial cells to populate the inner lumen surface. This would dramatically improve the functionality of the implant. The porous structure would allow wide scale integration of the implant, as the cells can go through all the thickness of the implant over long implantation periods (together with the effect of polymer degradation); but since the inner surface would facilitate epithelialization this would not result in restenosis. This system might be further used in other target areas for cell separation too [28]. This design is currently being tested in new Zealand rabbits as tracheal implants.

## Materials and Methods

### Pore gradient formation within titanium implants

Macroporous titanium implants of 2 mm thickness and 11 mm diameter formed of medical grade Titanium beads with an open pore structure were provided by Protip (Strasbourg, France) and laser cutting by IREPA laser (Illkirch, France). 4% or 6% of PLLA (Sigma-Aldrich) solution was prepared in Dioxane/Water binary mixture (v:v 87/13%) and then heated to 60°C up until a homogenous solution was obtained [29]. The hot solution was poured into the titanium implants via precision glass syringes in a two-piece custom-made Teflon mold up until all the pores are filled and the samples were either directly frozen or incubated at room temperature for 30 minutes before the freezing step. In this setting one face of the implant faces the Teflon which restricts the movement of extraction liquid in one direction and also affects the freezing of the solution. Samples were frozen overnight at −80°C. The next day, solvent exchange was achieved by immersion of the

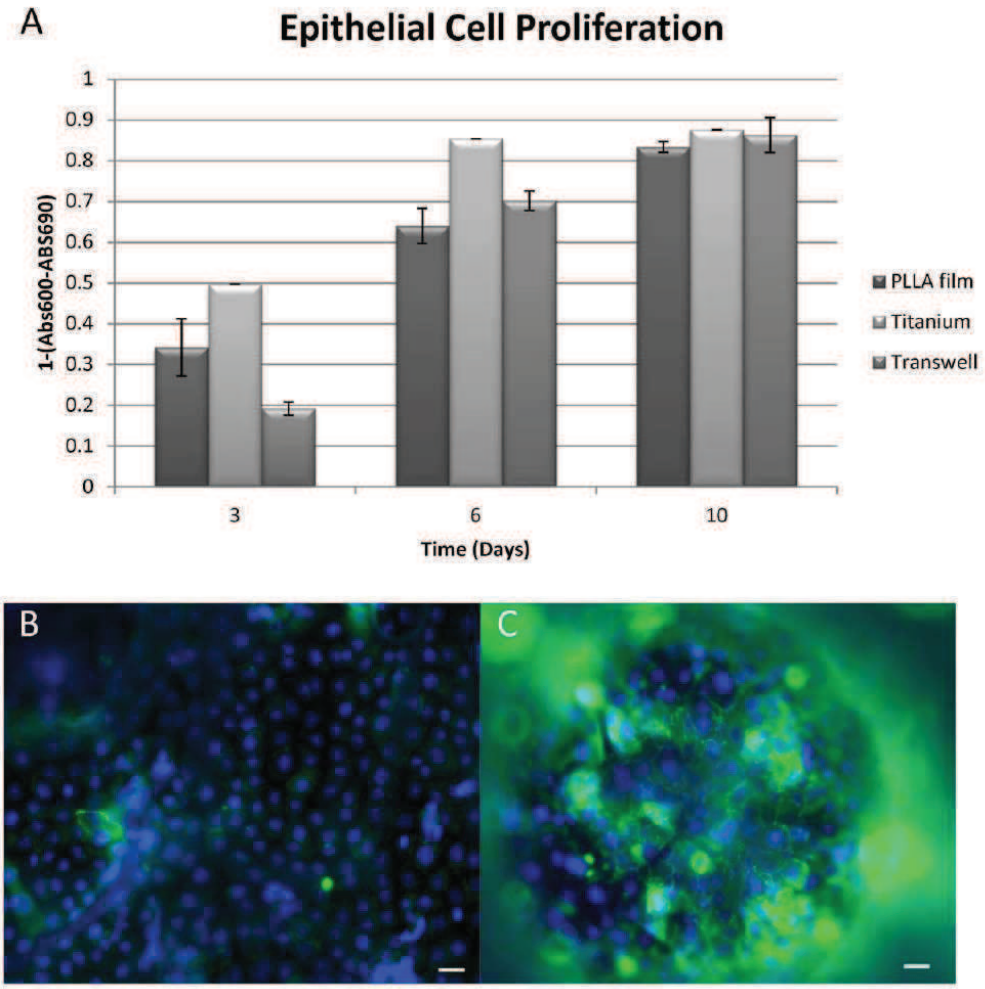


**Figure 6. Epithelial cell proliferation and positioning.** a) Human respiratory epithelium growth on transwell (positive control, hybrid implant with a nanoporous PLLA film and hybrid implant without a film b)presence of the film layer kept the epithelium on the same level for promoting the monolayer formation c) whereas in the absence of the film, epithelial cells grew on different levels (Scale bars: 10 μm).
doi:10.1371/journal.pone.0020480.g006

samples in the mold into pre-chilled 80% Ethanol solution at −20°C overnight [30]. Samples were removed from the molds and air dried. The morphology of the final product was observed with environmental SEM (Hitachi TM100, Japan) and the average pore size distribution and overall porosity was determined with mercury porosimetry analysis. To quantify the pore size difference between the back and front faces of the implants images of both sides (n>6) were processed and analyzed by Image J (NIH, USA) in which at least 50 definite, unconnected pore structures were measured per image to obtain the average surface porosity for each surface.

### Non porous/Nanoporous film formation on PLLA/titanium hybrids

After formation of the Ti/PLLA hybrid, to form the nanoporous top layer , 1% PLLA solution was dissolved in a more volatile solvent (Chloroform (Merck)) and 20 μl of the solution was applied on to the surface of Titanium/PLLA hybrid with precision glass syringes and then immersed in pure ethanol to induce phase separation [31]. After incubation in the non-solvent samples were removed and air-dried. The surface morphology, roughness and porosity were determined with Atomic force microscopy (Veeco). Thickness of the film layer and the morphology of the underlying porous layer and the effect of film formation on the porosity of the bottom layer were determined by confocal microscopy (Zeiss LSM 510), by utilizing the autofluorescence of PLLA.

### Fibroblast Cell culture and Cell migration assay

NIH-3T3 fibroblast cell line was cultured in RPMI 1640 medium (Gibco) with 10% Foetal bovine serum and 1% Penicillin/Streptomycin under standard culture conditions [22].

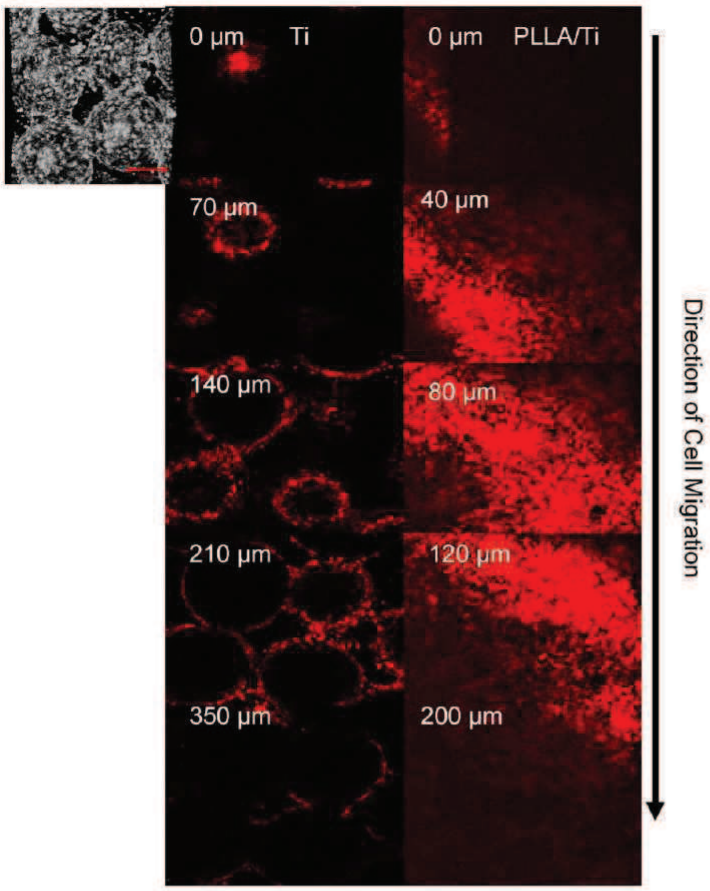


**Figure 7. Vertical movement of 3T3 cells in Ti and Ti/PLLA implants.** Distribution of 3T3 fibroblast after 7 day of culture from back to front for (Left hand side) Titanium Titanium/PLLA hybrid (Right hand side). Last images shows the depth through the scaffold where the signal (cell number) decreases significantly (~350 µm and 200 µm respectively). Cells were able to move towards the front surface of the implant for both scaffold but the number of cells significantly decreased towards the front; where the migration degree was much higher in titanium scaffolds.
doi:10.1371/journal.pone.0020480.g007

Titanium/PLLA hybrid and titanium only implants were sterilized by 70% Ethanol for 2 hours and then washed with sterile PBS and placed into 11 mm transwell cell culture inserts (Transwell) in order to restrict the movement of the cells to vertical direction after seeding. Confluent cells were removed with Tryple express enzyme cocktail (invitrogen), counted with a a haemocytometer and then marked with PKH26 fluorescent red cell linker (Sigma Aldrich) according to the providers instructions. Marked cells were seeded onto the implants in transwell inserts at a concentration of $2\times10^6$ cells/implant and fed both from top and bottom. Medium was changed twice a day and at day 7, samples were fixed with 3.7% paraformaldehyde and observed with confocal microscopy ($n\geq3$). For each sample at least 12 stacks were analyzed between the top layer (where the cells were seeded) and the layer where when the signal got nearly undetectable. Cell number at each thresholded stack was determined by Image J particle analyzer tool with a manual follow-up for noise reduction. To determine cell proliferation, samples were seeded with $1\times10^5$ cells/implant and then cell numbers were determined over a course of 1 week with MTT cell proliferation assay (Promega) and validated with TOX8 (Resazurin based) assay (Sigma-Aldrich) ($n\geq6$).

## Human Respiratory Epithelium Cell Isolation and Culture

For respiratory epithelial cell culture, freshly removed human nasal polyps were used for cell isolation as described before [32]. The use of human tissues was authorized by the bioethical law 94–654 of the Public Health Code of France, with a written consent from the patients. The study has been approved by the French committee "Comité de Protection des Personnes" (CPP-Est III, Nancy), statement n° DC-2008-374. The specimens used were polyps that needed to be removed, no surgeries were performed with the specific aim of obtaining polyps for the described experiments. Isolated cells were grown on tissue culture plates upon confluency. Cells were then seeded on hybrid Titanium/PLLA implants in transwell inserts at a concentration of $5\times10^4$ cells/implant. Cell proliferation was observed by TOX8 assay

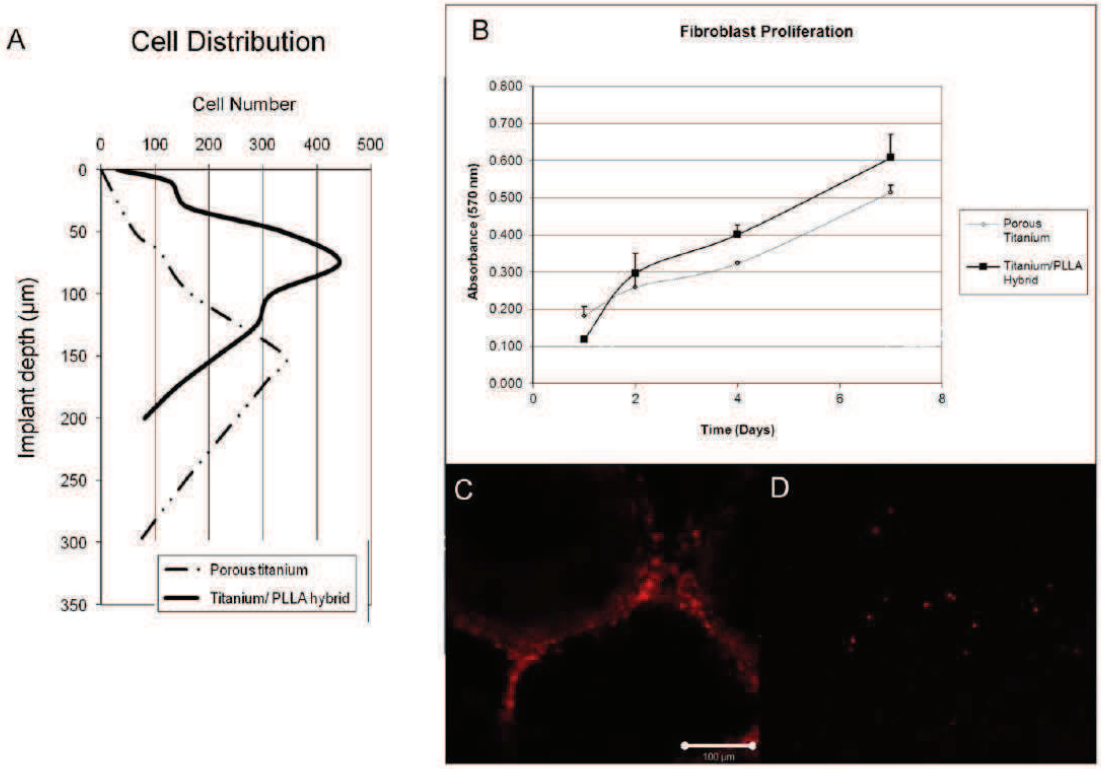


**Figure 8. 3T3 proliferation and the ability to reach to the other face of the implant.** a) Depth of cell movement in Titanium only and Titanium/PLLA hybrids, cells moved considerably deeper in titanium only implants. The point were there was a significant drop in the signal (cell number) notified the final depth; b) MTT assay results for 3T3 proliferation: overall cell number was higher in PLLA/titanium hybrids due to decreased migration and the availability of more niches to proliferate; c) Confocal images of the front surfaces of the implants. A significant number of cells has reached the face of titanium only implants after 7 days of culture d) whereas only occasional cells can be observed in the case of Titanium/PLLA hybrids.
doi:10.1371/journal.pone.0020480.g008

over a 10 days period of time (n≥3). Culture was stopped at several time points and cell-cell contact formation and cell coverage of implant surface was observed by phase-contrast microscopy and by fluorescence microscopy after DAPI nuclei staining and ZO-1 immunodetection. Briefly, cultures were fixed for 10 min at −20°C in precooled methanol. After a wash in PBS (Gibco), they were saturated for 2 h in PBS containing 3% (vol/vol) of Bovine Serum Albumin (BSA, Sigma) to prevent unspecific bindings, then incubated overnight at 4°C with mouse anti-ZO-1 antibodies diluted at 1/100 in PBS/BSA 1% (Zymed). After 3 washes in PBS under gentle agitation, cultures were incubated with Alexe Fluor®-coupled goat anti-mouse IgG (Molecular Probe) at 1/200 in PBS for 1 h at room temperature (RT). After washes in PBS under gentle agitation, cell nuclei are finally stained with 4′,6-diamidino-2-phenylindole (DAPI; 1 mg/ml in PBS) for 15 min at RT, and cultures are mounted under coverslip in Aquapolymount antifading solution (Polysciences). Cultures were observed under an AxioImager fluorescence microscope (Zeiss) equipped with an Apotome device. Images were recorded with a CCD video camera (Coolsnap, Roper Scientific) at 57 successive z levels (1 µm between each z level) at ×20 magnification.

### Statistical Analysis

For determination of statistical significance Student's t-test was utilized for comparison of two conditions with significance level was set as $p \leq 0.05$, for tests involving more than two conditions ANOVA tests were performed with the same statistical significance level and Tukey's honest significance test as follow-up.

## Supporting Information

**Figure S1 Confluent Epithelial Cells on the film layer.** Phase-contast images of confluent human respiratory epithelial cells as observed in the film areas which lie on the macropores of the titanium body.
(TIF)

## Acknowledgments

We are grateful to Dr. A. Walder for providing titanium samples, to Dr. M. Erhardt for his help with SEM images (IBMP, Strasbourg Esplanade Cellular Imaging Facility, funded by CNRS, INSERM, Louis Pasteur University and Alsace Region). We thank K. Benmlih for the build-up of the Teflon molds.

## Author Contributions

Conceived and designed the experiments: NEV CD DV PL. Performed the experiments: NEV AD CC. Analyzed the data: NEV PL AD. Contributed reagents/materials/analysis tools: NEV CC CD. Wrote the paper: NEV PL.

## References


1. Karp JM, Langer R (2007) Development and therapeutic applications of advanced biomaterials. Current Opinion in Biotechnology 18: 454–459.
2. Singh M, Berkland C, Detamore MS (2008) Strategies and Applications for Incorporating Physical and Chemical Signal Gradients in Tissue Engineering. Tissue Engineering Part B: Reviews 14: 341–366.
3. Kojima K, Bonassar LJ, Roy AK, Mizuno H, Cortiella J, et al. (2003) A composite tissue-engineered trachea using sheep nasal chondrocyte and epithelial cells. FASEB J 17: 823–828.
4. Macchiarini P, Jungebluth P, Go T, Asnaghi MA, Rees LE, et al. (2008) Clinical transplantation of a tissue-engineered airway. The Lancet 372: 2023–2030.
5. Wolf MH, Farhadi J, Candrian C, Martin I, Barbero A (2008) European Cells and Materials. 15: 1–10.
6. Muller S, Koenig G, Charpiot A, Debry C, Voegel JC, et al. (2008) VEGF-Functionalized Polyelectrolyte Multilayers as Proangiogenic Prosthetic Coatings. Advanced Functional Materials 18: 1767–1775.
7. Schultz P, Vautier D, Charpiot A, Lavalle P, Debry C (2007) Development of tracheal prostheses made of porous titanium: a study on sheep. European Archives of Oto-Rhino-Laryngology 264: 433–438.
8. Schultz P, Vautier D, Richert L, Jessel N, Haikel Y, et al. (2005) Polyelectrolyte multilayers functionalized by a synthetic analogue of an anti-inflammatory peptide, [alpha]-MSH, for coating a tracheal prosthesis. Biomaterials 26: 2621–2630.
9. Grillo HC (2002) Tracheal replacement: a critical review. The Annals of Thoracic Surgery 73: 1995–2004.
10. Zani BG, Kojima K, Vacanti CA, Edelman ER (2008) Tissue-engineered endothelial and epithelial implants differentially and synergistically regulate airway repair. Proceedings of the National Academy of Sciences 105: 7046–7051.
11. Schultz P, Vautier D, Egles C, Debry C (2004) Experimental study of a porous rat tracheal prosthesis made of T40: long-term survival analysis. European Archives of Oto-Rhino-Laryngology 261: 484–488.
12. Kipshidze N, Dangas G, Tsapenko M, Moses J, Leon MB, et al. (2004) Role of the endothelium in modulating neointimal formation: Vasculoprotective approaches to attenuate restenosis after percutaneous coronary interventions. J Am Coll Cardiol 44: 733–739.
13. Ho M-H, Kuo P-Y, Hsieh H-J, Hsien T-Y, Hou L-T, et al. (2004) Preparation of porous scaffolds by using freeze-extraction and freeze-gelation methods. Biomaterials 25: 129–138.
14. Budyanto L, Goh Y, Ooi C (2009) Fabrication of porous poly(L-lactide) (PLLA) scaffolds for tissue engineering using liquid–liquid phase separation and freeze extraction. Journal of Materials Science: Materials in Medicine 20: 105–111.
15. Leong KF, Chua CK, Sudarmadji N, Yeong WY (2008) Engineering functionally graded tissue engineering scaffolds. Journal of the Mechanical Behavior of Biomedical Materials 1: 140–152.
16. Moroni L, Curti M, Welti M, Korom S, Weder W, et al. (2007) Anatomical 3D Fiber-Deposited Scaffolds for Tissue Engineering: Designing a Neotrachea. Tissue Engineering 13: 2483–2493.
17. Sargeant TD, Guler MO, Oppenheimer SM, Mata A, Satcher RL, et al. (2008) Hybrid bone implants: Self-assembly of peptide amphiphile nanofibers within porous titanium. Biomaterials 29: 161–171.
18. Mathieu LM, Mueller TL, Bourban P-E, Pioletti DP, Müller R, et al. (2006) Architecture and properties of anisotropic polymer composite scaffolds for bone tissue engineering. Biomaterials 27: 905–916.
19. Ma H, Hu J, Ma PX (2010) Polymer Scaffolds for Small-Diameter Vascular Tissue Engineering. Advanced Functional Materials 20: 2833–2841.
20. Lutolf MP, Hubbell JA (2005) Synthetic biomaterials as instructive extracellular microenvironments for morphogenesis in tissue engineering. Nat Biotech 23: 47–55.
21. Baharloo B, Textor M, Brunette DM (2005) Substratum roughness alters the growth, area, and focal adhesions of epithelial cells, and their proximity to titanium surfaces. Journal of Biomedical Materials Research Part A 74A: 12–22.
22. Grossin L, Cortial D, Saulnier B, Felix O, Chassepot A, et al. (2009) Step-by-Step Build-Up of Biologically Active Cell-Containing Stratified Films Aimed at Tissue Engineering. Advanced Materials 21: 650–+.
23. Fuchs JR, Hannouche D, Terada S, Vacanti JP, Fauza DO (2003) Fetal tracheal augmentation with cartilage engineered from bone marrow-derived mesenchymal progenitor cells. J Pediatr Surg 38: 984–987.
24. Kanzaki M, Yamato M, Hatakeyama H, Kohno C, Yang J, et al. (2006) Tissue engineered epithelial cell sheets for the creation of a bioartificial trachea. Tissue Eng 12: 1275–1283.
25. Coraux C, Hajj R, Lesimple P, Puchelle E (2005) Repair and regeneration of the airway epithelium. M S-Medecine Sciences 21: 1063–1069.
26. Bucheler M, Haisch A (2003) Tissue engineering in otorhinolaryngology. DNA Cell Biol 22: 549–564.
27. Coraux C, Nawrocki-Raby B, Hinnrasky J, Kileztky C, Gaillard D, et al. (2005) Embryonic stem cells generate airway epithelial tissue. Am J Respir Cell Mol Biol 32: 87–92.
28. Keeney M, Pandit A (2009) The Osteochondral Junction and Its Repair via Bi-Phasic Tissue Engineering Scaffolds. Tissue Engineering Part B-Reviews 15: 55–73.
29. Pavia FC, La Carrubba V, Piccarolo S, Brucato V (2008) Polymeric scaffolds prepared via thermally induced phase separation: Tuning of structure and morphology. Journal of Biomedical Materials Research Part A 86A: 459–466.
30. Budyanto L, Goh YQ, Ooi CP (2009) Fabrication of porous poly(L-lactide) (PLLA) scaffolds for tissue engineering using liquid-liquid phase separation and freeze extraction. Journal of Materials Science-Materials in Medicine 20: 105–111.
31. Papenburg BJ, Bolhuis-Versteeg LAM, Grijpma DW, Feijen J, Wessling M, et al. (2010) A facile method to fabricate poly(L-lactide) nano-fibrous morphologies by phase inversion. Acta Biomaterialia 6: 2477–2483.
32. Skowron-Zwarg M, Boland S, Caruso N, Coraux C, Marano F, et al. (2007) Interleukin-13 interferes with CFTR and AQP5 expression and localization during human airway epithelial cell differentiation. Experimental Cell Research 313: 2695–2702.

# 4.3. Etude *in vivo* de l'implantation d'une prothèse de trachée hybride, Article 4

## 4.3.1. Introduction à l'article 4

Nous avons vu dans le chapitre précédent que la prothèse hybride titane/ polymère PLLA avait les capacités de contrôler la migration des différents types cellulaires lors des études *in vitro.* Cependant la surface endoprothétique nanoporeuse pouvait être encore améliorée par l'utilisation d'un dépôt couche par couche d'un film constitué de collagène et d'alginate en remplacement du film nanoporeux de PLLA déposé dans la partie endoluminale. Nous avons réalisés l'implantation des prothèses hybrides PLLA/titane et film de collagène/alginate, en remplacement d'un segment de trachée sur un modèle animal, le lapin. Le changement de modèle animal a été motivé par différentes raisons. Tout comme le porc, il est phylogénétiquement plus proche de l'homme que ne l'est la brebis. Ce modèle animal est particulièrement intéressant pour l'étude de pathologies cardiorespiratoires telle la cardiomyopathie familiale ou la mucoviscidose. Son épithélium respiratoire est très proche de celui de l'homme. De plus, il présente une structure anatomique du larynx, de la trachée et des bronches souches quasi identique à l'homme (Calasans-Maia et al., 2009). Le lapin est un modèle pertinent dans l'étude expérimentale sur la biocompatibilté de matériaux prothétiques. Il s'agit d'un animal facilement manipulable et observable, permettant de travailler sur un grand nombre d'individus. De plus, son coût (achat, stabulation, histologie) est beaucoup plus faible que celui de la brebis. Enfin, une animalerie lapin est située sur le site de la Faculté de Médecine de Strasbourg (laboratoire de virologie, Dr G. Prévost). Cette situation permet une surveillance optimale des animaux par notre équipe. Pour toutes ces raisons, nous avons ainsi décidé de poursuivre les expérimentations d'implantation trachéale sur le lapin blanc néozélandais.

Nous avons implanté des prothèses hybrides PLLA/titane contenant film de collagène/alginate, en remplacement d'un segment de trachée sur 10 lapins blancs

néozélandais et comparé les résultats du comblement tissulaire des pores des prothèses de trachée à ceux de prothèses implantées en intramusculaire.

Nous avons réalisé un suivi régulier des animaux de manière clinique et par un monitoring des taux de CRP, de CGA par chromatographie en phase liquide (HPLC). Après explantation des analyses histologiques ont été réalisées.

Nous avons également mis en culture des cellules épithéliales humaines, obtenues à partir de polypes nasaux. Ces cellules ont servies à ensemencer *in situ*, lors du remplacement d'un segment de trachée, la face endoluminale des prothèses hybrides qui avaient été précédemment mises en jachère dans un muscle de la cuisse.

L'ensemble des protocoles réalisés sur le modèle du lapin et leurs résultats sont décrit dans ce quatrième article.

## 4.3.2. Résumé de l'article 4

Nous avons vu précédemment que les prothèses en titane macroporeux, colonisées *in vivo* par un épithélium endoluminale et par un tissu conjonctivo-vasculaire dans l'épaisseur de l'implant, était un transplant valable chez la brebis (Dupret-Bories et al., 2011) pour le remplacement d'un segment trachéal, mais nécessitait plusieurs procédures chirurgicales. Afin de réduire le nombre d'étapes chirurgicales et donc de simplifier la procédure, un nouveau biomatériau a été développé dans cette étude. Une prothèse de trachée microporeuse hybride PLLA/titane poreux a été développée afin de réduire le risque de sténose endoprothétique et d'obtenir une surface endoluminale de porosité adaptée à la migration d'un épithélium respiratoire. Nous avons implanté ces substituts trachéaux hybrides sur des lapins blancs néozélandais.

De plus, une surface endoluminale recréant une membrane basale a été obtenue grâce à la méthode de dépôt couche par couche de films de collagène et d'alginate. Les résultats ont montré qu'une prévention du risque de sténose endoprothétique était obtenue avec l'implant hybride microporeux PLLA/titane.

Afin de déterminer le temps nécessaire à l'épithélialisation de l'implant trachéal après implantation, nous avons réalisés des prélèvements sanguins réguliers avec mesure du profil de la CRP et de la CGA par HPLC et comparés ces résultats à ceux de l'analyse histologique des implants. Le délai moyen pour que l'épithélialisation de l'épaisseur de l'implant autorise une colonisation endoluminale était de 3 semaines. Cela a été confirmé par l'attachement de cellules épithéliales marquées par Calcein-AM sur la surface endoprothétique visible dès 3 semaines d'implantation. Après une élévation initiale durant la première semaine post-implantatoire, le taux de CRP était stable et conforme à des valeurs considérées comme normales.

La surface endoprothétique obtenue à partir d'alginate et de collagène déposés « couche par couche » était nanofibrillaire et constituait un film uniforme sans modifier la structure microporeuse de l'épaisseur de l'implant hybride PLLA/titane. Cette surface, sur laquelle sont déposées des cellules épithéliales respiratoires humaines précédemment mises en culture, constitue une meilleure alternative par rapport au film nanoporeux endoprothétique de PLLA (Vrana et al., 2011).

En conclusion, le dépôt couche par couche de collagène et d'alginate sur la face endoprothétique d'implants hybrides PLLA/titane avec épithélialisation *in situ* de la face

endoluminale de l'implant représente un avantage conséquent dans la stratégie pour le remplacement d'un segment de trachée.

## 4.3.3. Article 4

ARTICLE

BIOTECHNOLOGY AND BIOENGINEERING

# Modification of Macroporous Titanium Tracheal Implants With Biodegradable Structures: Tracking In Vivo Integration for Determination of Optimal In Situ Epithelialization Conditions

Nihal Engin Vrana,[1] Agnes Dupret-Bories,[1,2] Charlotte Bach,[1,3] Christophe Chaubaroux,[1] Christelle Coraux,[4] Dominique Vautier,[1,3] Fouzia Boulmedais,[5] Youssef Haikel,[1,3] Christian Debry,[1,2] Marie-Helene Metz-Boutigue,[1,3] Philippe Lavalle[1,3]

[1]Institut National de la Santé et de la Recherche Médicale, INSERM Unité 977, 11 Rue Humann, 67085 Strasbourg, France; telephone: +33-3-68-85-30-61; fax: +33-3-68-85-33-79; e-mail: philippe.lavalle@inserm.fr

[2]Hôpitaux Universitaires de Strasbourg, Service Oto-Rhino-Laryngologie, 67098 Strasbourg, France

[3]Faculté de Chirurgie Dentaire, Université de Strasbourg, 1 Place de l'Hôpital, 67000 Strasbourg, France

[4]Institut National de la Santé et de la Recherche Médicale, INSERM Unité 903, 51092 Reims, France

[5]Centre National de la Recherche Scientifique, UPR 22, Institut Charles Sadron, 23 rue du Loess, BP 84037, 67034 Strasbourg Cedex 2, France

**ABSTRACT:** Previously, we showed that macroporous titanium implants, colonized in vivo together with an epithelial graft, are viable options for tracheal replacement in sheep. To decrease the number of operating steps, biomaterial-based replacements for epithelial graft and intramuscular implantation were developed in the present study. Hybrid microporous PLLA/titanium tracheal implants were designed to decrease initial stenosis and provide a surface for epithelialization. They have been implanted in New Zealand white rabbits as tracheal substitutes and compared to intramuscular implantation samples. Moreover, a basement membrane like coating of the implant surface was also designed by Layer-by-Layer (LbL) method with collagen and alginate. The results showed that the commencement of stenosis can be prevented by the microporous PLLA. For determination of the optimum time point of epithelialization after implantation, HPLC analysis of blood samples, C-reactive protein (CRP), and Chromogranin A (CGA) analyses and histology were carried out. Following 3 weeks the implant would be ready for epithelialization with respect to the amount of tissue integration. Calcein-AM labeled epithelial cell seeding showed that after 3 weeks implant surfaces were suitable for their attachment. CRP readings were steady after an initial rise in the first week. Cross-linked collagen/alginate structures show nanofibrillarity and they form uniform films over the implant surfaces without damaging the microporosity of the PLLA body. Human respiratory epithelial cells proliferated and migrated on these surfaces which provided a better alternative to PLLA film surface. In conclusion, collagen/alginate LbL coated hybrid PLLA/titanium implants are viable options for tracheal replacement, together with in situ epithelialization.

Biotechnol. Bioeng. 2012;109: 2134–2146.



**KEYWORDS:** titanium; trachea; implant; epithelialization; porosity; in vivo; CGA; collagen

Correspondence to: P. Lavalle
Contract grant sponsor: Région Alsace
Contract grant sponsor: PMNA (Pôle Matériaux et Nanosciences d'Alsace)
Additional supporting information may be found in the online version of this article.
Received: 19 October 2011; Revision received: 18 January 2012;
Accepted: 26 January 2012
Accepted manuscript online 13 February 2012;
Article first published online 2 March 2012 in Wiley Online Library (http://onlinelibrary.wiley.com/doi/10.1002/bit.24456/abstract)
DOI 10.1002/bit.24456

## Introduction

Respiratory system diseases are one of the most common causes of death, especially in high income countries. For example, tracheal restenosis might become a problem that

can necessitate surgery. Moreover, tracheal damages due to cancer and congenital diseases are quite common and even though end-to-end anastomosis can solve the problem for short lengths (<5 cm) (Roomans, 2010), implants are necessary if the problem is recurrent or the damaged area is above the limits of end-to-end anastomosis. In recent years several commendable efforts in the area of trachea tissue engineering have given very promising results, especially the systems by Macchiarini et al. (2008) and Delaere et al. (2010) have shown possible routes to improve the life quality of the patients. However these systems are dependent on allograft availability and long production periods with high level of expertise, which has also been stated by the authors themselves in their recent reviews (Bader and Macchiarini, 2010). It was also discussed widely whether a more in situ approach might be more beneficial, as trachea is surgically accessible. In such a scheme, some elements of the regeneration were either induced within the body or added after the initial implantation. It has been suggested that the in situ epithelialization might be a more attractive option as the survival of the epithelial cells seeded initially is low (Nakamura et al., 2009; Omori et al., 2008). Thus more widespread and easily transferable solutions are still necessary. Current systems available are either dependent on cartilage production for the airway stability and prevention of collapse or in vivo migration of epithelial cells or epithelial graft for remodeling. Porous titanium technology is an interesting venue to provide biointegrable implants without any concerns on mechanical stability. It is composed of titanium microbeads put together with an electrical arc, which provides a macroporous, low density and yet stable implant system, with an easier production procedure compared to most of porous metal implants (Ryan et al., 2006). We have previously utilized the titanium tracheal implants in mice and sheep with success (Schultz et al., 2002, 2004). Other groups also had success with titanium implants in respiratory area (Janssen et al., 2009, 2010). Trachea is an advantageous area for reconstruction as it is a thin tissue with relatively low oxygen requirements (Kalathur et al., 2010). The main problems encountered in the previous studies were the absence of epithelium for large defects for which there is no possibility of epithelium grafting (skin, mouth, etc.) and an extensive risk of restenosis. Grafting can be a viable route but its availability is a difficulty and more importantly the differentiated state of the graft might cause problems in the target area (such as hair growth or excessive keratinization), so a surface that would facilitate epithelial growth is a preferred option. Utilization of the advantageous properties of two material types either as hybrids or composites is generally necessary in the field of biomaterials (Nicole et al., 2010). Thus utilizing a biodegradable structure, such as a polymer foam, within a biocompatible metallic template is feasible to control cellular movement also in vivo. A prerequisite for colonization of a porous tracheal implant is also to prevent restenosis of the lumen. For example, macropores with a microporous body might slow down cellular movement and prevent restenosis as we have shown previously (Vrana et al., 2011). However, advantages of a single operation procedure can be overshadowed by the extent of immune response. Also the level of epithelial migration might not be enough for full coverage of the implant surface. For this end, a surface coating which would provide a better medium for epithelial movement would be useful. Layer-by-Layer (LbL) film production methodology can be used for this aim with natural molecules such as collagen to make surface properties more basement membrane-like. LbL films are extremely simple to build up and they are also very versatile, that is, thickness, surface charge, mechanical parameters can be tuned easily by changing the number of deposited layers or the buildup conditions.

In order to decide for the right conditions for in situ epithelialization, monitoring of implant integration is necessary. Also since in trachea, implant failures can be fatal, their strict monitoring is crucial (Grillo, 2002). For this end, rabbits are appropriate models as the shape and relative size of their trachea is a good mimic of that of humans when normalized with respect to their size (ten Hallers et al., 2004). Moreover, rabbits are very susceptible to pulmonary infections, as such infections have been cited as one of the most common causes of death in rabbits (Rougier et al., 2006). This is relevant in the sense that, after implantation due to the unsterile environment of the tracheal passage, the implants might be prone to development of infection. This should be taken into account as the products are developed for clinical trials, for example, abrupt loss of animals has regularly been reported during similar interventions (Tatekawa et al., 2010). Due to these problems, detection of infections and removal of pathogens are extremely important. Determination of pathogen related peptides and monitoring of inflammation/immune system response related molecules by HPLC can thus provide crucial information on post-operational care of the implant. It has been utilized in a wide range of in vivo detection problems such as transplant rejection or cytotoxic material presence (Horuk et al., 2001; Tseng et al., 2005). C-reactive protein (CRP) is a common marker of inflammation and infection which has found clinical applications. Recently Chromogranin A (CGA, a severity marker) has also been shown to be a potent agent for infection and inflammatory response detection. In this study, a hybrid implant for tracheal implantation was monitored in vivo for its effectiveness in cell movement control and for determination of the right time period for secondary seeding of autologous epithelial cells with respect to animal health and tissue integration. The monitoring of animal condition was done by regular blood tests based on CRP levels and characterization of blood samples by HPLC and subsequent peptide sequencing. Also a surface modification of the implant was done with LbL methodology to provide a more basement membrane like structure for migration of respiratory epithelium cells.

## Materials and Methods

### Materials

Rabbit CRP ELISA kit was obtained from Helica Biosystems (Fullerton, CA) and Triple Express from Gibco/Life Technologies (Saint Aubin, France). Collagen type I (source: Bovine) was obtained from Symatese (Lyon, France) and alginate from Novamatrix (Pronova UPLVG medical grade, FMC Biopolymers AS Novamatrix, Sandvika, Norway). The rest of the products including, poly(L-lactic acid) (PLLA), chloroform, dioxane, and TOX-8 were purchased from Sigma–Aldrich (Saint Quentin Fallavier, France).

#### *Animal Model*

Adult White New Zealand rabbits ($n = 10$) between 14 and 16 weeks of age and weighing an average of 3 kg were used for this study. Each animal received care in compliance with the Guide for the Care and Use of Laboratory Animals (National Research Council, 2010) and were housed in our institution at the Faculty of Medicine of Strasbourg (France). They were fed with a standard laboratory diet and tap water ad libitum.

### Methods

#### *Implant Production*

Porous titanium implants with an inner diameter of 7 mm and an outer diameter of 10 mm were produced by previously defined electric-arc discharge method by using 400–500 μm diameter beads. The final length of the implants was 2 cm. A circular insert of 6 mm was cut out of the implant body with a laser beam (IREPA Laser, Illkirch, France) for posthumous investigations. The body of the implant was filled with a porous PLLA structure as described previously (Vrana et al., 2011). Briefly a 6% PLLA solution in dioxane/water binary mixture (v:v 87/13%) was heated to 60°C and then poured into a Teflon mold that contains the titanium implant. Then the system was left for gelation at room temperature for 30 min and then frozen at −70°C overnight. The system was rendered porous by freeze extraction with an extraction step in cold 80% ethanol (Goh and Ooi, 2008). The outer element of the mold has been previously removed and only the mandrel was left. This creates an open pore gradient from extraluminal side to intraluminal side. Finally a layer of 1% PLLA film was laid into the lumen and then precipitated with the application of EtOH (Fig. 1). The final structure was washed several times with PBS and then sterilized in an antibiotic/antimitotic cocktail as suggested previously (Shearer et al., 2006) followed by UV sterilization.

#### *In Vivo Experiments*

*Anesthesia.* All surgeries were performed under general anesthesia. Anesthesia was induced by intramuscular administration of ketamine (30 mg/kg, Ketamine® 500; Virbac, Carros, France) in combination with midazolam (0.2 mg/kg, Mydazolam®; Mylan, Saint Priest, France) and xylazine (3 mg/kg, Rompun®; Bayer AG; Leverkusen, Germany) and assisted ventilation (O2:1 L/min). Postoperative analgesia was maintained by fentanyl patch (3 μg, Fentanyl-Mepha®; Mepha Pharma, Aesch, Switzerland) for 6 days.

*Surgical technique.* All operations were performed under sterile conditions. With the animal in the supine position after a vertical midline cervicotomy, the infrahyoid muscles were separated from the tracheal axis. After dissecting to the level of the thyroid, a tracheal segment of three to four rings (15 mm) was resected. Each tracheal extremity was then inserted into the prosthesis, which replaced the defect. A silicone tube was placed in the titanium prosthesis and sutured to the prosthesis with one proximal stitch (vicryl 4.0). The porous titanium prosthesis and the tracheal extremities were joined by four proximal and distal sutures (vicryl 4.0). Before closing the skin and the subcutaneous layers without drainage, a myoplasty was performed to cover the prosthesis and limit possible peritracheal leakage.

A tracheal segment, silicone tubes (stents) were used for the endoluminal calibration of the porous titanium prostheses for the in vivo experiments. They were 40 mm long with an internal diameter of 5 mm. They protruded from each end of the prosthesis by 10 mm, thus providing protection of the tracheo-prosthetic anastomoses.

#### *Implant Follow-Up*

A daily clinical follow-up was performed. Data regarding the general well-being of the animals and their weight were recorded throughout the duration of the experiment.

Implantation period was 6 weeks and regular CRP readings were taken weekly by an ELISA kit to determine the level of inflammation as per the instructions of the manufacturer. Blood was obtained from the auricular veins and centrifuged at 5,000 rpm at 4°C for 20 min, the supernatant was obtained and tested for CRP levels. The rest of the plasma was utilized for further characterization.

#### *Plasma Characterization*

*Purification of proteic material by reverse phase HPLC.* Soluble biological material was obtained by acidic extraction with 0.1% of trifluoroacetic acid of rabbit plasma (1/1, v/v). The soluble extract was purified using a Dionex HPLC system (Ultimate 3000; Sunnyvale, CA) on a nucleosil reverse-phase 300-5C18-column (4 mm × 250 mm; particle size 5 μm; porosity, 300 Å, Macherey Nagel, Hoerdt, France). Absorbance was monitored at 214 and 280 nm, and the solvent system consisted of 0.1% ( v/v)

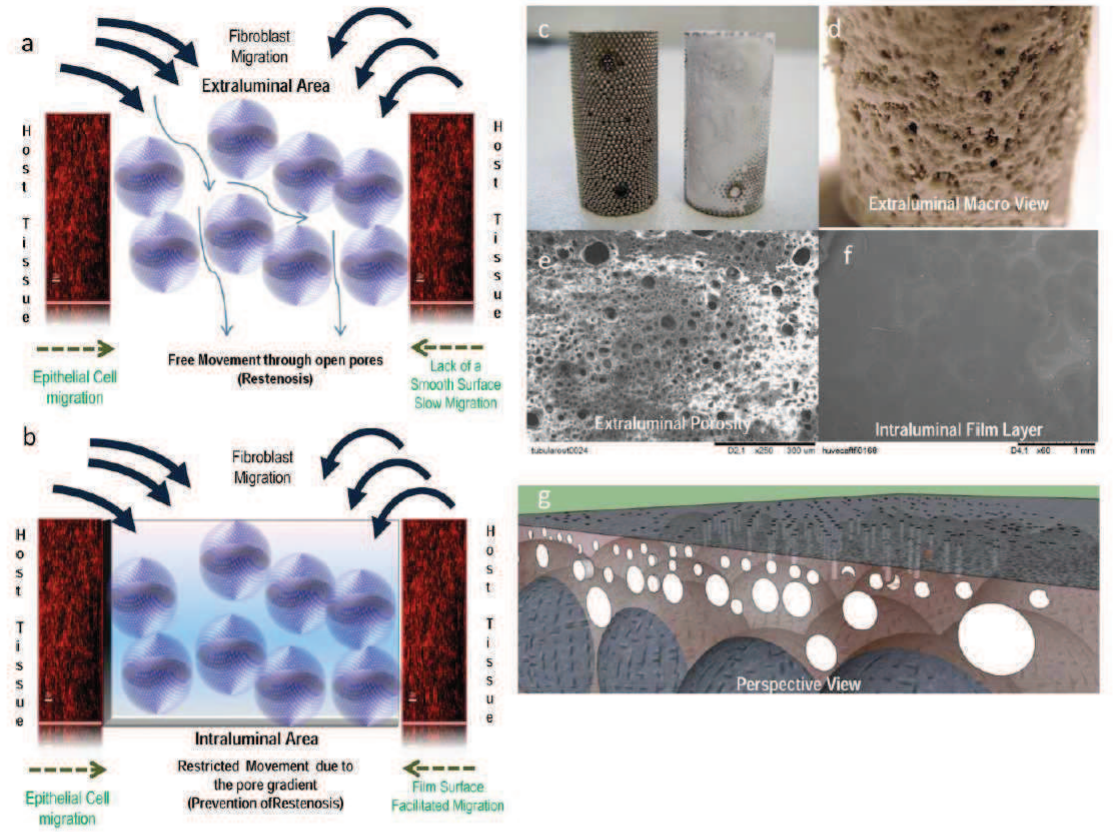


**Figure 1.** Scheme of the proposed implant, as macroporous structure of titanium implants does not hinder cell movement (**a**). A hierarchically porous PLLA body with a thin film layer facing the lumen has been introduced (**b**). **c,d**: Macroscopic view of titanium only and titanium PLLA implants. SEM images of (**e**) extraluminal and (**f**) intraluminal surfaces of the implant (from microporous surface to a smooth surface). **g**: The perspective view of the final implant model, where the titanium beads are engulfed by the hierarchically porous PLLA body.[Color figure can be seen in the online version of this article, available at http://wileyonlinelibrary.com/bit]

trifluoroacetic acid (TFA) in water (solvent A) and 0.09% (v/v) TFA in 70% (v/v) acetonitrile–water (solvent B). Elutions were performed at a flow rate of 700 $\mu$L/min using gradients indicated on chromatograms. Each peak fraction was collected and concentrated by evaporation, but not to dryness with the speed-vac.

*Western blotting.* Samples were loaded on 15% SDS–PAGE and then transferred to PVDF membrane (HyBond$^{TM}$-P, GE Healthcare). During migration a voltage of 50 V was applied for the first 10 min and then 120 V till end and during transfer 75 V was used for 90–100 min. For immunodetection Millipore Snap i.d. protein detection system was used using 0.5% of bovine serum albumin as blocking agent. Antibodies used were monoclonal anti-CGA (anti-$CGA_{47–68}$). Secondary antibodies used were goat anti-mouse immunolabeled bands were visualized by using the imager system ChemiDoc XRS (Bio-Rad, Marne-la-Coquette) after addition of ECL reagent (Amersham Bio-Science, Buckinghamshire, UK). To compare with our previous technique (intramuscular implantation prior to tracheal replacement) (Dupret-Bories et al., 2011), the CGA tests were also done for the samples obtained from animals who received a tracheal titanium implant with or without epithelial cells after 3 weeks of intramuscular implantation. Briefly, the steps were (i) implantation of titanium endoprosthetic tube under the infrahyoid muscles (day 0); (ii) implantation of the prosthesis to replace a resected tracheal segment (day 21). After placing the animal in the supine position, a cervicotomy was performed with a midline vertical incision, allowing access to the infrahyoid muscles, which was separated from the tracheal axis. The prosthesis was placed between the infrahyoid muscles and the trachea. Then a silicon tube was inserted into the porous titanium prosthesis. The skin and subcutaneous layers were then closed with separated stitches of Vicryl 2.0. After 21 days, the cervical cutaneous incision was reopened.

The initial silicon tube was removed from the titanium prosthesis and replaced with a new silicone tube (placed inside the porous titanium prosthesis) that was sutured to the prosthesis with one proximal stitch (Vicryl 4.0). The prosthesis was laterally transposed (with its endoluminal surface covered with epithelium) to replace a 2 cm tracheal segment which was resected during the same operation. The proximal and distal tracheal extremities were inserted into the titanium prosthesis and the junctions of the prosthesis and the tracheal extremities were joined with 6 sutures of vicryl 4.0. Before closing the skin and subcutaneous tissue, a myoplasty was performed to improve coverage and limit future leakage.

*Automatic Edman sequencing of peptides derived from the plasma.* The N-terminal sequence of purified peptides was determined by automatic Edman degradation on a Procise microsequencer (Applied Biosystems, Courtaboeuf, France). Samples purified by HPLC were loaded to polybrene-treated glass-fiber filters. Phenylthiohydantoin-amino acids (Pth-Xaa) were identified by chromatography on a $C_{18}$ column (PTH C-18, 2.1 mm × 200 mm) (Gasnier et al., 2004). For the identification of the sequence SWISS-Prot database was used by Blast software.

### *Histological Analysis*

After an observation period ranging from 1 to 6 weeks, the rabbits were euthanized with an intravenous overdose of sodium pentobarbital (120 mg/kg, CEVA Santé Animale, Libourne, France) after intramuscular administration of anesthesia (the same protocol previously described). A block resection, including surrounding tissues as well as the prosthesis, was performed. After explantation, the inserts where removed and observed with scanning electron microscopy (SEM) and confocal microscopy to check the structure and the presence of PLLA respectively. The implants were explanted at 2nd, 3rd, and 6th weeks of implantation and the histological cuts and hemotoxylin and eosin staining was done as reported previously (Schultz et al., 2007). Histological analyses were performed at the IMM (Institut Mutualiste Monsouris, Paris, France), where the blinded analyses were performed by two pathologists not involved in the project.

### *Collagen/Alginate LbL Production*

Collagen type I and Alginate were dissolved at 0.5 mg/mL in 0.15 M NaCl buffer at pH 4. LbL films were constructed on PLLA/titanium implants with an automated dipping robot where for each layer a 1:1 ratio of each polyelectrolyte was applied for equal time periods. The duration of dipping was 8 min for each polyelectrolyte with 5 min washing steps in between until 24 bilayers were reached. During the film construction, all the rinsing steps were performed with a 10 mM citrate buffer containing 0.15 M NaCl at pH 4. Cross-linking of the film layers on the implants was achieved by chemical cross-linking via genipin. Genipin solution (20 mg/mL) was prepared by dissolving 20 mg of the genipin powder in DMSO/buffer (0.15 M NaCl, pH 4) mixture (1:5). The cross-linking agent solution was let in contact with the coated PEM film for 12 h, followed by several rinsing steps. Formed film layers were characterized by atomic force microscopy (AFM) and SEM imaging.

### *Epithelial Cell Culture*

The use of human tissues was authorized by the French committee "Comité de Protection des Personnes" (CPP-Est III, Nancy), statement number DC-2008-374. Nasal polyps were taken with a written consent from the patients. Human respiratory Epithelial cells were obtained from freshly removed nasal polyps as described before (LeSimple et al., 2007). Cells were seeded on collagen/alginate covered hybrid PLLA/titanium implants as $5 \times 10^4$ cells/implant. Cell proliferation was observed by a Resazurin-based proliferation assay ($n \geq 6$) and morphology of the cells by fluorescence microscopy (DAPI and ZO-1 immuno-staining). Migration of the epithelial cells was quantified by time lapse microscopy and compared to the positive controls, collagen type IV and collagen type I coatings ($n \geq 40$).

## Results

### Implant Patency and Fibroblast Movement

The developed method produces a PLLA body within the titanium template with a porosity of 40–60 μm at the extraluminal part to 5–10 μm intraluminally. This structure enables the entry of fibroblasts and macrophages but prevents their migration into the lumen area (Vrana et al., 2011). The addition of the PLLA film layer in the intraluminal side was necessary to provide a surface for epithelial cells to migrate from anastomosis sites. The film layer was a surface visible on the structure of the implant (Fig. 1e). It has been previously shown that such systems can affect the movement of cells in vitro (Matschegewski et al., 2010).

All animals survived the surgical procedure. Implantations went uneventful except removal of the sutures by two rabbits 1 day after implantation. This rabbits were treated with local antiseptics, but one of them was lost at week 4 due to deep infection of the wound site. Another rabbit was lost due to peri-implantitis. Upon explantation, all implants were in contact with the native trachea wall, both in proximal and distal ends. In histological sections, fibroblasts are observed together with occasional multinucleated cells (Fig. 2). For fibroblast migration a similar behavior to that of in vitro conditions was seen in vivo, as there was a distinct decrease in the fibroblast movement in hybrid implants compared to titanium only implants. In the case of hybrid implants the fibroblast were able to get into the polymer body (cells were visible inside the foam after 2 weeks and their depth of movement gradually increased), but they

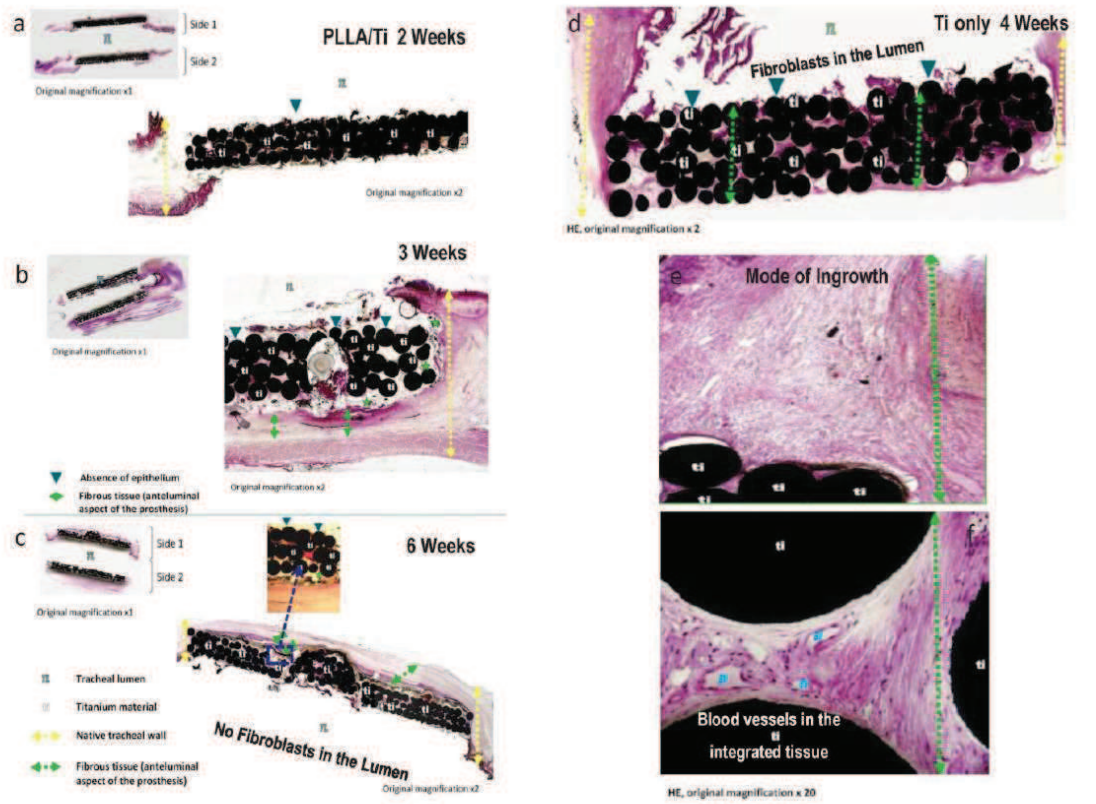


**Figure 2.** Histology after explantation. For PLLA/titanium implants cellular movement was controlled by PLLA presence; fibroblasts were restricted to the surrounding area in week 2 (**a**) then their movement into the implants was more apparent by week 3 (**b**) and week 6 (**c**). By week 6 whole implant was covered with the fibrovascular tissue with the tissue ingrowth into the implant, without the presence of fibroblasts in the lumen. On the other hand, only titanium implant was infiltrated with fibrotic tissue after 1 month (**d**) but the lumen has been started to be colonized which will end up in restenosis. **e**: The mode of ingrowth was from the extraluminal side. The tissue within the implants had distinct blood vessels. Epithelium movement was restricted to the areas close to the anastomosis sides and even though the amount was higher in PLLA/titanium implants, the middle area of the implants lacked epithelial cells. Thus, after initial integration an in situ seeding of autologous epithelial cells might be necessary. [Color figure can be seen in the online version of this article, available at http://wileyonlinelibrary.com/bit]

have not been able to reach the lumen side over a 6-week period (Fig. 2a–c). During this period, fibrovascular tissue surrounded the implant with noticeable growth into the polymer body, which has reached the middle part of the implant after 6 weeks (Fig. 2c, inset). The only titanium implants were colonized totally in 1 month period (Fig. 2d) and there was no way of keeping cell growth away from the lumen, thus fibroblasts in the lumen area were clearly visible, which suggested that longer periods would result in restenosis. Effectively the hybrid system is a temporary obstacle for the fibrovascular tissue infiltration which prevents the overcome of epithelial growth by fibroblasts. In other words, presence of polymer body kept the growth of the fibrous tissue back to give epithelium enough time to grow.

### CRP, CGA, and Blood Protein Levels

The change in rabbit health was monitored by CRP levels. CRP is an acute phase protein and it has been established as a good method to monitor inflammation. In this scheme, inflammation might come from two sources: inflammation due to reaction to the implant and inflammation due to infection. When there is no infection symptoms CRP readings dropped after an initial hike in the first week and stayed only slightly over the baseline of healthy animals over 6 weeks, but they were still below the acceptable limit for CRP in rabbits (5 ng/mL) (Fig. 3a). CRP readings for normal animals were around the levels of previously published reports (below 5 ng/mL) (Alvarez et al., 2008). However, when there was an infection, before the symptoms became

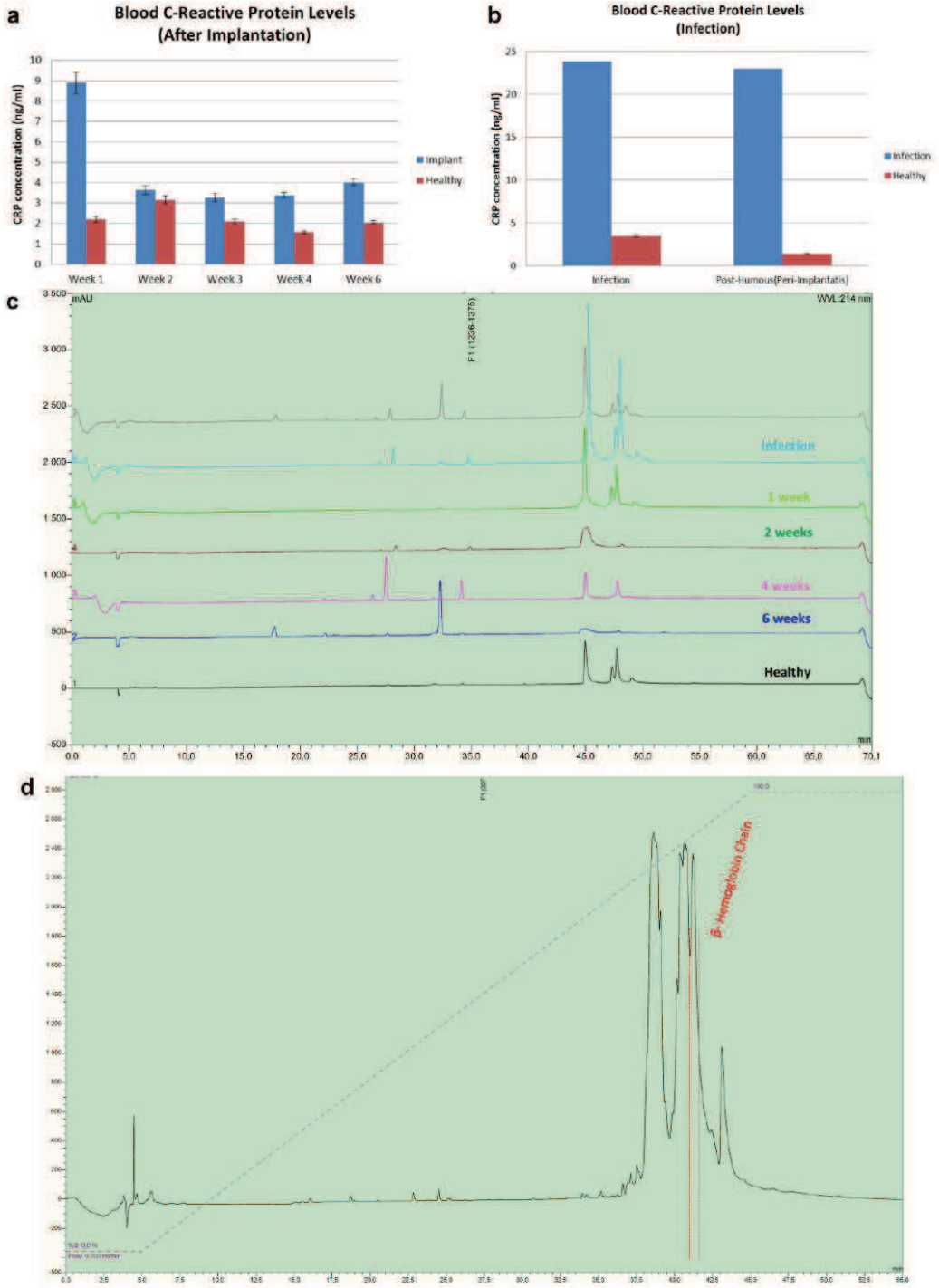
a
Blood C-Reactive Protein Levels
(After Implantation)
CRP concentration (ng/ml)
Week 1
Week 2
Week 3
Week 4
Week 6
Implant
Healthy
b
Blood C-Reactive Protein Levels
(Infection)
CRP concentration (ng/ml)
Infection
Post-Humous(Peri-Implantatis)
Infection
Healthy
c
mAU
WVL:214 nm
F1 (1236-1376)
Infection
1 week
2 weeks
4 weeks
6 weeks
Healthy
min
d
β- Hemoglobin Chain

**Figure 3.**

apparent, CRP levels elevated steeply (Fig. 3b). For example, one of the animals had elevated CRP levels (above 20 ng/mL) and then started to show infection symptoms. This animal's trachea was cleared with a small intervention and animal was healthy afterwards and survived up until the pre-determined sacrifice date. This showed that CRP levels are a good early warning method (Löbler et al., 2002). To further check this trend the proteome analysis were done in the serum samples over a timeline of 6 weeks, 1 animal who died of a wound site infection was used as negative control and a healthy animal as positive control. The HPLC profile showed distinct peaks corresponding to alpha and beta hemoglobin ½ as determined by Edman sequencing (Fig. 3c,d). Animals with tracheal implants show an increase in both hemoglobin alpha and beta ½ amount after 1 week of implantation compared to healthy animals, followed by a progressive decrease in 2, 4, and 6 weeks. Similar to the CRP readings, in case of an infection there was a very strong increase in alpha and beta hemoglobin ½ readings.

When the levels of CGA was checked at time points 3, 4, and 6 weeks, the level of unprocessed CGA (72 kDa) stayed stable, but an increase in the processed CGA (20 kDa) was observed (Fig. 4a). This processed CGA fragment (20 kDa) is known to be involved in improving cell attachment (Colombo et al., 2002). As CGA has been previously shown to be an even better indicator of stress (Shooshtarizadeh et al., 2010; Zhang et al., 2009), this check would be robust warnings for the set of infection and subsequent treatment. Moreover, they provide a means to compare different protocols in their influence in body response. When compared to our previous two-step method (intramuscular implantation and after 21 days, tracheal implantation), the PLLA/titanium hybrid system had less complete CGA. Processed CGA levels of two steps method after 1 week of tracheal implantation were at the level of 6 weeks for PLLA/titanium hybrid system (Fig. 4b). This methodology would open up a venue for checking the implantation behavior in a broader sense and specific to each animal, as tracheal replacement is a debilitating process and such methods for patient-based monitoring are necessary. When collaborated with the histology and CRP results, these results suggested that for initial fibrovascular population of the implants, 3 weeks period was necessary, during this period the initial immune response to implantation decreases but also the animals gradually become more prone to respiratory infections, mainly due to the lack of epithelium. Thus, after in vivo colonization of implant by the surrounding tissue for 3 weeks, the structure will be ready for local antibiotic treatment and subsequent in situ epithelialization.

### Epithelialization

The luminal surface of the implant is designed as a smooth film layer to facilitate epithelial cell attachment and migration. SEM imaging of the implant inserts after explantation showed that the film layer was largely intact after 4 weeks of in vivo incubation (Fig. 5). This layer has

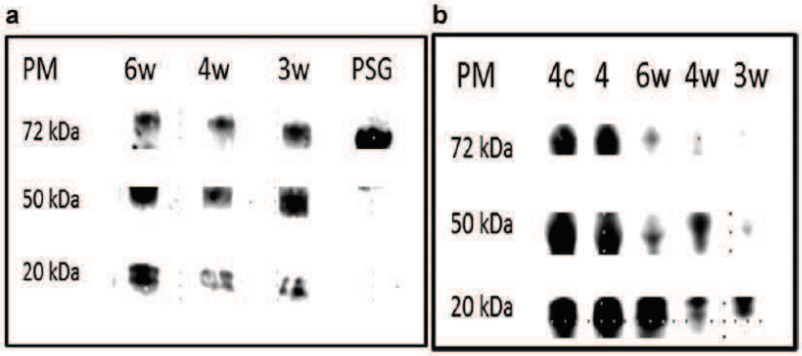


**Figure 4.** Western blots for determination of complete and/or digested CGA during the course of implantation. **a**: Animals which were implanted with PLLA/titanium implants over 6 weeks, complete CGA levels were similar, but the digested CGA (an N-terminal fragment) increased over time. **b**: comparison of PLLA/titanium hybrid implant procedure (3, 4, and 6 weeks denoted 3w, 4w, and 6w respectively) with two steps implantation protocol developed previously (Dupret-Bories et al., 2011) (intramuscular implantation, followed by tracheal implantation denoted 4 and 4c, where c corresponds to addition of epithelial cells. PSG stands for Positive control. The CGA levels were significantly higher in the cases of two steps implantation.

**Figure 3.** Animal health checks. **a**: CRP readings on healthy and implanted animals over 6 weeks, CRP levels decrease over implantation period after an initial increase. **b**: when there is infection an increase in CRP signal was observed. **c**: HPLC separation of plasma samples obtained from the animals over the course of implantation, where the profile of an healthy animal and a sick animal were used as positive and negative controls respectively. **d**: a representative of the readings where a distinct peak corresponding to hemoglobin beta ½ chain is marked, the comparison of the relative size of the peaks at different time points showed a correlation of the peak with implant integration. [Color figure can be seen in the online version of this article, available at http://wileyonlinelibrary.com/bit]

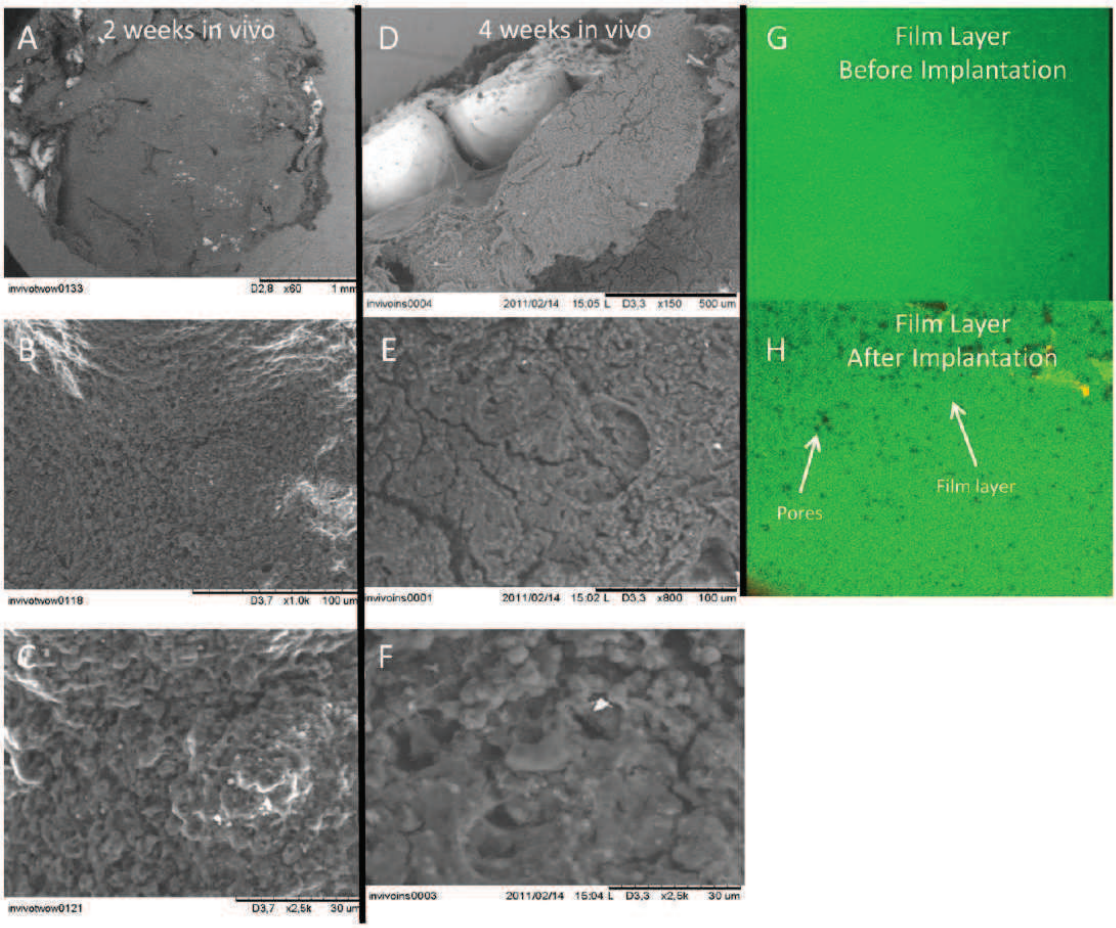


**Figure 5.** Stability of the film layer. The presence of film layer was monitored (**a**–**c**) after 2 weeks, (**d**–**f**) after 4 weeks of implantation. The film layer was in place but effects of degradation was apparent, with occasional cracks and an increase in the surface roughness. Confocal images of the film layer acquired at (**g**) time 0 and (**h**) after 4 weeks of in vivo implantation. The film layer was mostly intact, but the formation of further pores on the surface was visible (magnification 20×). [Color figure can be seen in the online version of this article, available at http://wileyonlinelibrary.com/bit]

been previously shown to support human respiratory cell proliferation. However in the view of the histological results, in vivo growth of epithelium was still slow (limited to the close proximity of the anastomosis sites). Epithelialization is generally a long process, basically due to the mode of growth of epithelium (Fong et al., 2010) and can only be overcome by surface treatments with growth factor gradients to a certain extent, as the boundary conditions cannot be changed. However, surface coatings can further improve the outcome. Previously in canine specimens the replacement of epithelium was observed on a polycaprolactone (PCL) based lumen coating of a collagen-based scaffold, but only after 18 months following the surgery (Sato et al., 2010). The authors state that there was a distinct improvement in epithelialization in the presence of the film coating. In this model, no prior autologous cell seeding was done. When decellularized tracheal scaffolds were used, Go et al. (2010) reported a distinct improvement in the case where autologous cells were seeded. Initial attachment of the cells becomes important, which can be very limited depending on the surface properties of the implant.

To further improve the implant design, we coated the lumen of the implants with collagen/alginate polyelectrolyte multilayers cross-linked with genipin. This cross-linking step was necessary to stabilize the film in physiological conditions (pH 7.4). The cross-linking was effective between collagen chains. Genipin acts on collagen molecules with primary amine groups and has the ability to form both intra and intermolecular cross-links (Hwang et al., 2011). However, we demonstrate that, alginate molecules from

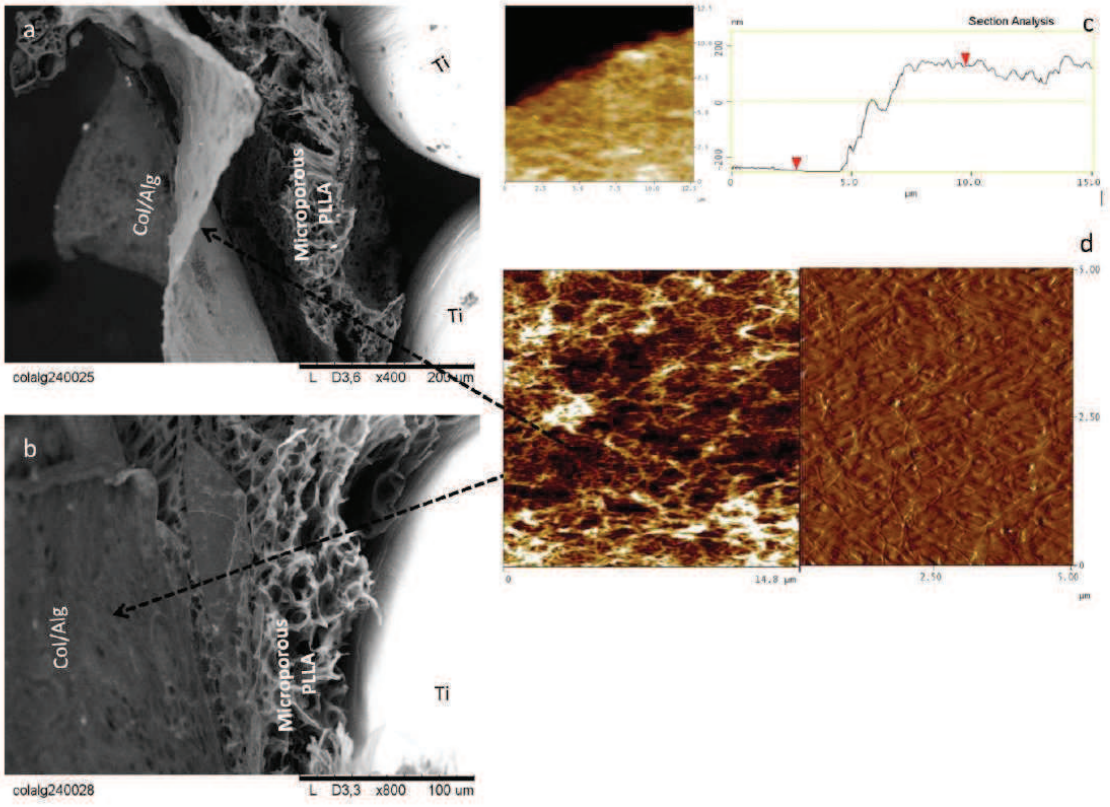


**Figure 6.** Development of collagen/alginate multilayers on the implant lumen. **a**: A Thin layer of the collagen/alginate film covers the surface of the implant over the titanium beads and microporous PLLA body after 24 bilayers were deposited (**b**) which showed a strong attachment to the implant body. **c**: Films have on average a thickness around 400 nm as determined by scratch tests (**d**) and they depicted a highly nanofibrillar structure. [Color figure can be seen in the online version of this article, available at http://wileyonlinelibrary.com/bit]

the cross-linked film were maintained in physiological conditions (Fig. S1). The exact mechanism of cross-linking is not fully described, even though a mechanism based on nitrogen-iridoid formation between C3 of genipin and the primary amines of lysine, hydroxylysine and arginine (Sundararaghavan et al., 2008) could be considered. When these layer were built at high bilayer numbers (24), a thick layer of film on top of the porous PLLA/titanium hybrid can be obtained (Fig. 6a,b). When the titanium samples are dipped into the polyelectrolyte solutions, the solutions cannot flow into the pore areas and they form thin films even in the absence of PLLA, but these films have wrinkled surface features compared to the smooth surface obtained in the case of PLLA/titanium. The thickness of this film layer determined by AFM was around 400 nm and the components of the film layer had a nanofibrillar structure which is known to improve the cell attachment due to its similarity to basement membrane. This structure had a surface roughness of 20 nm which is also appropriate for epithelial cell culture (Fig. 6c,d).

Human respiratory epithelial cells attached and proliferated on these structures, with near confluent layers obtained by 10 days (Fig. 7a–e). Cells proliferated faster on these structure compared to standard epithelial cell culture on Transwell inserts and also the cell numbers were higher compared to our previous results with PLLA films (Vrana et al., 2011). Transwell inserts were selected as control since they are widely used for in vitro differentiation of epithelial cells to ciliated epithelium by air–liquid interface culture method, which is crucial for respiratory epithelium. Moreover, in long term culture periods which are necessary for differentiation, long-term viability of epithelial cells was higher on collagen/alginate multilayers compared to Transwell. Cells stayed on the implant surface even after 19 days of culture (Fig. 7d), whereas in the case of Transwell and PLLA films, cell numbers saw a decrease after 13 days. To check the rate of migration, epithelial cells were observed with time lapse microscopy and their migration rates were calculated. In general cells migrated slower on collagen type IV than on multilayer counterparts ($P < 0.05$), whereas pure

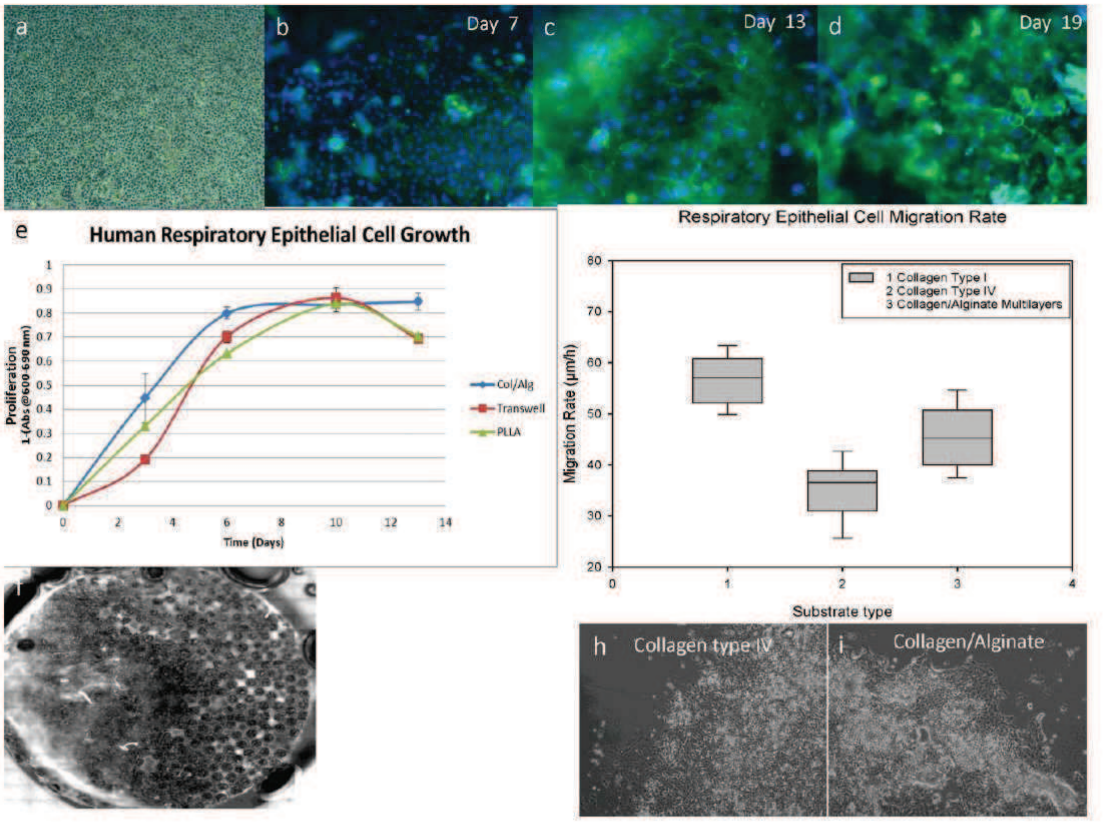


**Figure 7.** Human respiratory epithelial cell growth and migration on collagen/alginate coated implants. Collagen/alginate multilayers provided a better surface for cell growth than Transwell. Cell numbers were significantly higher than our previous system with PLLA films too. **a**: Phase-contrast micrographs of confluent respiratory epithelium cells. **b–d**: DAPI/ZO-1 staining of the cells on the implants after days 7, 13, and 19 (magnification 10×). **e**: Epithelial cell proliferation curve on collagen/alginate multilayers versus Transwell and PLLA systems. Cell numbers were significantly higher on collagen/alginate multilayers at days 3, 6, and 13. **f**: Macroscopic view of the coated cell seeded implant. **g**: Rate of migration (μm/h) of respiratory epithelial cells on three substrates: collagen type I, collagen type IV, and collagen/alginate multilayers ($n > 40$). **h,i**: Representative images of migration tests. [Color figure can be seen in the online version of this article, available at http://wileyonlinelibrary.com/bit]

collagen type I coating was a better surface for migration. However, collagen type I by itself is not a good substrate for respiratory epithelium proliferation, thus by using the LbL technology a surface that behaves better than pure collagen can be created. An additional coating of a collagen/alginate multilayer would help the epithelialization of implants, however with an average migration rate of 45.6 μm/h, a 2 cm defect can only be covered in about 10 days, if the movement is unidirectional from the both anastomosis sites.

Thus our next step was to seed the epithelial cells to an implant that has already been integrated with the body (after 3 weeks of implantation). This can be done endoscopically with the modification of already available endoscopical intervention equipment. A possible option would be a tubing system that will provide the airflow together with a cartridge facing the lumen of the surface that needs to be epithelialized filled with freshly isolated autologous epithelium in autologous serum. This might provide an "on-site" method for the epithelialization of the implant. In such a method, the epithelium would not need to deal with the initial inflammation and it can grow on an integrated structure thus the delay in vascularization can be eliminated. As a proof of concept, Calcein-AM labeled respiratory epithelial cells have been seeded on implants just after explantation. These implants were previously remodeled for 3 weeks between the infrahyoid muscles and the trachea. The epithelial cells have attached and spread on these surfaces in an hour (Fig. 8), which indicates that in situ epithelialization is an achievable goal in a clinical setting.

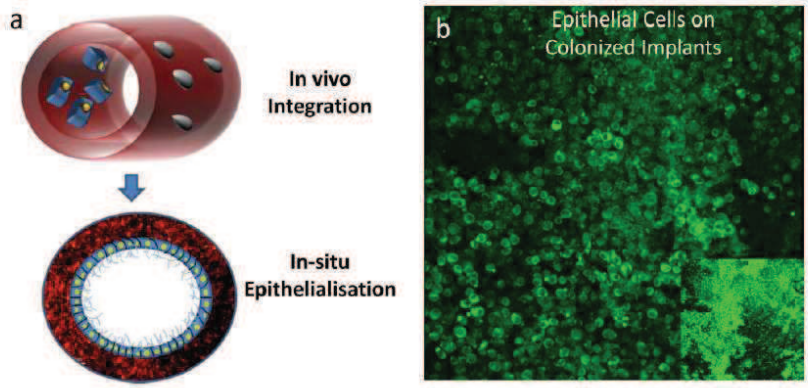


**Figure 8.** a: Proposed in situ epithelialization system, where the implant was left for integration in vivo and then epithelial cells were seeded in vitro to obtain a functional epithelium. b: Seeding of Calcein-AM labeled respiratory epithelial cells on implant surfaces after 3 weeks of in vivo incubation; the surface created via colonization provided a suitable substrate for epithelial cell attachment and spreading (after 1 day of in vitro incubation). [Color figure can be seen in the online version of this article, available at http://wileyonlinelibrary.com/bit]

## Conclusion

The hybrid PLLA/titanium tracheal implants can stop the initial ingrowth of the fibroblasts into the lumen. The histology and blood characterization results showed that the 3 weeks time-point is the optimal time delay for in situ seeding of epithelial cells. Analysis of CRP and CGA levels are viable methods to check the process of implant integration. A further modification of inner surface of the implants with collagen/alginate multilayers resulted in a 400 nm thick fibrillar film which can support epithelial cell growth and migration. As the next step, these implants will be used for in situ epithelialization experiments.

Authors would like to thank Dr. A. Walder for providing titanium samples. We thank K. Benmlih for the build-up of the Teflon molds and Dr. G. Prevost for his help with animal experimentation. We acknowledge the Région Alsace and PMNA (Pôle Matériaux et Nanosciences d'Alsace) for financial contribution.

## References

Alvarez H, Castro C, Moujir L, Perera A, Delgado A, Soriano I, Evora C, Sanchez E. 2008. Efficacy of ciprofloxacin implants in treating experimental osteomyelitis. J Biomed Mater Res B Appl Biomater 85B(1): 93–104.

Bader A, Macchiarini P. 2010. Moving towards in situ tracheal regeneration: The bionic tissue engineered transplantation approach. J Cell Mol Med 14(7):1877–1889.

Colombo B, Longhi R, Marinzi C, Magni F, Cattaneo A, Yoo SH, Curnis F, Corti A. 2002. Cleavage of chromogranin A N-terminal domain by plasmin provides a new mechanism for regulating cell adhesion. J Biol Chem 277(48):45911–45919.

Delaere P, Vranckx J, Verleden G, De Leyn P, Van Raemdonck D, Leuven Tracheal Transplant Group. 2010. Tracheal allotransplantation after withdrawal of immunosuppressive therapy. N Engl J Med 362(2):138–145.

Dupret-Bories A, Vrana NE, Lavalle P, Vautier D, Debry C. 2011. Development of surgical protocol for implantation of tracheal prostheses in sheep. J Rehabil Res Dev 48(7):851–864.

Fong E, Tzlil S, Tirrell DA. 2010. Boundary crossing in epithelial wound healing. Proc Natl Acad Sci USA 107(45):19302–19307.

Gasnier C, Lugardon K, Ruh O, Strub JM, Aunis D, Metz-Boutigue MH. 2004. Characterization and location of post-translational modifications on chromogranin B from bovine adrenal medullary chromaffin granules. Proteomics 4(6):1789–1801.

Go T, Jungebluth P, Baiguero S, Asnaghi A, Martorell J, Ostertag H, Mantero S, Birchall M, Bader A, Macchiarini P. 2010. Both epithelial cells and mesenchymal stem cell-derived chondrocytes contribute to the survival of tissue-engineered airway transplants in pigs. J Thorac Cardiovasc Surg 139(2):437–443.

Goh YQ, Ooi CP. 2008. Fabrication and characterization of porous poly(L-lactide) scaffolds using solid–liquid phase separation. J Mater Sci Mater Med 19(6):2445–2452.

Grillo HC. 2002. Tracheal replacement: A critical review. Ann Thorac Surg 73(6):1995–2004.

Horuk R, Shurey S, Ng HP, May K, Bauman JG, Islam I, Ghannam A, Buckman B, Wei GP, Xu W, Liang M, Rosser M, Dunning L, Hesselgesser J, Snider RM, Morrissey MM, Perez HD, Green C. 2001. CCR1-specific non-peptide antagonist: Efficacy in a rabbit allograft rejection model. Immunol Lett 76(3):193–201.

Hwang Y-J, Larsen J, Krasieva TB, Lyubovitsky JG. 2011. Effect of genipin crosslinking on the optical spectral properties and structures of collagen hydrogels. ACS Appl Mater Interfaces 3(7):2579–2584.

Janssen LM, van Osch G, Li JP, Kops N, de Groot K, Von den Hoff JWV, Feenstra L, Hardillo JAU. 2009. Tracheal reconstruction mucosal survival on porous titanium. Arch Otolaryngol Head Neck Surg 135(5):472–478.

Janssen LM, van Osch G, Li JP, Kops N, de Groot K, Feenstra L, Hardillo JAU. 2010. Laryngotracheal reconstruction with porous titanium in rabbits: Are vascular carriers and mucosal grafts really necessary? J Tissue Eng Regenerat Med 4(5):395–403.

Kalathur M, Baiguera S, Macchiarini P. 2010. Translating tissue-engineered tracheal replacement from bench to bedside. Cell Mol Life Sci 67(24): 4185–4196.

LeSimple P, van Seuningen I, Buisine MP, Copin MC, Hinz M, Hoffmann W, Hajj R, Brody SL, Coraux C, Puchelle E. 2007. Trefoil factor family 3

peptide promotes human airway epithelial ciliated cell differentiation. Am J Respir Cell Mol Biol 36(3):296–303.

Löbler M, Saß M, Kunze C, Schmitz K-P, Hopt UT. 2002. Biomaterial implants induce the inflammation marker CRP at the site of implantation. J Biomed Mater Res 61(1):165–167.

Macchiarini P, Jungebluth P, Go T, Asnaghi MA, Rees LE, Cogan TA, Dodson A, Martorell J, Bellini S, Parnigotto PP, Dickinson SC, Hollander AP, Mantero S, Conconi MT, Birchall MA. 2008. Clinical transplantation of a tissue-engineered airway. Lancet 372(9655):2023–2030.

Matschegewski C, Staehlke S, Loeffler R, Lange R, Chai F, Kern DP, Beck U, Nebe BJ. 2010. Cell architecture-cell function dependencies on titanium arrays with regular geometry. Biomaterials 31(22):5729–5740.

Nakamura T, Sato T, Araki M, Ichihara S, Nakada A, Yoshitani M, Itoi S, Yamashita M, Kanemaru S, Omori K, Hori Y, Endo K, Inada Y, Hayakawa K. 2009. In situ tissue engineering for tracheal reconstruction using a luminar remodeling type of artificial trachea. J Thorac Cardiovasc Surg 138(4):811–819.

National Research Council. 2010. Guide for the care and use of laboratory animals. Washington, DC: National Academies Press.

Nicole L, Rozes L, Sanchez C. 2010. Integrative approaches to hybrid multifunctional materials: From multidisciplinary research to applied technologies. Adv Mater 22(29):3208–3214.

Omori K, Tada Y, Suzuki T, Nomoto Y, Matsuzuka T, Kobayashi K, Nakamura T, Kanemaru S, Yamashita M, Asato R. 2008. Clinical application of in situ tissue engineering using a scaffolding technique for reconstruction of the larynx and trachea. Ann Otol Rhinol Laryngol 117(9):673–678.

Roomans GM. 2010. Tissue engineering and the use of stem/progenitor cells for airway epithelium repair. Eur Cell Mater 19:284–299.

Rougier S, Galland D, Boucher S, Boussarie D, Valle M. 2006. Epidemiology and susceptibility of pathogenic bacteria responsible for upper respiratory tract infections in pet rabbits. Vet Microbiol 115(1–3):192–198.

Ryan G, Pandit A, Apatsidis DP. 2006. Fabrication methods of porous metals for use in orthopaedic applications. Biomaterials 27(13):2651–2670.

Sato T, Araki M, Nakajima N, Omori K, Nakamura T. 2010. Biodegradable polymer coating promotes the epithelization of tissue-engineered airway prostheses. J Thorac Cardiovasc Surg 139(1):26–31.

Schultz P, Vautier D, Chluba J, Marcellin L, Debry C. 2002. Survival analysis of rats implanted with porous titanium tracheal prosthesis. Ann Thorac Surg 73(6):1747–1751.

Schultz P, Vautier D, Egles C, Debry C. 2004. Experimental study of a porous rat tracheal prosthesis made of T40: Long-term survival analysis. Eur Arch Otorhinolaryngol 261(9):484–488.

Schultz P, Vautier D, Charpiot A, Lavalle P, Debry C. 2007. Development of tracheal prostheses made of porous titanium: A study on sheep. Eur Arch Otorhinolaryngol 264(4):433–438.

Shearer H, Ellis MJ, Perera SP, Chaudhuri JB. 2006. Effects of common sterilization methods on the structure and properties of poly(D,L-lactic-*co*-glycolic acid) scaffolds. Tissue Eng 12(10):2717–2727.

Shooshtarizadeh P, Zhang D, Chich JF, Gasnier C, Schneider F, Haikel Y, Aunis D, Metz-Boutigue MH. 2010. The antimicrobial peptides derived from chromogranin/secretogranin family, new actors of innate immunity. Regul Pept 165(1):102–110.

Sundararaghavan HG, Monteiro GA, Lapin NA, Chabal YJ, Miksan JR, Shreiber DI. 2008. Genipin-induced changes in collagen gels: Correlation of mechanical properties to fluorescence. J Biomed Mater Res A 87A(2):308–320.

Tatekawa Y, Ikada Y, Komuro H, Kaneko M. 2010. Experimental repair of tracheal defect using a bioabsorbable copolymer. J Surg Res 160(1):114–121.

ten Hallers EJ, Rakhorst G, Marres HA, Jansen JA, van Kooten TG, Schutte HK, van Loon JP, van der Houwen EB, Verkerke GJ. 2004. Animal models for tracheal research. Biomaterials 25(9):1533–1543.

Tseng WC, Cheng GW, Lee CF, Wu HL, Huang YL. 2005. On-line coupling of microdialysis sampling with high performance liquid chromatography and hydride generation atomic absorption spectrometry for continuous in vivo monitoring of arsenic species in the blood of living rabbits. Anal Chim Acta 543(1–2):38–45.

Vrana NE, Dupret A, Coraux C, Vautier D, Debry C, Lavalle P. 2011. Hybrid titanium/biodegradable polymer implants with an hierarchical pore structure as a means to control selective cell movement. PLoS ONE 6(5):e20480. DOI: 10.1371/journal.pone.0020480.

Zhang D, Lavaux T, Sapin R, Lavigne T, Castelain V, Aunis D, Metz-Boutigue MH, Schneider F. 2009. Serum concentration of chromogranin A at admission: An early biomarker of severity in critically ill patients. Ann Med 41(1):38–44.

# Partie 5 : Modification de la taille des billes de la prothèse de trachée, études *in vitro* et *in vivo*

# Partie 5 : Modification de la taille des billes de la prothèse de trachée, études *in vitro* et *in vivo*

# 5.1. Introduction à l'article 5

Dans les études précédentes nous avons amélioré l'intégration de la prothèse de trachée en titane poreux par la modification du protocole opératoire (article 1) et l'ajout de polymère PLLA (article 2, 3) ainsi que d'un film nanoporeux endoprothétique de collagène/alginate (article 4).

Nous n'avions jusqu'à présent pas testé l'effet de la modification de la structure en titane macroporeuse de la prothèse elle-même.

Il apparaît que le contact des cellules entre elles (contact cellule/cellule) (Mills et al., 2011) est un élément majeur favorisant leur migration et prolifération. Nous avons décidé de tester l'effet de la diminution de la taille des billes de titane et donc de la taille des pores (avec une porosité constante de 35%). Ceci doit améliorer le contact entre les cellules et ainsi leur prolifération entre les billes de titane.

Trois prothèses, faites de microbilles de titane assemblées sous forme de plaque, différentes par la taille des billes utilisées ont été testées : 500, 300 et 150 µm de diamètre. Nous avons réalisé, dans cette étude, des expérimentations *in vitro* et *in vivo* sur l'intégration de ces implants en fonction de la taille des billes. Le comportement *in vitro* des fibroblastes, à savoir leur capacité de migration et de prolifération pour ces trois implants a été testée. La rapidité de l'intégration des implants, en fonction de la taille des billes, a été testée *in vivo* par l'implantation des 3 types de plaques en sous-cutané, au contact d'un muscle, sur le modèle animal lapin blanc néozélandais et le modèle rat Wistar.

Les protocoles des expérimentations et leurs résultats sont résumés dans le cinquième article.

# 5.2. Résumé de l'article 5

Les implants poreux constituent un terrain favorable à l'intégration par des tissus mous. Pour des applications cliniques en oto-rhino-laryngologie nous avons développé des implants constitués de microbilles de titane, l'espace entre les billes (pores) constituant un environnement favorable à la migration cellulaire des tissus environnants. In vivo, cette structure poreuse a pour but de promouvoir la progression d'un tissus fibro-vasculaire dans l'épaisseur de l'implant. Cependant ce processus nécessite plusieurs semaines, ce délai favorisant notamment les processus inflammatoires dans des sites exposés aux sécrétions aériennes comme la trachée. Par des études *in vivo* et *in vitro*, nous déterminons les conséquences entrainées par la modification de la structure de l'implant telle que la vitesse d'intégration de celui-ci, élément primordial pour les applications cliniques.

Par le suivi des cellules en microscopie confocale, nous avons quantifié la distribution des cellules à travers les implants. Nous avons mis en évidence le fait que la taille des billes et la distance entre les billes modifiaient de manière significative la capacité des cellules à développer un contact entre elles et à combler les pores. Le marquage des cellules par des fluorophores a montré que plus la taille des billes était faible, meilleure était la probabilité d'observer un comblement des pores dans un délai de 7 jours. La taille des billes affecte également l'attachement et la distribution des cellules, ainsi que la production de collagène par les fibroblastes : la sécrétion de matrice extracellulaire (ECM) augmente lors de l'utilisation d'implants ayant des billes de 150 µm. L'obtention d'un comblement rapide de l'implant autorise également un système de co-culture *in vitro*, où le nombre et la distribution d'un second type cellulaire est boosté par la présence d'une premier type de cellules. Ce concept a été utilisé dans cette étude pour améliorer l'attachement des cellules vasculaires endothéliales en plaçant une couche première de fibroblastes. Cette technique peut être utilisée afin d'améliorer la vascularisation *in vitro* des implants.

En réduisant la taille des billes, la colonisation globale de l'implant est significativement améliorée après 3 semaines d'implantation *in vivo*. La modification de la taille des billes entraine des résultats similaires chez le lapin et le rat, avec une colonisation plus rapide de l'implant lorsque l'on réduit la taille des billes. L'utilisation de billes de titane

de plus petite taille pourrait améliorer la réalisation d'un implant fonctionnel au niveau clinique.

# 5.3. Article 5

adhm201200369.sgm Generated by PXE using XMLPublish[SM] June 4, 2013 11:18 APT: WF JID: AHM

Full Paper

Biomedical Implants

N. E. Vrana,* A. Dupret-Bories, P. Schultz, C. Debry, D. Vautier, P. Lavalle .....x–xx

**Titanium Microbead-Based Porous Implants: Bead Size Controls Cell Response and Host Integration**

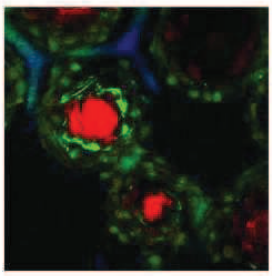

**Microbead-based porous titanium implants with different granulometries significantly affect cell behavior both in vitro and in vivo.** By using smaller microbead, faster filling of the pores is achieved in vitro and also implants with smaller bead size integrated faster with the host in rat and rabbit models. Utilization of such physical features for controlling implant integration can ensure fast, robust attachment for many applications such as dental, tracheal, and hip implants.

adhm201200369.sgm Generated by PXE using XMLPublish[SM] June 4, 2013 11:18 APT: WF JID: AHM

adhm201200369(201200369)

Materials Views
www.MaterialsViews.com

ADVANCED HEALTHCARE MATERIALS
www.advhealthmat.de



Full Paper

# Titanium Microbead-Based Porous Implants: Bead Size Controls Cell Response and Host Integration

*Nihal Engin Vrana,* Agnès Dupret-Bories, Philippe Schultz, Christian Debry, Dominique Vautier, and Philippe Lavalle*

**Keywords:** host *integration; in* vivo; porous implants; titanium; trachea

**ABSTRACT:** Openly porous structures in implants are desirable for better integration with the host tissue. We develop sintered microbead-based titanium implants for oto-rhinolaryngology applications, which create an environment where the cells can freely migrate in the areas between the microbeads. This structure promotes fibrovascular tissue formation within the implant in.vivo. However, this process can take several weeks and might pose risk of infection in implant areas such as trachea. In this study, we determine to what extent these events can be controlled by changing the physical environment of the implants both in vitro and in vivo as obtaining a fast integration of the implant is an important clinical goal. By cell tracking with confocal microscopy, we quantified the distribution of cells within the implants and observed that the size of the beads and the distance between the neighboring beads significantly affect the ability of cells to develop cell-to-cell contacts and to bridge the pores. Live cell staining shows that as the bead size gets smaller (from 500 to 150 µm), the probability to observe cells that fill the porous areas is higher in 7 d. This also affects the initial attachment and distribution of the cells and collagen secretion by fibroblasts (higher extracellular matrix secretion in 150 µm beads over 21 d, $P < 0.05$). Obtaining a fast coverage of the system also enables coculture systems in vitro where, the number and the distribution of the second cell type are boosted by the presence of the first. This concept is utilized in the present study to increase the attachment of vascular endothelial cells by an initial layer of fibroblasts, which can be used for in vitro vascularization. By decreasing the bead diameter, the overall colonization of the implant can be significantly increased in vivo within 3 weeks. The effect of bead size has a similar pattern both in rats and rabbits, with faster colonization of smaller bead-based structures. Using smaller beads would improve clinical outcomes as faster integration facilitates the attainment of functionality by the implant. Overall, integration of titanium microbead-based implants can be finely controlled by changing the bead size, which provides an outline for integration of other implants with well-defined topographical features.

Q1

## 1. Introduction

Titanium is a widely used biomaterial, with a long list of clinical successes in orthopedic and dental implant fields. However, implant integration remains a crucial problem and to overcome this issue, surface modifications have been generally used for improving cell interaction with implants. These modifications involved changing surface roughness,[1] geometry,[2] or applying coatings[3] such as hydroxyapatite. Recently, development of metallic foams with porosities that would allow in-growth of cells in vivo has become a very active area of research.[4]

Dr. N. E. Vrana, A. Dupret-Bories, Dr. P. Schultz, Prof. C. Debry, Dr. D. Vautier, Dr. P. Lavalle, INSERM, UMR-S 1121, "Biomatériaux et Bioingénierie", 11 rue Humann, F-67085 Strasbourg Cedex, France
Dr. N. E. Vrana, Dr. D. Vautier, Dr. P. Lavalle, Université de Strasbourg, Faculté de Chirurgie Dentaire, 1 place de l'Hôpital, 67000 Strasbourg, France, E-mail: engin.vrana@protip.fr
A. Dupret-Bories, Dr. P. Schultz, Prof. C. Debry, Hôpitaux Universitaires de Strasbourg, Service Oto-Rhino-Laryngologie, 67098 Strasbourg, France
**10.1002/adhm.201200369**

adhm201200369.sgm Generated by PXE using XMLPublish[SM] June 4, 2013 11:18 APT: WF JID: AHM

Full Paper



Utilization of metallic foams enables utilization of titanium in soft tissue applications such as tracheal replacement where mechanical properties of the structure are vital.[5] In such structures, understanding the mechanisms of the interactions of the 3D titanium structures with soft tissues is important, but it has not been as widely studied as the interaction of titanium with hard tissues.

There are three modes of integration for metallic implants: (i) in situ where the implant interacts with the cells surrounding it upon implantation; (ii) in vivo where the implant is first implanted in a different area (such as subcutaneous implantation) promoting the integration in a controlled way before the implant is moved to the main target area; *(iii)* in vitro where the relevant cells for the target area are used before implantation. As a good integration improves the functionality of the implants and prevents infection related problems, the development of methods to obtain robust integration in a fast manner is very important for the patients' well being. The topographical properties of the implants are one of the main determinants in all these processes. Effects of topography on the behavior of cells are well documented,[6] where cells respond to topographical cues by alignment, differentiation, self assembly, etc.[7] The micropatterning experiments showed that the distance between the patterns and the size of the patterns are important determinants of cell behavior.[8] Recently, it was also shown that this can even be used for exclusion of microbial attachment on surfaces.[9] As some implantation areas are not sterile (such as tracheal implants), it is important that the integration of implants happens faster than possible biofilm formation by bacteria.

However, there is a gray area between well-controlled 2D topographical features[10] and 3D topographical structures obtained by solid freeform fabrication methods and inherently complex structure of 3D implants and scaffolds,[11] where cells come across a wide array of 3D features. Microbead-based structures falls somewhere in between random pore distribution and fabricated pores, as microbead assembly results in a naturally ordered structure where the bead size determines the size of the pores of the structure (**Figure 1**). Previously, efforts to quantify the effect of 3D pore architecture on cell behavior was mostly done with open and closed cell foams, but since lyophilization and other methods generates random pore size distributions, the results cannot be highly reproducible.[12] Actually reports have shown that in the structurally heterogeneous environment of a foam, cells behave as in 2D cultures when they interact exclusively with the surface of pore walls. But they change their behavior when the pore structure prevents them from spreading in one plane. There is also another line of study that has focused on the effect of the pore size for different cell types to determine the optimal pore sizes that promote colonization. For example, it was shown that polymeric substrates with pores larger than 20 μm can have an adverse effect on vascular endothelial cell growth.[13] *In vivo* this would affect the period of invasion of the scaffold by cells. However, how highly defined 3D pores can be used to modify host integration in vivo has not yet been described. Also, pore size studies have focused on polymeric systems where the pore size can change with cellular activity and degradation, whereas in a metallic system it will be stable during the course of integration.

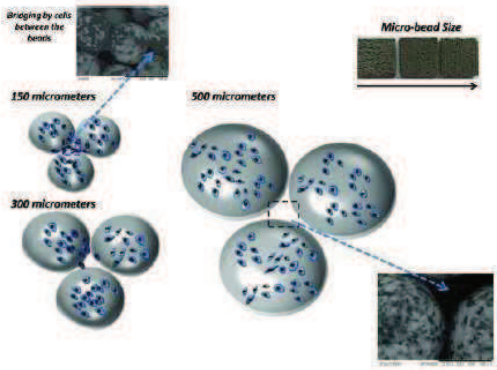


**Figure 1.** Production of implants with different granulometry. It is possible to obtain with different titanium microbeads robust implants with a similar total porosity. Because of the differences in the pore sizes, the attachment and distribution of the cells is distinctly different for different bead size implants, which can be useful for controlling integration period. Inset: the macroscopic view of sample subcutaneous implants with different bead sizes (150, 300, and 500 μm in diameter, respectively).

Microbead-based structures have the advantage of a naturally open pore structure, which would improve in vivo integration. Also, since the interconnectivity is complete, formation of pouches of bacterial growth can be prevented, which is an important advantage in vivo in areas where the implant is in contact with air. Previously we have used microbead-based implants in vivo for tracheal replacement experiments[14] and also checked how coating them with angiogenic factors would affect their vascularization capacity.[15] We have also reported a tracheal implant development protocol in sheep where a first step was intramuscular implantation of the implant for fast colonization and the addition of an epithelial layer on the colonized structure was the second step.[16] However, the integration process was rather slow and we observed through both in vivo and in vitro approaches that 500 μm beads resulted in spaces that took several weeks to become filled by newly formed tissue. We have previously shown how these structures can be improved using a composite based on association of porous titanium with a hierarchically porous system composed of polymers. This hybrid system allowed a better control of colonization and the depth movement of the cells.[17] But such control brings an additional limitation based on polymer degradation, as the pore sizes will change over time due to degradation. Thus, we hypothesized that the size of the individual microbeads can be used to control in vivo implant integration process. By decreasing the bead size, the bridging between the pore areas by the cells can be increased as their ability to move between the subsequent beads is related to the distance. To check this hypothesis, we seeded 3T3 fibroblasts to implants having an identical total thickness but composed of different bead sizes

adhm201200369.sgm Generated by PXE using XMLPublish[SM] June 4, 2013 11:18 APT: WF JID: AHM



and we monitored cell migration in *z* direction. We also quantified the distribution of the cells on the beads and how this was affected by the bead size. Then, we validated our results with in vivo tests. Our previous in vivo experiments showed that the infiltration and filling by fibrovascular tissue might take up to 6 weeks with large beads (500 µm in diameter), thus we checked whether there is a significant difference between different bead size samples in shorter periods of time (2–3 weeks). Another possibility of improving the integration of the implant systems is the seeding of the implants with coculture systems.[18] It has been shown previously that the coculture of vascular endothelial cells (Human Umbilical Cord Vascular Endothelial Cells, HUVEC) with osteoblasts can induce neovessel formation and that the presence of the osteoblasts is an important promoter of this event.[19] Thus, in our study, we also checked whether it would be possible to improve the attachment and proliferation of HUVEC cells over fibroblasts as an additional way to facilitate integration. By utilizing these tools, it would be possible to colonize and functionalize an implant, in our case a tracheal implant, within a shorter time interval.

## 2. Results and Discussion

Control of the bead size should lead to discrepancies in four areas: *(i)* migration and thus distribution of the cells in the 3D architecture; *(ii)* initial cell attachment due to bead curvature; *(iii)* filling of the pore volumes; *(iv)* in vivo integration. For both in vitro and in vivo conditions using smaller beads led to significant differences in these properties.

### 2.1. 3D Distribution of Cells

We first started by observing the distribution of fibroblast cells by scanning electron microscopy (SEM) and confocal microscopy. In SEM images, it was possible to distinguish the difference between the level of interaction of the cells on different beads (**Figure 2**). From large beads to small beads, the cell–cell contacts between the beads changed from nonexistent at 500 µm beads to extensive in 150 µm beads. In 150 µm bead samples, the areas between the beads were occasionally fully filled with cells and possibly with extracellular matrix (ECM) secretions. To quantify and verify ECM presence, the secreted collagen content of the implants were measured over time and it was found that it was significantly higher in the case of 150 µm beads at each time point during a 21-day culture period ($P < 0.05$) (**Table 1**).

To see the position of the cells in these structures after 1 week of seeding, live cells were labeled with Calcein-AM. Confocal images showed that cellular groups holding onto each other were present in the pores of small bead size samples (150 µm), this was not the case for 500 µm beads where cells only stayed on the bead surfaces (**Figure 3**). For large beads, the distance between them is high enough to prevent large-scale cell-to-cell contact between different beads after 7 d. To understand better the extent of this difference and for determining the distribution of the cells after 1 week, *z*-stacks of PKH-26-labeled cell seeded implants were done. PKH-26 is

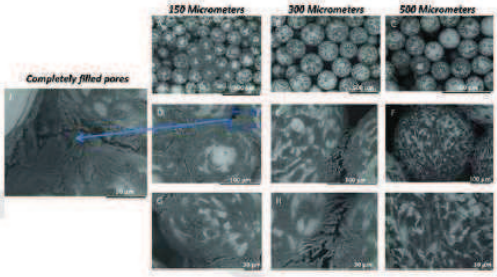


**Figure 2.** SEM images of fibroblasts after 7 d of culture on different bead sizes. For 150 µm bead samples A), D), G), and J), after 7 d, the pores where totally or partially covered by the cells. The dense nature of these areas suggests presence of ECM, which is quantified to be higher in the case of 150 µm beads (Table 1). Bead to bead cell contacts were available but much less in the case of 300 µm beads B), E), and H), whereas for 500 µm beads, they were nearly nonexistent and cells covered preferentially on the surface of the beads C), F), and I) particularly the top part.

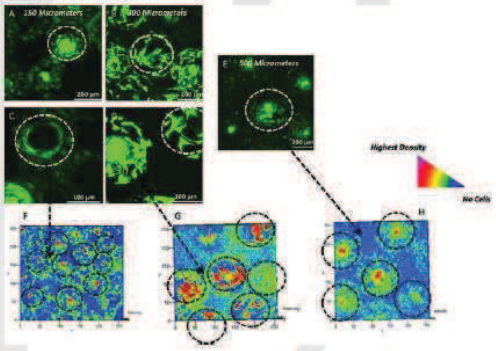


**Figure 3.** A–E) Calcein-AM staining of the fibroblasts on different bead sizes after 7 d, the areas between the beads is bridged by groups of cells in the case of 150 µm beads, whereas similar bridging is scarce in the case of 300 µm beads. Cells were solely present on the beads for 500 µm samples. F–H) Contour graphs of PKH-26-labeled cells after 7 d, red color means high number of cells, blue color means absence of cells, and green color means intermediate level. Cell presence in the pores distinctly decreases from small beads to larger beads also distribution of the cells shows distinct differences, a more diffuse hot spot regions for 300 µm beads, concentration on the apex for 500 µm beads and a more equilibrated distribution for 150 µm beads.

an appropriate dye to monitor long-term migration.[20] The intensity of the signal was converted to contour graphs by color encoding the fluorescence signal intensity within the 3D reconstructions (Zeiss LSM Confocal Imaging Software, Germany) (Figure 3F–H). These graphs show that the cells' preference

adhm201200369.sgm Generated by PXE using XMLPublish[SM] June 4, 2013 11:18 APT: WF JID: AHM



Materials Views
www.MaterialsViews.com

ADVANCED HEALTHCARE MATERIALS
www.advhealthmat.de

**Table 1.** Secreted collagen amounts by fibroblasts seeded on different bead size samples. Mean values of $n \geq 3$ samples and standard deviations.

| Collagen amount [μg] | 150 μm | 300 μm | 500 μm |
|---|---|---|---|
| Day 7 | 6.56 ± 0.60 | 5.97 ± 0.02 | 4.74 ± 0.27 |
| Day 14 | 15.72 ± 0.65 | 7.40 ± 0.44 | 9.74 ± 0.30 |
| Day 21 | 23.37 ± 1.03 | 16.81 ± 0.53 | 15.77 ± 0.37 |

changes significantly with respect to bead size. For all bead sizes, it was possible to see a high cell concentration at the apex, but as the bead size gets smaller cells start to follow the curvature of the beads and the distribution around the beads themselves gets higher. For 500 μm beads, cells were mostly on the top of the beads and the pore areas were nearly empty. In 300 μm beads there were hotspots for cells (higher cell density areas) as streaks on large areas of the bead surface but the pore areas were still scarce in cells. In 150 μm bead size samples, it was possible to observe from 3D stacks, cells around the central portion of the beads and also in between the beads (data not shown). So with respect to the location of the cell signal, it was seen that most of the cells in the case of large beads are located on the top of the beads, whereas in the case of the 300 μm beads, more cells could be seen in the periphery. In the case of 150 μm beads, cells were not only on the periphery of the beads but also in between the bead areas. After 7 d, there were pores in 150 μm samples that were partially covered.

### 2.2. Fibroblast Migration

The ability of the lamellapodia of the fibroblastic cells to assess the material surface and to determine the movement direction of the cells is a well-defined process.[21] Fibroblastic cells send lamellapodia to sense the surface chemistry and topography in front of them. The decision to move forward would then depend on establishment of a strong contact with the target area. This mechanism is well known in 2D movement however in in vivo conditions the presence of lamellapodia is less significant.[22] The movement in a porous structure is more similar to 2D migration since the cells interact with a 2D surface and then make decisions on how to navigate in the 3D environment. This is unlike in vivo conditions where the cells are surrounded by ECM. Thus, while moving within porous structures, especially when the pore walls are distant to each other, a cell might not be able to extend across the walls. So as a result, in the case of microbead-based structures, the cell would prefer to reside on the bead it has already attached to and to move on it. The previously observed results of the differential effect of pore sizes on cellular movement can be attributed to the fact that, the migration of fibroblastic cells in 3D would have a better chance of encompassing the distances between the small pores. However, classical porous systems that are created by methods like freeze-drying, freeze-extraction, etc., have their pore interconnectivity *via* junctions, which can act as bottlenecks for overall cellular movement. In the open porous structure in the current study, this effect was not a problem and the differences observed were solely due to the limitations on the cellular movement.

To see how the microbead-defined pore structure affect 3D migration in our implants, the next step was the determination of the effect of the bead size in the movement of the cells in $z$ direction. For this end, PKH-26-labeled cells were monitored at days 4, 7, and 14 by confocal microscopy up to the depth where no cells were observed (maximum migration distance), to quantify overall movement of the cells (**Figure 4**). The migration pattern of the cells within the different bead size structures was significantly different ($P < 0.05$ at depth 200 μm at day 4 and at depth 50 μm at days 7 and 14). Cells initially went deeper in larger bead size implants, but their distribution on each layer was sparser compared with smaller bead size counter parts. Surface curvature seems to be an important factor in the distribution of the cells: as the bead sizes gets larger, the surface curvature decreases (where mean curvature is $1/R$) and cells experience a more planar surface where they can attach and spread easily. Whereas, as the bead size gets smaller, cells face a more curved surface which pushes them more to the central areas than the apex. Also decreasing the bead size decreases the specific surface area per bead which gives less area to cells to attach thus forcing them to move between the beads. However, this effect is compensated by the packing effect, as more small beads can be packed in a given volume, thus decreasing the contribution of the specific surface area between a 3D structure made of small beads and large beads. The sintering of the beads also creates contact points between the beads which facilitates movement of the cells. Moreover, cells tend to accumulate around these areas and then are able to cross the pores which provides them with more area to move. The cells were able to reach to the other side of the implant, as evidenced by their presence observed by confocal microscopy (Figure 4B). The decrease in the depth on day 14 was due to the amplified diffusion limitations due to the increase in overall cell number in all implants. Recently, it has been shown that the responses of the cells to the geometrical obstacles are an important parameter for their behavior.[23] As fibroblastic cells tend to migrate as a whole front, when they come across an obstacle they can go through it by bridging, whereas this would not be possible for cells that migrate alone. This property of fibroblasts is an important contributor to the results observed in this study.

### 2.3. In Vivo Integration

*In* vivo, cellular response followed a similar pattern, regardless of the model animal, where smaller bead sizes caused increased infiltration and also maturation of the infiltrated tissue. First, subcutaneous implantation of the different bead size implants to rats was tested (**Figure 5**). The outer surfaces of the implants were more covered with tissue in the case of small bead sizes

adhm201200369.sgm Generated by PXE using XMLPublish[SM] June 4, 2013 11:18 APT: WF JID: AHM





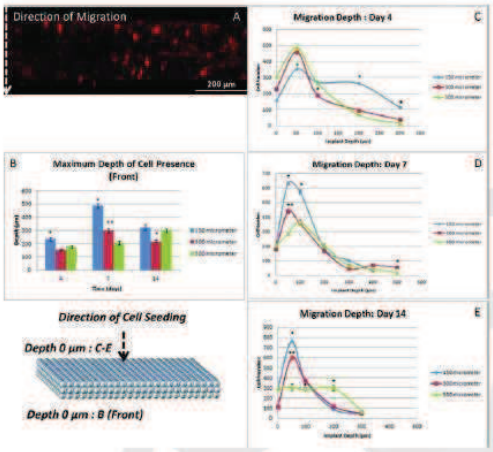


**Figure 4.** Fibroblast migration through the implants with different bead sizes. A) Representative cross-section of the migration samples. B) The maximum depth where cells were detected to the opposite face to where the cells were seeded (front). Depth 0 denotes the point where the implants touch the transwell surface where cells are seeded at the other side (which would denote 1,500 µm depth). For days 4 and 7, depth of reach was significantly higher for 150 µm samples ($P < 0.05$) ($n \geq 3$, error bars denote standard deviation. * signifies statistical significance with the marked sample with the others and ** signifies statistically significant difference between all three samples).C–E)z-direction distribution of cells on different bead size implants over course of 2 weeks with respect to their movement from their seeding position (Denoted as 0 depth). Initially, on 150 µm bead samples, cells were able to settle deeper, whereas over the course of migration, thick layers of cells closer to the seeding surface prevailed. A similar, but less pronounced behavior was observed for 300 µm bead samples, whereas for 500 µm bead samples initial movement was mostly limited to first 100 µm and then a homogenous distribution of the cells close to the implant surface was observed after 14 d. Cell number is calculated with an average of 26 stacks and image sizes of 920 × 920 µm$^2$ ($n = 8$ for each time point, with three images per stack for each sample).

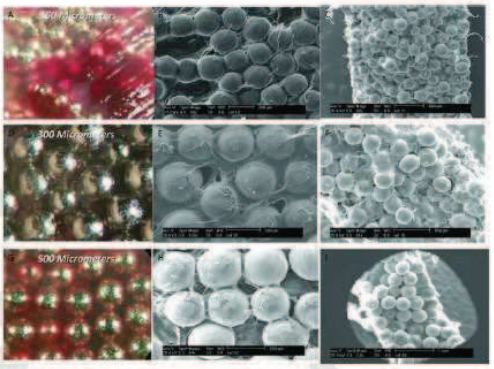


**Figure 5.** Subcutaneous implantation of the different bead size implants to rats for a 3-week period. A), D), and G) Macroscopic view of the freshly explanted implants, 150, 300, and 500 µm bead size respectively. B), E), and H) Surface of the explanted implants. The coverage by the cells decreases for the 500 µm bead size implants. Unlike in vitro conditions cells tend to move deeper into the implants. C), F), and I) SEM images of the cross-section of the explanted implants; colonization of the core of the implant decreases as the bead size increases. Large empty areas were visible in the case of 500 µm bead size.

(Figure 5A, D, and G). The attachment of the implant to the subcutaneous area was not significantly different as the measurements of the mean force necessary to remove the implants during explantation with a custom-made dynamometer were not statistically significant (data not shown). At the surface, similar to the in vitro observations, the filling of the pores was more effective than in the small bead size samples (Figure 5B, E, and H). The SEM analysis of the cross-section of the implants showed that the migration was impeded into the depth of the larger bead size implants, whereas in smaller bead size implants, the coverage was full (Figure 5C, F, and I). The main difference between the in vivo and in vitro observations was that in vivo the colonization of the middle implant zone was faster due to the increased speed of migration for all implants, particularly for 300 µm bead implants. Distribution of the cells proved that the implant shape related differences in cell behavior persist under in vivo conditions and by controlling the bead size, the rate of integration of the implant can be easily controlled. Another discrepancy observed was at certain areas 300 µm bead implants had higher infiltration, due to the high compaction of 150 µm beads in some areas. This effect can be rectified by using a mixture of different bead size to control the compaction of the beads, i.e., the pore size.

All implants were mostly covered, but the vascularization of the smaller bead size implants was better. In rabbits, angiogenesis was even more apparent in smaller bead sizes as well developed veins and arteries were visible on the implants (**Figure 6**).

Histological analysis of the samples explanted from rabbits after subcutaneous implantations showed that the bead size also has a qualitative effect on the integration process. For 150 and 300 µm samples, a maturing connective tissue was clearly present between the beads deep into the scaffolds (the extent of the tissue was higher for 150 µm samples), whereas only a fibrous tissue coverage was present in the case of 500 µm samples (Figure 6). There is a clear correlation between our in vitro observations and the integration process monitored in.vivo. This will be especially beneficial for having control over initial inflammatory response as the interaction of macrophages with implant surfaces is an important determinant of successful implant integration.[24]

  

adhm201200369.sgm Generated by PXE using XMLPublish[SM] June 4, 2013 11:18 APT: WF JID: AHM



Materials Views
www.MaterialsViews.com

ADVANCED HEALTHCARE MATERIALS
www.advhealthmat.de

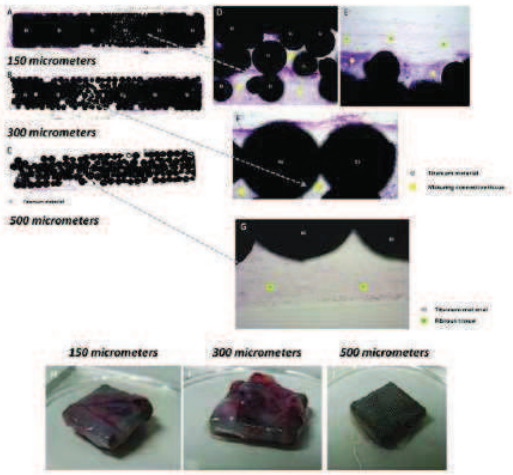


**Figure 6.** H&E staining of implants with different bead sizes after subcutaneous implantation in rabbits: A), D), E) 150 µm; B), F) 300 µm, and C), G) 500 µm. A maturing connective tissue penetrated into the pore areas for 150 and 300 µm samples, whereas the in-growth and tissue maturation was lower when the bead size was bigger. H–J) Explants of different bead sizes from rabbits. The level of tissue integration vascularization was higher on 150 and 300 µm bead samples.

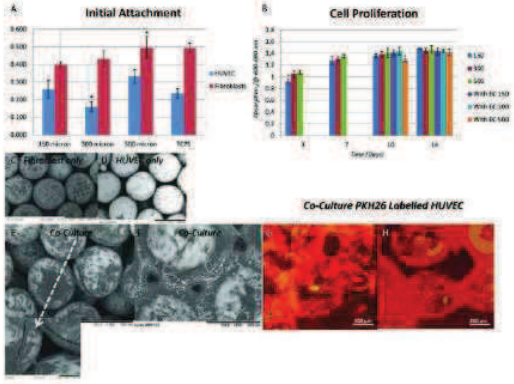


**Figure 7.** Fibroblast cell attachment and proliferation on different bead sizes and coculture with vascular endothelial cells. A) Cell attachment was higher on bigger bead sizes. B) Cell proliferation followed a similar rate for all bead sizes for 14 d, which shows that the difference in integration is independent of cell growth (bead size was 500 µm, EC denotes endothelial cell presence). SEM images of: C) only fibroblasts; D) only HUVEC cells after 7 d; E) when fibroblasts and HUVEC cells were cocultured, surface coverage dramatically improved after 7 d; F) after 7 d of coculture some pores were totally covered. G) and H) Confocal images showed that PKH-26-labeled HUVEC cells contributed to the coverage more when they are cocultured.

### 2.4. Coculture Conditions

To assess whether the cell behavior discrepancies observed on different bead size samples is cell type dependent, we have quantified the cell initial attachment and proliferation for 3T3 fibroblasts and HUVEC both alone and in coculture (**Figure 7**). As the cell suspension goes through the implant, the 500 µm beads provide a large surface for cells to attach and to form a layer on them. Because of this, the initial attachment quantified as the cell number 24 h post-seeding on the 500 µm bead implants was the highest (Figure 7A). This tendency was similar for both 3T3 and HUVEC cells. However, this does not directly result in a higher proliferation in long term (Figure 7B). The differences in proliferation were not always statistically significant ($P > 0.05$) and by 14 d, the cell numbers were at comparable levels for all bead sizes. Thus, the differences in the integration are not related to the differential cell numbers. Cell growth was not the main driving force behind the differences observed in the cell distribution as the cell numbers are similar for all bead sizes.

For both cell types tested, the trend was similar in the case of initial attachment where larger bead sizes caused higher attachment of cells overall. The size of the beads do not influence cell proliferation in the case of 3D structures presented in this work, but for single alginate microcarrier beads, it has been recently shown that an inverse relationship between the bead size and cell proliferation was observed.[25] However, this was done under bioreactor conditions, where also the shear stress can be a major affecting factor. In the current work, the differences seen in the mode of integration is due to the cell distribution and their differential ability to interact on beads with different sizes. With smaller beads, cells on adjacent beads can form contacts and move between the beads, which enable an increased filling of the structure without a strong increase in cell proliferation.

Previous works concerning the relation between pore size and cell behavior used the pore size as the main parameter[26] while the geometrical structure induced by the pores is generally not considered. The importance of the distinction between the pore architecture and porosity has been recently shown with the behavior of mesenchymal stem cells on CAD designed gyroid-shaped PLLA scaffold versus salt leached scaffolds of comparable porosity. The gyroid structure by virtue of having an equal interconnection at each point had better cell distribution compared with the salt leached counterpart.[27]

The cell movement largely depends on the geometry and the surface properties such as charge[28] which can be tuned by applying certain coating procedures, as demonstrated previously for anti-inflammatory response on titanium surfaces.[29] Another possibility is to use a "precursor" layer of fibroblasts as a coating to improve the behavior of another cell type. This concept has been used with vascular endothelial cells, which are important actors in the cases where in vitro vascularization is necessary.[30] By themselves, HUVEC cells were able to attach titanium implants but their proliferation and ability to cover titanium surfaces was quite low (Figure 7D). However, when

adhm201200369.sgm Generated by PXE using XMLPublish[SM] June 4, 2013 11:18 APT: WF JID: AHM









they are seeded onto fibroblast seeded implants (Figure 7E), this caused an increase in their distribution even for the 500 μm bead implants. Moreover, their ability to bridge the beads is also increased as evidenced by PKH-26 stained samples (Figure 7G and H). Large areas were covered under these conditions and sprouting structures were observed showing that a natural coating of the surface by cells can act as a promoter of a secondary cell attachment. It has been shown previously that endothelial cells sprout within hydrogel environments.[31] In the present case, the contacts and the secretions of the underlying fibroblasts provided these cues. The functionality of HUVEC cells was checked with NO secretion levels which were similar for all bead size implants and not detectable where only fibroblasts were seeded on the samples (data not shown). The ability of fibroblast layers to support HUVEC cells were also validated by 2D experiments of preseeded fibroblasts, which showed that a 7-d culture period provides a better surface for cell attachment. As controlling bead size affects fibroblast population, together with the effect of fibroblast presence on HUVEC cells, an exponential decrease in the integration period can be foreseen by using this strategy mix.

## 3. Conclusion

The ability to control the colonization by changing the bead size of the building blocks is an example of how modular approaches in biomedical field can be used for improving in vivo outcomes. The current study shows that by arranging the architecture of a porous structure, it is possible to influence and facilitate cellular migration and host integration. The ability to cover open volumes by cells in vitro and in vivo will enable faster formation of functional tissue. By controlling the interaction of the cells with single beads, it might also be possible to obtain better osteoblast infiltration for bone applications or better periodontal closure in dental applications. We have been working on demonstrating that the surfaces obtained after subcutaneous implantation are suitable for promoting respiratory epithelium,[32] which would improve dramatically the clinical success of these implants as tracheal substitutes. Our current work focuses on utilization of this system for tissue substitution, particularly for full tracheal replacement in rabbits.

## 4. Experimental Section

*Implant Production* Medical grade pure titanium beads with different granulometry ranges were separated into three groups (150–250, 300–400, and 400–500 μm, respectively) and then in molds were meshed together with an electrical arc. After sintering, the final implants that are 1.5 mm thick were cleaned in acetone in an ultrasonicated bath and sterilized first with UV and then 70% ethanol before in vitro cell culture experiments and implantation.

*Cell Culture*: i) Fibroblast Cell Culture: NIH-3T3 fibroblasts were cultured in RPMI 1640 medium (Gibco, USA) with 10% fetal bovine serum and Pen/strep. The implants were sterilized by 70% ethanol for 2 h and then washed with sterile PBS and placed into cell culture plates. Confluent cells were removed with triple express enzyme cocktail (Invitrogen, USA). Total cell number was determined with a a hemocytometer and the cells were marked with PKH26 fluorescent red cell linker (Sigma–Aldrich) according to the providers instructions. Marked cells were seeded onto the implants at a concentration of $2 \times 10^6$ cells implant$^{-1}$. Medium was changed twice a day and at day 7, samples were fixed with 4% glutaraldehyde and gold coated and observed with SEM ($n \geq 3$). For each bead size sample at day 7, cells were labeled with Calcein-AM used as per instructions of the provider (Invitrogen). Briefly the culture was then supplemented with Calcein-AM containing medium with the final concentration of Calcein-AM as 5 μM. Then the cells were incubated at 37 °C for 1 h, washed with medium and PBS, and fixed with 3.7% paraformaldehyde. The cell–cell interactions of Calcein-AM-labeled cells were checked with confocal microscopy (Zeiss LSM 510, Germany) to see the bridging of the pores by multiple cells. For the migration of the cells fibroblasts were labeled with PKH-26 and the *z*-stacks of the samples from both bottom and top were taken at days 4, 7, and 14. For each sample, at least 26 stacks were analyzed by Image J software (NIH, USA) between the top layer (where the cells were seeded) and the layer where when the signal is lost. Cell number at each stack was determined.

To determine cell proliferation, samples were seeded with $1 \times 10^5$ cells implant$^{-1}$ and then cell numbers were determined over a course of 2 weeks with TOX8 (Sigma–Aldrich) assay. This is a Resazurin-based assay, where cell number can be inferred from the decrease in the absorption of the dye in 600 nm due to metabolic activity. The level of cell attachment was determined with a test at 24 h time point. The test was done on samples up to 14 d with a 2 h of incubation and with readings at reference wavelength of 690 nm. As positive control TCPS was used ($n \geq 6$).

ii) HUVEC Culture and Coculture Experiments: HUVEC (PromoCell, Germany) were used at passage 4–5 for all experiments. Cell culture was done with Endothelial Cell Growth Medium (PromoCell, Germany) with supplement mix and 1% Pen/Strep. For coculture experiments, fibrobalst seeded samples were seeded with $1 \times 10^5$ HUVEC at day 7 and the total medium is changed to endothelial growth medium. Separate experiments with the fibroblasts showed that this medium does not cause death of the fibroblasts but stops their growth. To differentiate between the fibroblasts and HUVEC cells, HUVEC cells were marked with PKH-26 and after 7 d they were observe with both confocal microscopy and SEM (Hitachi TM100) after fixation.

iii) Collagen Determination: The amount of collagen over a course of 3 weeks was determined by Chondrex Semi-Quantitative Collagen Micro-assay kit (Chondrex, USA) as per providers instructions. Briefly, the samples were incubated in Kit dye solution for 30 min and after washing with PBS, the dye that bind to collagen was extracted with extraction solution and the absorption of the solution was measured at 540 and 605 nm (Multiplate reader Multiskan EX from Thermo Scientific, France). The amount of collagen (in μg) was calculated from

  

adhm201200369.sgm Generated by PXE using XMLPublish[SM] June 4, 2013 11:18 APT: WF JID: AHM



Materials Views
www.MaterialsViews.com

ADVANCED HEALTHCARE MATERIALS
www.advhealthmat.de

the following equation:

$$\text{Collagen amount} = [OD_{540\,nm} - (OD_{605} * 0.291)]/37.8 * 1000$$

*In Vivo Experiments:* i) Rats: After Wistar rats ($n \geq 6$) were anesthetized with intraperitoneal administration of ketamine (20 mg kg$^{-1}$, Ketamine 500®; Virbac France) in combination with midazolam (10 mg kg$^{-1}$, Mydazolam®; Mylan, France) and atropine (0.25 mg kg$^{-1}$). They were placed in the prone position.[14] Surgical procedures were performed under standard aseptic conditions. A single dorsal incision was made in the lower back to expose the paraspinal muscles.

Four titanium plates with same porosimetry were implanted into sockets made within the paraspinal muscle (two on the right side and two on the left side of the incision). Each plate was sutured to the muscles with one stitch (vicryl 4.0). After rinsing with saline, the wound was closed in layers. Two weeks after surgery, the animals were euthanized with an overdose of sodium thiopenthal (100 mg kg$^{-1}$). The implants with surrounding tissues were excised.

ii) Rabbits: The surgery was performed under general anesthesia. Anesthesia was induced by intramuscular administration of ketamine (30 mg kg$^{-1}$) in combination with midazolam (0.2 mg kg$^{-1}$), and xylazine (3 mg kg$^{-1}$) and assisted ventilation ($O_2$:1 min$^{-1}$).[32]

The operation was performed under sterile conditions. With the animal (New Zealand White Rabbits) in the prone position a single dorsal incision was performed in the lower back to expose the paraspinal muscles.

Four titanium plates with different porosimetry were implanted into sockets made within the paraspinal muscle (two on the right side and two on the left side of the incision). Each plate was sutured to the muscles with one stitch (vicryl 3.0). After rinsing with saline, the wound was closed in layers. Postoperative analgesia was maintained by fentanyl patch (3 µg, Fentanyl-Mepha®;Mepha Pharma, Austria) for 3 d. Two weeks after the rabbit was euthanized with an intravenous overdosed of sodium pentobarbital (120 mg kg$^{-1}$) after intramuscular administration of anesthesia (same protocol previously described). The implants with surrounding tissues were excised.

iii) Explantation and Histology: After 3 weeks, the subcutaneous implants were explanted after intramuscular administration of anesthesia. Sectioning of the implants and hemotoxylin and eosin staining was done as reported previously.[14] Histological analyses were performed at the IMM (Institut Mutualiste Monsouris, Paris, France), where the blinded analyses were performed by two pathologists not involved in the project.

iv) Statistical analysis: Statistical significance between different bead sizes was tested with one-way ANOVA test together with Tukey's honest significant difference test for each time point (significance limit $P \leq 0.05$).

## Supporting Information

Supporting Information is available online from the Wiley Online Library or from the author.

*Acknowledgements*

Authors would like to thank Dr. A. Walder from ONERA, (Office National d'Etudes et de Recherche Aérospatiale) for providing titanium samples. We thank Pr. J.-H. Lignot from IPHC-DEPE-CNRS (Strasbourg) for SEM and Dr. G. Prevost from Institute of Bacteriology (University of Strasbourg) for his help with animal experimentation. We acknowledge the PMNA (Pôle Matériaux et Nanosciences d'Alsace), Région Alsace, Communauté Urbaine de Strasbourg and EuroTransBio "BiMoT" project (ETB-2012-32) for financial contribution

Received: MM DD, YYYY
Revised: MM DD, YYYY
Published online: MM DD, YYYY

[1] B. Baharloo, M. Textor, D. M. Brunette, *J. Biomed. Mater. Res. Part A.* **2005**, *74A*, 12.
[2] C. Matschegewski, S. Staehlke, R. Loeffler, R. Lange, F. Chai, D. P. Kern, U. Beck, B. J. Nebe, *Biomaterials* **2010**, *31*, 5729.
[3] S. Werner, O. Huck, B. Frisch, D. Vautier, R. Elkaim, J. C. Voegel, G. Brunel, H. Tenenbaum, *Biomaterials* **2009**, *30*, 2291.
[4] G. Ryan, A. Pandit, D. P. Apatsidis, *Biomaterials* **2006**, *27*, 2651.
[5] L. M. Janssen, G. van Osch, J. P. Li, N. Kops, K. de Groot, L. Feenstra, J. A. U. Hardillo, *J. Tissue Eng. Regener. Med.* **2010**, *4*, 395.
[6] K. Anselme, P. Davidson, A. M. Popa, M. Giazzon, M. Liley, L. Ploux, *Acta Biomater.* **2010**, *6*, 3824.
[7] J. N. H. Shepherd, S. T. Parker, R. F. Shepherd, M. U. Gillette, J. A. Lewis, R. G. Nuzzo, *Adv. Funct. Mater.* **2011**, *21*, 47.
[8] E. Vrana, N. Builles, M. Hindie, O. Damour, A. Aydinli, V. Hasirci, *J. Biomed. Mater. Res. Part A.* **2008**, *84A*, 454.
[9] Y. Wang, G. Subbiahdoss, J. Swartjes, H. C. van der Mei, H. J. Busscher, M. Libera, *Adv. Funct. Mater.* **2011**, *20*, 3916.
[10] M. M. Stevens, J. H. George, *Science* **2005**, *310*, 1135.
[11] V. Karageorgiou, D. Kaplan, *Biomaterials* **2005**, *26*, 5474.
[12] Y. Huang, M. Siewe, S. V. Madilhally, *Biotechnol. Bioeng.* **2006**, *93*, 64.
[13] D. Narayan, S. S. Venkatraman, *J. Biomed. Mater. Res., Part A.* **2008**, *87A*, 710.
[14] P. Schultz, D. Vautier, A. Charpiot, P. Lavalle, C. Debry, *Arch. Oto-Rhino-Laryngol.* **2007**, *264*, 433.
[15] S. Muller, G. Koenig, A. Charpiot, C. Debry, J. C. Voegel, P. Lavalle, D. Vautier, *Adv. Funct. Mater.* **2008**, *18*, 1767.
[16] A. Dupret-Bories, P. Schultz, N. E. Vrana, P. Lavalle, D. Vautier, C. Debry, *J. Rehabil. Res. Dev.* **2011**, *48*, 851.
[17] N. E. Vrana, A. Dupret, C. Coraux, D. Vautier, C. Debry, P. Lavalle, *PLoS ONE* **2011**, *6*.
[18] C. J. Kirkpatrick, S. Fuchs, R. E. Unger, *Adv. Drug Deliv. Rev.* **2011**, *63*, 291.
[19] A. Hofmann, U. Ritz, S. Verrier, D. Eglin, M. Alini, S. Fuchs, C. J. Kirkpatrick, P. M. Rommens, *Biomaterials* **2008**, *29*, 4217.
[20] W. Christian, T. S. Johnson, T. J. Gill, *J. Biomed. Sci. Eng.* **2008**, *1*, 163.
[21] G. Albrechtbuehler, *J. Cell Biol.* **1976**, *69*, 275.
[22] J. S. Harunaga, K. M. Yamada, *Matrix Biol.* **2011**, *30*, 363.
[23] R. J. Mills, J. E. Frith, J. E. Hudson, J. J. Cooper-White, *Tissue Eng. Part C* **2011**, *17*, 999.
[24] S. Gordon, *Nat. Rev. Immunol.* **2003**, *3*, 23.
[25] J. J. Schmidt, J. Jeong, H. Kong, *Tissue Eng. Part A* **2011**, *17*, 2687.
[26] F. J. O'Brien, B. A. Harley, I. V. Yannas, L. J. Gibson, *Biomaterials*

  

adhm201200369.sgm Generated by PXE using XMLPublish[SM] June 4, 2013 11:18 APT: WF JID: AHM









**2005**, *26*, 433.
[27] F. P. W. Melchels, A. M. C. Barradas, C. A. van Blitterswijk, J. de Boer, J. Feijen, D. W. Grijpma, *Acta Biomater.* **2010**, *6*, 4208.
[28] D. Vautier, J. Hemmerle, C. Vodouhe, G. Koenig, L. Richert, C. Picart, J. C. Voegel, C. Debry, J. Chluba, J. Ogier, *Cell Motil. Cytoskeleton* **2003**, *56*, 147.
[29] P. Schultz, D. Vautier, L. Richert, N. Jessel, Y. Haikel, P. Schaaf, J. C. Voegel, J. Ogier, C. Debry, *Biomaterials* **2005**, *26*, 2621.
[30] A. Alajati, A. M. Laib, H. Weber, A. M. Boos, A. Bartol, K. Ikenberg, T. Korff, H. Zentgraf, C. Obodozie, R. Graeser, S. Christian, G. Finkenzeller, G. B. Stark, M. Heroult, H. G. Augustin, *Nat. Meth.* **2008**, *5*, 439.
[31] K. T. Morin, R. T. Tranquillo, *Biomaterials* **2011**, *32*, 6111.
[32] N. E. Vrana, A. Dupret-Bories, C. Bach, C. Chaubaroux, C. Coraux, D. Vautier, F. Boulmedais, Y. Haikel, C. Debry, M.-H. Metz-Boutigue, P. Lavalle, *Biotechnol. Bioeng.* **2012**, *8*, 2134.

  

# Partie 6 : Le larynx artificiel, première application clinique

# Partie 6 : Le larynx artificiel, première application clinique

# 6.1. Introduction à l'article 6

Après plus d'une dizaine d'année de travail de recherche, notre équipe a réalisé la première implantation clinique mondiale d'un larynx artificiel chez un patient ayant bénéficié d'une laryngectomie totale pour raison carcinologique (Implantation of an artificial larynx after total laryngectomy- Protocol NCT01474005 http://clinicaltrials.gov/).

Le larynx artificiel est constitué de 2 parties, une structure inamovible d'une part, qui vise à prolonger la trachée proximale qui reste après laryngectomie totale et une valve supérieure d'autre part, structure amovible, synchronisant les fonctions respiratoire et digestives.

La partie inamovible est constituée d'un assemblage de microbilles de titane et de titane plein. Sa conception, ainsi que le protocole opératoire d'implantation, découlent directement des expérimentations réalisées chez le gros animal (article 1). Les procédures d'autorisation d'un tel essai clinique étant très longues à obtenir, nous n'avons pu intégrer à cette prothèse les modifications qui auraient été nécessaires au vu des résultats des expérimentations décrites dans les articles 2, 3, 4 et 5. Ces éléments seront intégrés lors de la conception de nouvelles prothèses pour les essais ultérieurs.

La partie amovible de la prothèse, créée grâce à un partenariat industriel (PROTiP, France), est formée d'un système de double valve autorisant la respiration et la déglutition. Cette prothèse amovible a fait l'objet de tests cliniques parallèles pour la prise en charge de troubles majeurs de la déglutition au sein de notre service au CHU de Strasbourg (« Mise en place d'une prothèse intralaryngée avec valve trifonction dans les troubles majeurs de la déglutition », Etude HUS 3866). La prothèse était alors implantée, sous endoscopie, entre les cordes vocales, les valves surplombant le niveau des arythénoïdes de 1.5 cm. Aucune obstruction des prothèses n'a été mise en évidence.

Dans cet article nous décrivons les 2 étapes chirurgicales nécessaires à la mise en place du larynx artificiel et analysons les résultats de cette première implantation clinique avec un suivi de 8 mois. L'article 6 est en cours de révision dans la revue Head and Neck.

# 6.2. Résumé de l'article 6

**Introduction :** La laryngectomie totale induit pour les patients une perte de leur intégrité physique avec des retentissements psychologiques majeurs. L'objectif du larynx artificiel est de remplacer les fonctions laryngées et ainsi d'améliorer la qualité de vie des patients devant bénéficier d'une laryngectomie principalement pour raison carcinologique.

**Méthodes:** Nous rapportons, avec un suivi de 8 mois, le premier cas d'implantation d'un larynx artificiel chez un patient ayant bénéficié d'une laryngectomie totale pour un carcinome épidermoïde du sinus piriforme. Nous décrivons la prothèse laryngée, les 2 étapes chirurgicales d'implantation et le devenir du patient. Le larynx artificiel est composé de 2 structures: i) une prothèse inamovible incluant un anneau en titane poreux qui prolonge la trachée restante après laryngectomie totale, implantée lors de la première procédure chirurgicale. ii) une prothèse amovible constituée de 2 valves concentriques autorisant la respiration et la déglutition; cette prothèse est implantée sous endoscopie dans un second temps opératoire. Les suivis de la tolérance clinique de l'implant et de son intégration aux tissus ont été réalisés par des contrôles nasofibroscopiques rétrogrades via l'orifice de trachéotomie et par imagerie (tomodensitométrie, transit œsogastroduodénal).

**Résultats:** En post-opératoire, les fonctions de respiration, déglutition, d'odorat par les voies aériennes supérieures ont été partiellement restaurées. Le patient a été capable de parler avec une voix chuchotée lors de la fermeture provisoire de l'orifice de trachéotomie. A 8 mois le processus de colonisation de l'anneau en titane poreux de l'implant était visible. Aucune fistule pharyngo-cervicale n'a été mise en évidence (transit œsogastroduodénal).

**Conclusions:** La description de ce cas montre que, par l'utilisation du larynx artificiel, la fermeture de l'orifice de trachéotomie chez un patient laryngectomisé est envisageable de même que la restauration des fonctions laryngées. Par l'amélioration de la prothèse, nous espérons pouvoir restaurer totalement les fonctions laryngées et ainsi éviter la réalisation d'un trachéostome définitif chez les patients laryngectomisés.

# 6.3. Article 6

LARYNGEAL REPLACEMENT WITH AN ARTIFICIAL LARYNX AFTER TOTAL LARYNGECTOMY: IS IT POSSIBLE TO RESTORE LARYNX FUNCTIONALITY IN THE FUTURE?

**Christian Debry[1,2,3*], MD, PhD; Agnes Dupret-Bories[1,3], MD; Nihal Engin Vrana[4], PhD; Patrick Hemar[3], MD; Philippe Lavalle[1,2], PhD; Philippe Schultz[1,3], MD, PhD**

[1]Institut National de la Santé et de la Recherche Médicale, INSERM, UMR-S 1121, "Biomatériaux et Bioingénierie", 11 rue Humann, F-67085 Strasbourg Cedex, France

[2]Faculté de Chirurgie Dentaire, Université de Strasbourg, 1 Place de l'Hôpital, 67000 Strasbourg, France

[3]Hôpitaux Universitaires de Strasbourg, Service Oto-Rhino-Laryngologie, 67098 Strasbourg, France

[4] Protip SAS, 8 Place de l'Hôpital, 67000, Strasbourg, France

*To whom correspondence should be addressed: Prof. Christian Debry, Phone: +33 38 8127652 , e-mail: christian.debry@chru-strasbourg.fr

**Funding**:
This study has been funded by Fédération de Médecine Translationnelle de Strasbourg (FMTS), Université de Strasbourg, France, and Ligue contre le cancer Alsace, France.

**Running Title:** Laryngeal Replacement with an Artificial Larynx

**Keywords:** Laryngectomy, Tracheostomy, Titanium, Artificial Larynx, Cancer

**Abstract**:

**Background:** Most patients perceive total laryngectomy as a mutilation carrying with it a loss of physical and psychological integrity. Thus, an artificial larynx system that can replace the laryngeal functions would significantly improve the life quality of the afflicted patients.

**Methods:** This report presents the first case- in an ongoing clinical trial- of laryngeal rehabilitation using an artificial larynx following total laryngectomy for squamous cell carcinoma, for an eight month follow-up period. We depict the prosthesis' features, our two-step surgical procedure, and the outcome. The prosthesis is formed of two parts: i) a tracheal prosthesis with a porous titanium junction with trachea which was implanted in the first step to ensure its colonization. ii) a removable part composed of concentric valves that enables inhalation and exhalation. The second part was implanted endoscopically. The implant was monitored with retrograde nasofibroscopy of the tracheal prosthesis lumen and CT scans over a course of eight months.

**Results:** The patient's functioning in the relevant postoperative problem areas, such as swallowing, breathing, and smelling has significantly improved. The patient was able to talk in a whispering fashion while the tracheostomy was temporarily closed. The implants porous part was in the process of being colonized by the surrounding tissue and no fistulas were observed evidenced by barium swallow.

**Conclusions:** As the current case shows, tracheotomy closure can be performed, and laryngeal functions are restored, by means of an implant. With further improvements, this system

can alleviate the need for a permanent tracheostomy after total laryngectomy, while maintaining important larynx functions intact.

## Introduction

Head and neck cancer is the sixth most common cancer worldwide. In 2008, an estimated 635,000 new head and neck cancers were diagnosed globally, including 47,500 cases in the USA and 95,500 in Europe [1]. In 2012, 12,360 new cases of laryngeal cancer and 13,510 new cases of pharyngeal cancer were diagnosed in the United States (http://www.cancer.gov). For advanced tumors, the most common surgical option is a total laryngectomy, which negatively impacts patients' quality of life not so much because of the loss of voice and speech abilities, but rather due to the conspicuous tracheostomy and its particularly deleterious physical and social consequences. The most significant impacts are changed patient self-image, a worsened relationship with their partners, reduced sexuality, and increased social isolation. Furthermore, some authors conclude that a definitive tracheostomy has a negative impact on adjustment postoperatively and that it may have a more severe impact on "Quality of Life" than loss of voice [2]. Over 57,000 laryngectomees live in the United States, according to the International Association of Laryngectomees (http://www.theial.com). As yet, there is no total laryngeal replacement device that can considerably increase the patient's quality of life.

As an alternative to laryngectomy, this article proposes the use of an innovative artificial larynx as a replacement device. Herein we present the device's design: a titanium prosthesis with a double valve system allowing the patient to breathe via the upper respiratory airways while avoiding the aspiration of food. Results of the device's first clinical use within an ongoing clinical trial are provided**.**

## Materials and Methods

*Materials*

The artificial larynx (Figure 1) is the result of a collaboration between the *Hôpitaux Universitaires de Strasbourg-France* and PROTiP, a biomedical company (Strasbourg, France).

The implant comprises two parts that independently adapt to each patient's morphological features:

i) A non-removable tracheal prosthesis (TP), made of pure, porous titanium at its distal extremity, designed to be sutured to the proximal trachea. A temporary silicone tube is inserted into the tracheal prosthesis' lumen, offering support by calibrating the junction between tracheal prosthesis and proximal trachea, thereby preventing the development of a stenotic granuloma during wound healing. The TP's safe use is derived from experimental studies on animals such as sheep and New Zealand rabbits [3,4].

ii) A removable part (RP) also made of pure medical grade titanium, comprising a concentric valve system with double openings that allow air to be inhaled and exhaled. This RP must be implanted via endoscopy. Thanks to a micro-magnet, the valves remain closed at rest, and they open only when solicited by respiratory airflow.

*Patient*

We are reporting the case of a 65-year-old patient presenting with squamous cell carcinoma classified pT4pN2bM0 involving the left pyriform sinus. The patient's history revealed an

anterior frontal laryngectomy performed in 2002 for squamous cell carcinoma involving the left vocal cord and extending to the anterior commissure, along with tobacco-induced chronic obstructive pulmonary disease and centrilobular emphysema. Following discussions within the multidisciplinary team, it was decided to perform a total laryngectomy with bilateral cervical lymphadenectomy. After a thorough risk-benefit assessment of the possibility of surgically implanting an artificial larynx, the patient provided his written informed consent to participate in the clinical trial "Implantation of an artificial larynx after total laryngectomy," Protocol NCT01474005 (http://clinicaltrials.gov/). The trial inclusion criteria are: 18 years of age, with a carcinoma related airway pathology that necessitates total laryngectomy. The exclusion criteria are: less than 18 years of age, pregnancy, breast-feeding, contraindication against general anesthesia, and cases where there is an extension of the tumor (more than 1 cm) to infraglottic or basi-lingual.

*Tracheal prosthesis implantation via cervicotomy*

After an arciform skin incision was made four centimeters above the sternal notch, a second incision was performed below to accommodate a tracheotomy tube. Total laryngectomy and bilateral cervical lymphadenectomy were conducted according to standard surgical procedures, allowing for complete tumor excision with safe margins controlled under microscopic supervision. The proximal trachea was raised four centimeters without shifting its posterior part. Complete pharyngeal closure was accomplished by joining the mucosal flaps' edges. The TP and the trachea's proximal portion were joined without tension and sutured with six vicryl 2.0 stitches. The silicon tube (50 mm length, 20 mm diameter) was inserted into the prosthesis's lumen. The upper TP was sutured to the tongue's base using six vicryl® 2.0 stitches and temporarily closed using a cap. The infrahyoid muscles and the clavicular heads of the

sternocleidomastoid muscles were used to form the prosthesis's anterior covering, with its posterior part contacting the pharyngeal mucosa directly. The skin and subcutaneous layers were then closed over four aspiration drains.

*Implantation of the removable part via endoscopy*

Four months after the first surgical intervention, the cap was removed endoscopically following a pharyngeal mucosa incision. The decision was made due to our previous experience of the average colonization time for the porous titanium in several animal models (rat, rabbit, and sheep) and also by endoscopical analysis of the level of colonization. The removable part was then positioned and held in place by a clip under radioscopic control (Supplementary Video 1).

## Results

*Implant Follow-up*

The artificial larynx system is described in Materials and Methods part (Figure 1).

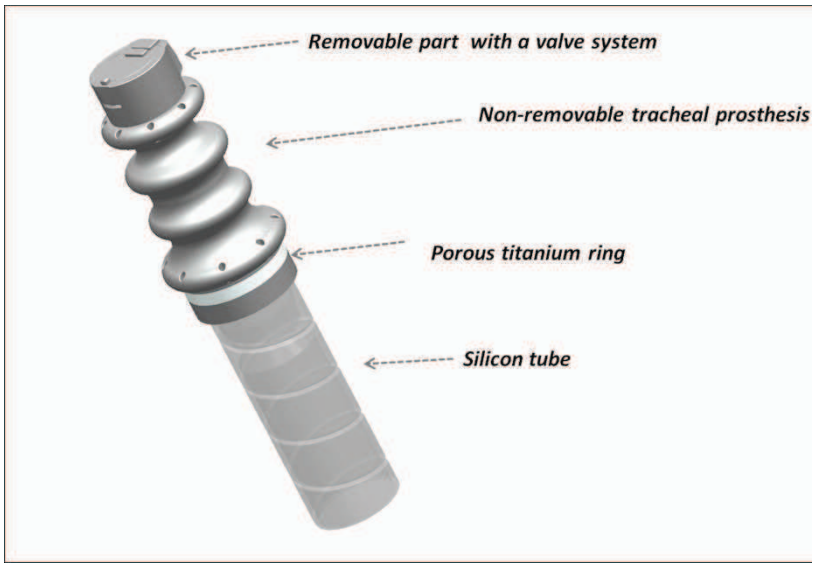


**Figure 1. Artificial Larynx Design.** Overall design and the parts of the Artificial Larynx System.

The positioning and the structure of the implant are as shown (Figure 2A). Postoperative follow-up was uneventful. Three weeks after surgery, three-dimensional computerized tomography scan (3D CT scan) confirmed the TP's good positioning (Figure 2B). A barium swallow showed the absence of fistula (Figure 2C). The patient was able to resume oral feeding.

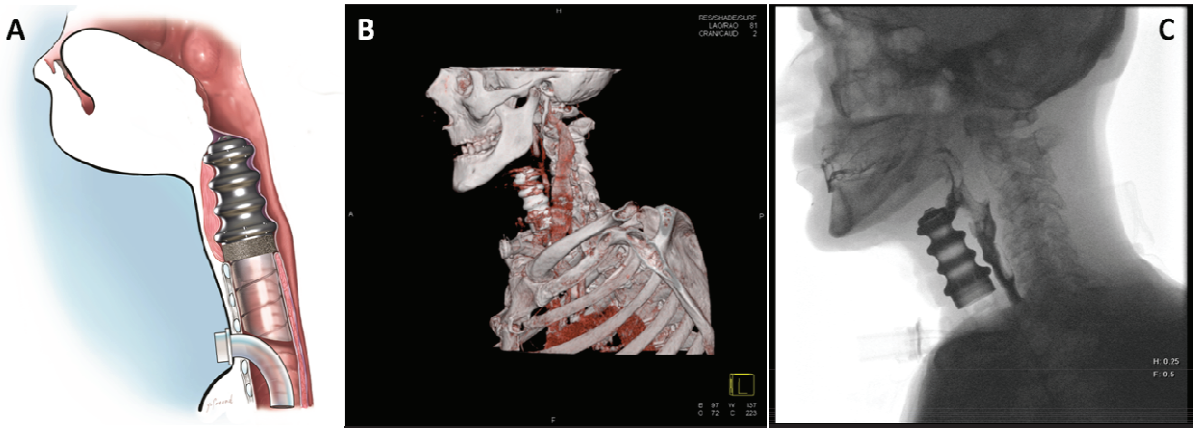


**Figure 2. First step of implantation of Artificial Larynx** **(A)** The Artificial Larynx system with the cap after the first surgical step **(B)** Cervical 3D CT scan showing the TP's good positioning after the first implantation step **(C)** Barium swallow test after the first implantation step confirmed absence of fistula.

Six weeks after surgery, the patient was treated using external-beam radiotherapy, directing 60 Gray (Gy) to the tumor site and 50 Gy to the cervical lymph nodes over five weeks. Presence of the prosthesis did not negatively affect radiotherapy, as any inflammatory reaction was observed. The patient complained neither of pain nor of dysphagia. Retrograde nasofibroscopy of the tracheal prosthesis lumen conducted on day (D) 15, revealed clean material with partial tissue colonization of the porous titanium beads (Supplementary Video 2). Retrograde nasofibroscopy of the tracheal prosthesis lumen at month one, two, three and five after tracheal prosthesis implantation confirmed that the endoluminal walls remained perfectly clean, with no stenotic granulation tissue covering the trachea-prosthesis anastomosis.

Four months after the first step, in a second procedure the cap was removed after sectioning of the pharyngeal mucosa by microscissors and the valve system was implanted endoscopically. During the patient's progressive awakening, the valves' movements were verified under endoscopic control (rigid optic; 0 degree angulation) by closing the tracheotomy orifice manually (Figures 3B). Due to the patient's chronic respiratory insufficiency, a cannula was inserted by precaution seven hours after the intervention.

Immediately after implanting the removable part, the tracheostomy was closed manually, allowing the patient to breathe through the upper airways (Supplementary Video 3). The patient was monitored in the intensive care unit. The patient was able to speak in an understandable whisper. His first words were "Merci" (Thank you). The patient can also speak such as counting numbers (Supplementary Video 4).

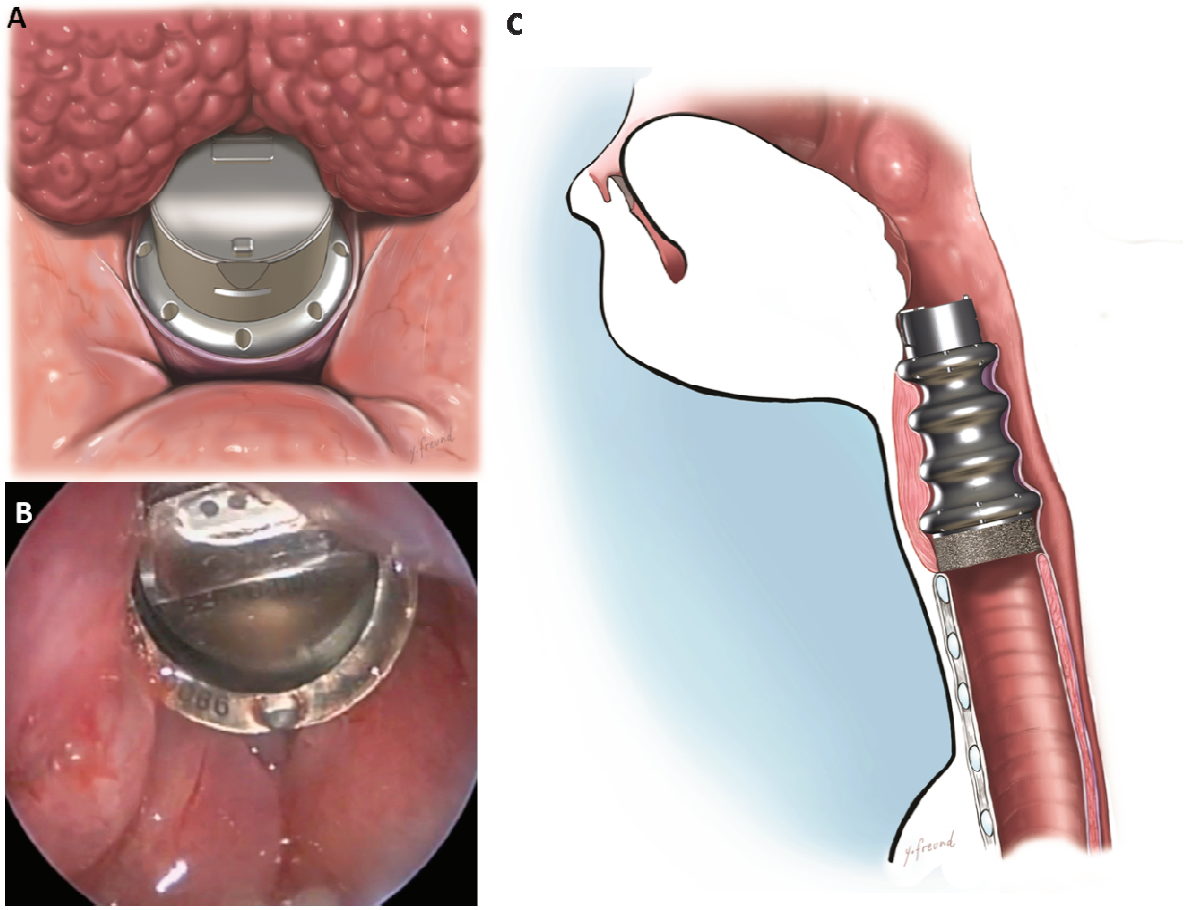

**Figure 3. Second step of implantation of artificial larynx (A)** Placement of the removable part **(B)** The valve system was functional after implantation and expiration and inspiration was achieved by the patient through the valve system **(C)** Profile view of the final, functional artificial larynx system, following the implantation of the removable part. The tracheostomy was left in position to permit swallowing test in complete safety.

At D8, D15, D30, and D60 following implantation of the removable prosthetic part, while the patient was seen in consultation, cannula removal attempts were made during intervals not exceeding several hours under arterial saturation oxygen monitoring. Three main functions were completely or partially restored:

i) normal breathing via the upper airways, with the tracheostomy closed, allowing the patient to expectorate efficiently despite the absence of the glottic sphincter;

ii) speaking in an understandable whisper. Phonation time was short (<15'') because of the absent glottic sphincter. Also the pharyngeal function was preserved and the movement of dry saliva without using false passages was confirmed. Tests using gelled water confirmed that an appropriate re-education is necessary to improve synchronization between respiration and swallowing; because of the potential and occasional problems with swallowing.

iii) The procedure did not cause pain or discomfort, confirming our previous experience concerning intralaryngeal prosthesis [5].

No systemic or local infection was observed, nor was there any subcutaneous inflammation.

To summarize, during the first four months in the absence of the removable prosthesis part, the patient had a tracheostomy, could not speak and but was able to resume oral feeding. After the insertion of the removable part, the tracheostomy could be manually closed for periods up to many hours. During these periods normal oronasal breathing was possible, also the patient was able to speak with a whispering voice while the tracheostomy was closed. The patient had a previous tracheostoma (the first operation) and the tracheostomy was not permanently closed, but was demonstrated that the implant was able to function while the tracheostomy was closed for extended periods, demonstrating that the permanent closure would be possible in the future.

The necessity of post-operational radiation therapy actually made it more difficult to obtain tracheal implant colonization. However, the level of colonization under these circumstances is encouraging for patients who would be only treated for laryngectomy alone where the possible radiation therapy related fibrosis would be absent.

**Discussion**

The prevalence of squamous cell carcinomas of the upper aerodigestive tract remains high, and 5-year survival rates are still limited (namely, 20-50% for Stage III and 10-30% for Stage IV). Preserving the larynx has been a major concern over the last few decades and extensive clinical research has been conducted in this area [6-8]. For advanced tumors, the common surgical option is total laryngectomy, of which Billroth performed the first in 1873. Yet this surgical intervention negatively impacts the patient's quality of life, not only due to the loss of voice, but also due to the conspicuous tracheostoma and its deleterious consequences [9]. At the beginning of the 20th century, therapy relying exclusively on radiation was made possible. In the 1970's, induction chemotherapy with sequential radiotherapy, and

then later on concomitant chemotherapy, contributed to gradual improvements in patient outcomes. The latter alternative has become the standard of care for larynx preservation. There is still room, however, for improvements in this area, most notably in laryngeal rehabilitation techniques for cases when the larynx cannot be preserved. Circumventing the need for a tracheostoma would likely lessen the patient's perception of physical and psychological integrity loss. Most studies conducted to date have focused on restoring normal phonation [10,11]. Yet, as no technique has succeeded in suppressing the tracheotomy orifice, it is still necessary to re-establish a common passage between the respiratory and digestive pathways.

Over the last decade, our team has focused on designing an implantable laryngeal prosthesis capable of replicating normal laryngeal functions [3,12-16]. This prosthesis comprises a non-removable tracheal ring and a removable part. Two types of studies, conducted in parallel, aimed to: i) research an ideal tracheal substitute, *i.e.*, the non-removable part (TP) designed to prolong the trachea [3,17], and ii) develop a movable part (RP), equipped with a valve system, designed to replace the aerodigestive crossroad.

The TP is made of a biomaterial composed of both porous titanium and massive titanium. Titanium was selected because it meets certain pre-specified criteria: it makes radiotherapy possible, does not contraindicate magnetic resonance imaging (MRI), integrates with surrounding tissues by cell colonization (porous titanium), is rigid (supporting surrounding tissues and preserving the respiratory lumen), and resists the aggressive intraluminal environment (pH, bacteria, mould, and humidity). The movable part is designed in a way that it can be removed for MRI, which is necessary.

Our main objective was to perform both a total laryngectomy and a laryngeal prosthesis implantation during the same surgical intervention, without delaying postoperative radiotherapy. The titanium implant did not cause any biocompatibility related issues. Re-

establishing a common passage between the respiratory and digestive pathways enabled the patient to breathe via the mouth, speak in an understandable whisper, and swallow his saliva. All these activities were achieved while keeping the tracheotomy orifice closed.

If necessary, the laryngeal prosthesis can be removed via cervicotomy, without sequelae. In this case, the preliminary tracheotomy orifice will then be transformed into a definitive tracheotomy, with or without implantation of a tracheoesophageal prosthesis.

Even though there are some recent attempts to obtain laryngeal transplants, a fully functional artificial larynx is still not available. In the literature, there are significant improvements in tissue engineered trachea systems, but same level of success has not been reported in the area of larynx yet. Recently, Baiguera *et al.* developed two new types of laryngeal transplants obtained from decellularized sections of cadaveric larynxes [18]. This is an innovative solution which would accommodate the graft completely and thus render pharmacological immunosuppression unnecessary, but this complex technique has not yet been evaluated or shown to preserve the larynx functions in clinical trials as in our case.

Two reports of laryngeal allografts have been published, one performed in 1998 [19,20] and the other performed more recently. Four years after the first graft, the larynx was objectively re-innervated, but closing the tracheotomy was not possible [21]. These procedures required long-term immunosuppression, and their main indications were: 1) trauma or benign tumors, or 2) cancer after progression-free survival. The immunosuppression requirement is hardly acceptable for patients with prior head and neck cancer[22,23]. The relative scarcity of laryngeal transplantation trials indicates that an implant based therapy option can be a feasible alternative in the area of larynx replacement.

For the perfection of the implementation of the artificial larynx in clinical settings, we continue to focus on improvements in both fundamental research and clinical aspects. Further improvements that will be made in the future include: i) surgical technique; ii) surface

modifications for precise control of implant integration; iii) optimal protection of respiratory airways; iv) postoperative re-education [24].

**Conclusion**

In conclusion, we are reporting on the first patient to have undergone artificial laryngeal prosthesis implantation following total laryngectomy for squamous cell cancer (T4 squamous cell carcinoma of the pyriform sinus). By demonstrating the concept's feasibility, our research opens the door for further optimized laryngeal rehabilitation in the oncology field. The proposed solution does not delay indispensible therapeutic options or generate life-threatening complications, for the perfection of the implementation of the artificial larynx in clinical settings; we continue to focus on improvements in both fundamental research and clinical aspects. Further improvements that will be made in the future include: i) surgical technique; ii) surface modifications for facilitation of implant integration to decrease the waiting period between two surgeries; iii) optimal protection of respiratory airways; iv) postoperative re-education.

Consequently, we continue our focus on both and currently recruiting patients for longer term studies to prove the effectiveness of the implant in improving patients' quality of life.

**Supplementary Materials**

**Movie S1.** Placement of the removable part and its mode of action during inspiration and expiration.

**Movie S2.** Colonization of the tracheal ring observed by endoscopy.

**Movie S3.** The patient breathing through the implant while the tracheostoma is closed.

**Movie S4.** The patient counts up to ten in French while the tracheostoma is closed.

**Acknowledgments:**

We would like to thank PROTiP Medical, France (Maurice Bérenger, CEO, Nicolas Perrin, Audrey Maniette and Jean-Marc Fressard) for providing the implants. Also, we acknowledge valuable contribution of Andre Walder and Gérard Caillieret who are co-founders of PROTIP Medical. We acknowledge Yvan Freund for his help in the preparation of the figures. We are indebted to Florence Guilleré, speech therapist (ENT department), Francis Veillon, MD, PhD, Sophie Riehm, MD, Jean-Francois Matern, MD (Radiology department),Strasbourg and to the many staff members of the ENT department of Strasbourg, France, who contributed to this patient's care.

**Author contributions**:

Study Design: CD, ADB, PH, PS; Data Acquisition: CD, ADB, PH, PS; Data Analysis: CD, ADB, NEV, PL; Implant Characterization: NEV, ADB, PL; Manuscript Preparation: NEV, ADB, CD.

**Competing interests**:

Prof. Christian Debry reports being a shareholder of Protip. Dr. Philippe Schultz reports being a shareholder of Protip. Philippe Lavalle reports being a shareholder of Protip. Engin Vrana reports being employed by Protip. No other potential conflicts of interest relevant to this article were reported.

**References**

1. Jégu J, Binder-Foucard F, Borel C, et al. Trends over three decades of the risk of second primary cancer among patients with head and neck cancer. Oral Oncology 2013;49:9-14.

2. Boscolo–Rizzo P, Maronato F, Marchiori C, et al. Long-Term Quality of Life After Total Laryngectomy and Postoperative Radiotherapy Versus Concurrent Chemoradiotherapy for Laryngeal Preservation. The Laryngoscope 2008;118:300-06.
3. Dupret-Bories A, Schultz P, Vrana NE, et al. Development of surgical protocol for implantation of tracheal prostheses in sheep. J Rehabil Res Dev 2011;48:851-64.
4. Vrana NE, Dupret-Bories A, Bach C, et al. Modification of macroporous titanium tracheal implants with biodegradable structures: Tracking in vivo integration for determination of optimal in situ epithelialization conditions. Biotechnology and Bioengineering 2012;109:2134-46.
5. Debry C, Charles X, Frenot M, et al. Intra-laryngeal endoprosthesis: an alternative therapeutic approach to surgical procedures of laryngeal exclusion. The Journal of Laryngology & Otology 2000;114:760-64.
6. Lefebvre JL, Pointreau Y, Rolland F, et al. Induction Chemotherapy Followed by Either Chemoradiotherapy or Bioradiotherapy for Larynx Preservation: The TREMPLIN Randomized Phase II Study. Journal of Clinical Oncology 2013;31:853-59.
7. Karp DD, Vaughan CW, Carter R, et al. Larynx Preservation Using Induction Chemotherapy plus Radiation Therapy as an Alternative to Laryngectomy in Advanced Head and Neck Cancer A Long-Term Follow-up Report. American Journal of Clinical Oncology 1991;14:273-79.
8. Forastiere AA, Goepfert H, Maor M, et al. Concurrent chemotherapy and radiotherapy for organ preservation in advanced laryngeal cancer. New England Journal of Medicine 2003;349:2091-98.
9. Noonan B, Hegarty J. The Impact of Total Laryngectomy: The Patient's Perspective. Oncology Nursing Forum 2010;37:293-301.
10. Singer S, Wollbrück D, Dietz A, et al. Speech rehabilitation during the first year after total laryngectomy. Head & Neck 2012:n/a-n/a.
11. Koike YA, Iwai HI, Morimoto M. Restoration of voice after laryngeal surgeries. The Laryngoscope 1975;85:656-65.
12. Schultz P, Vautier D, Dupret-Bories A, et al. [Replacement of the trachea using surgical reconstruction: current state of research]. In Annales d'oto-laryngologie et de chirurgie cervico faciale: bulletin de la Societe d'oto-laryngologie des hopitaux de Paris2009. 272.

13. Debry C, Schultz P, Vautier D. Biomaterials in laryngotracheal surgery: a solvable problem in the near future? Journal of laryngology and otology 2003;117:113-17.
14. Schultz P, Charpiot A, Vautier D, et al. [Research solutions to find the conception of artificial larynx]. Journal of otolaryngology-head & neck surgery= Le Journal d'oto-rhino-laryngologie et de chirurgie cervico-faciale 2010;39:410.
15. Schultz P, Vautier D, Charpiot A, et al. Development of tracheal prostheses made of porous titanium: a study on sheep. European archives of oto-rhino-laryngology 2007;264:433-38.
16. Vrana NE, Dupret A, Coraux C, et al. Hybrid titanium/biodegradable polymer implants with an hierarchical pore structure as a means to control selective cell movement. PloS one 2011;6:e20480.
17. Schultz P, Vautier D, Chluba J, et al. Survival analysis of rats implanted with porous titanium tracheal prosthesis. The Annals of thoracic surgery 2002;73:1747-51.
18. Baiguera S, Gonfiotti A, Jaus M, et al. Development of bioengineered human larynx. Biomaterials 2011;32:4433-42.
19. Birchall M, Lorenz R, Berke G, et al. Laryngeal transplantation in 2005: a review. American journal of transplantation 2006;6:20-26.
20. Strome M, Stein J, Esclamado R, et al. Laryngeal transplantation and 40-month follow-up. New England Journal of Medicine 2001;344:1676-79.
21. Lorenz RR, Hicks DM, Shields RW, et al. Laryngeal nerve function after total laryngeal transplantation. Otolaryngology--Head and Neck Surgery 2004;131:1016-18.
22. Hall A, Narula A. 'Voicing'considerations in laryngeal transplantation: a commentary of the Royal College of Surgeons working party final report. Clinical Otolaryngology 2012;37:56-57.
23. Bosetti C, Scelo G, Chuang SC, et al. High constant incidence rates of second primary cancers of the head and neck: a pooled analysis of 13 cancer registries. International journal of cancer 2011;129:173-79.
24. Hobson JC, Carney AS. Post laryngectomy speech and voice rehabilitation: past, present and future (Re: ANZ J. Surg. 2010; 80: 770–1). ANZ Journal of Surgery 2011;81:569-69.

# Partie 7 : Conclusion et Perspectives

Le larynx est un organe complexe jouant un rôle primordial dans les fonctions de respiration, déglutition et phonation. Il est le carrefour entre les voies aériennes et digestives, protégeant notamment, tel un sphincter, les voies respiratoires lors du passage du bol alimentaire.

La laryngectomie totale aboutit à l'abouchement de la trachée à la peau via un trachéostome. Outre la perte de la voix, la présence de ce trachéostome définitif induit une altération de l'intégrité physique et une souffrance psychologique majeure. La très grande majorité des laryngectomies totales sont pratiquées dans le cadre de carcinomes pharyngo-laryngés étendus. Afin de supprimer ce trachéostome définitif, en rétablissant la communication entre les voies aériennes et digestives, notre équipe a créée un larynx artificiel formé d'une structure prolongeant la trachée et d'une double valve remplissant le rôle de sphincter. Ne nécessitant aucun recours à un traitement immunosuppresseur, le larynx artificiel est composé de biomatériaux alliant le titane poreux, le titane plein, le silicone et les traitements de surfaces.

Les implants destinés à se substituer aux cartilages laryngés ou trachéaux doivent se rapprocher des qualités biofonctionnelles de l'arbre respiratoire, c'est-à-dire être suffisamment rigides pour éviter un collapsus des voies aériennes et être imperméables à l'air ou aux liquides. Les implants doivent être biocompatibles et capables de s'intégrer sans entraîner de réaction de rejet ou se dégrader dans les tissus environnants. Les voies respiratoires n'étant pas stériles, les biomatériaux sont par ailleurs supposés résister aux agressions bactériennes et limiter cette colonisation.

Schultz et al. ont réalisé des implantations de prothèses trachéales en titane poreux nu chez le rat (Schultz et al., 2002) avec des résultats encourageants qui les ont autorisés à procéder à l'implantation de prothèses trachéales chez la brebis (Schultz et al., 2007). Les premières implantations réalisées chez la brebis ont démontré une bonne tolérance immédiate, la période post-opératoire n'étant pas suivie de complication. Les complications et les décès sont survenus secondairement après infection et obstruction prothétique. L'obstruction des implants était due à un épaississement des moignons trachéaux par développement d'un granulome inflammatoire qui favorisait la stase bronchique qui était à l'origine d'infections

pulmonaires et de la formation de croûtes voire de bouchons muqueux. Des zones de nécrose étaient également présentes aux jonctions extrémités trachéales-prothèse.

Une deuxième étude chez la brebis, décrite dans le troisième chapitre de ce travail, suggérait que la calibration endoprothétique par un tube de silicone autorise une survie longue des animaux en entravant la formation des zones de sténose et de nécrose. Cependant, la face endoprothétique n'était que partiellement couverte par un épithélium respiratoire et ce uniquement pour les brebis aux survies longues (plus de 172 jours). L'importance de la calibration endoprothétique par un tube de silicone a pu être établie et a été être prise en compte pour les études suivantes. Aussi, la présence nécessaire d'un épithélium respiratoire devait encore être obtenue.

La couverture de la face endoprothétique par un épithélium est la clé du succès de ce type de reconstruction. Le rôle de l'épithélium est d'isoler et de protéger les tissus sous-jacents du milieu externe composé de sécrétions, d'air et de micro-organismes. Il doit favoriser le transport de l'air du larynx aux poumons et inversement, mais conduire les sécrétions bronchiques dans une seule direction vers les cavités pharyngolaryngées (rôle des cils vibratiles). Afin d'améliorer la couverture endoprothétique par un épithélium respiratoire, un polymère à base de PLLA a été utilisé en comblement des pores de la prothèse. Les résultats *in vitro*, et *in vivo*, décrits dans les chapitres 4, 5 et 6, de l'implant trachéal hybride PLLA/prothèse en titane poreux sont très prometteurs. Celui-ci, de par sa composition et le gradient de porosité qu'il crée au sein même de la prothèse favorise la migration des fibroblastes à partir de la périphérie tout en empêchant leur prolifération exophytique dans la lumière de la prothèse. Il améliore ainsi la colonisation des pores de la prothèse par un tissu de soutien nécessaire au développement d'un épithélium respiratoire sur la face endoluminale de la prothèse. De plus, l'ajout d'un film de surface (face endoluminale) de porosité encore diminuée, constitue le lit idéal à la migration d'un épithélium respiratoire déjà présent aux extrémités trachéales.

Nous avons également testé l'influence de la taille des billes de la prothèse en titane poreux sur l'intégration de la prothèse *in vitro* et *in vivo*. Cette étude est décrite dans un septième chapitre. Il s'est avéré que plus la taille des billes était réduite, plus rapide était l'intégration de la prothèse par les tissus environnants.

Suite à l'ensemble de ces résultats, nous avons réalisé la première application clinique mondiale du larynx artificiel. Un premier patient, ayant subi l'ablation du larynx pour raison carcinologique, a été implanté avec une prothèse de larynx artificiel fonctionnelle en 2 étapes chirurgicales au CHU de Strasbourg. La tolérance au matériel était très bonne. Le

rétablissement d'un néo-pharyngolarynx entre les voies respiratoires et digestives a permis au patient de respirer par la cavité buccale, de s'exprimer avec une voix chuchotée et de déglutir sa salive tout en maintenant l'orifice de trachéotomie fermé par intermittence. Cette application clinique nous a permis de progresser et d'améliorer pour les versions suivantes le concept de cette prothèse dont la faisabilité a été prouvée. L'implantation d'un larynx artificiel chez l'homme est une première mondiale et laisse entrevoir, depuis les premières laryngectomies réalisées en 1873, un véritable espoir de réhabilitation pour les patients devant subir cette mutilation majeure.

Avec des études de l'intégration de prothèse de trachée *in vitro* et *in vivo* (modèle brebis et lapin) et la première application clinique de larynx artificiel, ces travaux de recherches sont ininterrompues au sein de notre équipe chirurgicale et de l'équipe Inserm depuis plus de 10 ans. Notre équipe va poursuivre ces travaux dans les années à venir. Une des solutions très prometteuse afin d'améliorer l'intégration du larynx artificiel est la structuration nanométrique de surface du matériel titane pour lequel des études *in vitro* et *in vivo* sont en cours de réalisation.

De plus, en collaboration avec le laboratoire NMI (Natural and Medical Sciences Institute) et la société Cellendes (Reutligen, Allemagne), notre équipe de recherche a obtenu un financement européen (EuroTransBio) pour le projet BIMot pour une durée de 3 ans. Le projet repose sur la mise au point d'un biocapteur de mesure en temps réel de l'oxygénation, du pH et de l'impédancemétrie. Ceci permet de recueillir des informations sur l'intégration cellulaire, la vascularisation ou encore les phénomènes éventuels d'infection ou d'inflammation. Nous allons mener des études *in vitro* et *in vivo* au sein de notre laboratoire. Ce microcapteur avec un système télémétrique permettrait de mesurer *in situ* l'intégration des biomatériaux, d'où son importance pour une surveillance continue des prothèses de larynx.

En conclusion, l'ensemble de nos travaux décrits dans cette thèse représente une étape dans la création du larynx artificiel, jusqu'à la conception d'une prothèse idéale, parfaitement intégrée et ceci dans des délais cours. Fort d'une première application clinique, notre souhait de permettre à des patients devant subir une laryngectomie totale pour raison carcinologique de garder une intégrité physique grâce à l'implantation du larynx artificiel est proche de l'aboutissement. Ces résultats nous encouragent à poursuivre nos efforts dans l'amélioration de la prothèse et le suivi de son intégration.

# Annexes

# Publications rédigées dans le cadre du doctorat

1- Multi-scale modification of metallic implants with pore gradients, polyelectrolytes and their indirect monitoring in vivo.
Vrana NE, **Dupret-Bories A**, Chaubaroux C, Rieger E, Debry C, Vautier D, Metz-Boutigue MH, Lavalle P.
J Vis Exp. 2013;1;(77). doi: 10.3791/50533.

2- Titanium Microbead-based Porous Implants: Bead Size Controls Cell Response and Host integration.
Vrana NE, **Dupret-Bories A**, Schultz P, Vautier D, Lavalle P. Adv Healthc Mater. 2013;27. doi: 10.1002/adhm.201200369.

3**-** Modification of macroporous titanium tracheal implants with biodegradable structures: Tracking in vivo integration for determination of optimal in situ epithelialization conditions.
Vrana NE, **Dupret-Bories A**, Bach C, Chaubaroux C, Coraux C, Vautier D, Boulmedais F, Haikel Y, Debry C, Metz-Boutigue MH, Lavalle P. Biotechnol Bioeng. 2012;109(8):2134-46

4- Hybrid Titanium/Biodegradable Polymer Implants with a Hierarchical Pore Structure as a Means to Control Selective Cell Movement.
Vrana NE**, Dupret A**, Coraux C, Debry C, Vautier D, Lavalle P. PLoS One. 2011;6(5):e20480

5- Development of a surgical protocol for the implantation of tracheal prostheses in sheep.
**Dupret-Bories A**, Shultz P, Vrana NE, Lavalle P, Vautier D, Debry C. J Rehabil Res Dev. J 2011;48(7)

6- Avancées et perspectives en remplacement laryngé.
Debry C, **Dupret-Bories A**, Schultz P, Lavalle P.
E-Mémoires de l'Académie Nationale de Chirurgie. 2012

7- Replacement of the trachea using surgical reconstruction: current state of research.
Schultz P, Vautier D, **Dupret Bories A**, Debry C, Charpiot A. Ann Otolaryngol Chir Cervico Fac. 2009;126:272-7.

8- Laryngeal replacement with an artificial larynx after total laryngectomy.
Debry C, **Dupret-Bories A**, Vrana NE, Hémar P, Lavalle P and Schutz P. Head and Neck (soumission)

# Communications présentées dans le cadre du doctorat

1. Rehabilitation of laryngeal's functions by a new concept of intralaryngeal prosthesis. **Dupret-Bories A**, Vrana NE, Schultz P, Lavalle P, Guillere F, Riehm S, Debry C.

20th IFOS World Congress, Seoul, 2013

2. Laryngeal replacement after total laryngetomy.

Debry C, **Dupret-Bories A**, Hémar P, Lavalle P, Vrana NE, Schultz P.

20th IFOS World Congress, Seoul, 2013

3- Modification d'une prothèse de trachée en titane macroporeuse par ajout de matériels biodégradables: étude de la colonisation in vivo. (poster)

Dupret-Bories A, Vrana NE, Schultz P, Vautier D, Lavalle P et Debry C.

119ème Congrès français d'Oto-rhino-laryngologie et de Chirurgie de la face et du cou, Paris, 2012

4. Biocompatibility study of a tracheal prosthesis made of porous titanium.

**Dupret-Bories A**, Vrana NE, Schultz P, Lavalle P, Vautier D, Debry C.

Laryngology 2011. Londres, 2011

5. In-vitro and In-vivo Evaluation of Microporous Treatment PLLA/Macroporous Titanium Implants for Trachea Tissue Engineering

**Dupret-Bories A**, Vrana N E, Coraux C, Schultz P, Debry C, Vautier D, Lavalle P

24th European Conference on Biomaterials. Dublin, 2011.

6. Hierarchical pore structure within an hybrid Titanium/biodegradable polymer tracheal implant for controlling restenosis and epithelialization.

Vrana NE, **Dupret-Bories A**, Debry C, Vautier D, Lavalle P.

Second International Conference on Multifunctional, Hybrid and Nanomaterials

Strasbourg, 2011.

7- Etude de biocompatibilité d'une prothèse de trachée en titane poreux. (poster)

**Dupret-Bories A**, Vrana NE, Schultz P, , Lavalle P, Vautier D, Debry C.

Cancéropôle du Grand-Est, Strasbourg, 2011

8- Etude de biocompatibilité d'une prothèse de trachée en titane poreux.

**Dupret-Bories A**, Schultz P, Vrana NE, Lavalle P, Vautier D, Debry C.

Congrès des Matériaux, Nantes, 2010

9- Etude de biocompatibilité d'une prothèse de trachée en titane poreux. (poster)

**Dupret-Bories A**, Schultz P, Vrana NE, Lavalle P, Vautier D, Debry C.

117ème Congrès français d'Oto-rhino-laryngologie et de Chirurgie de la face et du cou, Paris, 2010. Prix Cancérologie

# Prix

1- Young Scientist Award

Rehabilitation of laryngeal's functions by a new concept of intralaryngeal prosthesis.

**Dupret-Bories A**, Vrana NE, Schultz P, Lavalle P, Guillere F, Riehm S, Debry C.

20th IFOS World Congress, Seoul, 2013

2- Lauréat de l'appel à candidatures « Congrès » du Cancéropole Grand Est, Strasbourg, 2011

3- Student Best Oral Presentations Awards:

In-vitro and In-vivo Evaluation of Microporous Treatment PLLA/Macroporous Titanium Implants for Trachea Tissue Engineering

**Dupret-Bories A**, Vrana NE, Coraux C, Schultz P, Debry C, Vautier D, Lavalle P

24th European Conference on Biomaterials. Dublin, 2011

4- Prix poster Cancérologie :

Etude de biocompatibilité d'une prothèse de trachée en titane poreux.

**Dupret-Bories A**, Schultz P, Vrana NE, Lavalle P, Vautier D, Debry C. 117ème Congrès français d'Oto-rhino-laryngologie et de Chirurgie de la face et du cou, Paris, 2010.

# Bibliographie

Alajati, A., Laib A.M., Weber H., Boos A.M., Bartol A., Ikenberg K., Korff T., Zentgraf H., Obodozie C., Graeser R., Christian S., Finkenzeller G., Stark G.B., Heroult M., and Augustin H.G. "Spheroid-Based Engineering of a Human Vasculature in Mice." *Nature Methods* 5, no. 5 (2008): 439-45.

Albrechtbuehler, G. "Filopodia of Spreading 3t3 Cells - Do They Have a Substrate-Exploring Function." *Journal of Cell Biology* 69, no. 2 (1976): 275-86.

Alvarez, H., Castro C., Moujir L., Perera A., Delgado A., Soriano I., Evora C., and Sanchez E. "Efficacy of Ciprofloxacin Implants in Treating Experimental Osteomyelitis." *Journal of Biomedical Materials Research Part B-Applied Biomaterials* 85B, no. 1 (2008): 93-104.

Akduman, D., Karaman, M., Uslu, C., Bilac, O., Turk, O., Deniz, M., and Durmus, R. Larynx cancer treatment results: survive and quality of life assessment. Kulak Burun Bogaz *Ihtis Derg* 20, (2010): 25-32.

Anoosh F., Hodjati H., Dehghani S., Tanideh N., and Kumar P.V.. "Tracheal Replacement by Autogenous Aorta." *Journal of Cardiothoracic Surgery* 4 (2009): 10.1186/1749-8090-4-23.

Anselme K., Davidson P., Popa A. M., Giazzon M., Liley M., and Ploux L.. "The Interaction of Cells and Bacteria with Surfaces Structured at the Nanometre Scale." *Acta Biomaterialia* 6, no. 10 (2010): 3824-46.

Azorin J. F., Bertin F., Martinod E., and Laskar M.. "Tracheal Replacement with an Aortic Autograft." *European Journal of Cardio-Thoracic Surgery* 29, no. 2 (2006): 261-63.

Babin E., Edy E., Bequignon A., and Hitier M.. "Total Laryngectomy or Identitary Metamorphosis." *Journal of Otolaryngology-Head & Neck Surgery* 37, no. 4 (2008): 495-501.

Bader A., and Macchiarini P.. "Moving Towards in Situ Tracheal Regeneration: The Bionic Tissue Engineered Transplantation Approach." *Journal of Cellular and Molecular Medicine* 14, no. 7 (2010): 1877-89.

Baharloo B., Textor M., and Brunette D.M.. "Substratum Roughness Alters the Growth, Area, and Focal Adhesions of Epithelial Cells, and Their Proximity to Titanium Surfaces." *Journal of Biomedical Materials Research Part A* 74A, no. 1 (2005): 12-22.

Baiguera S., Gonfiotti A., Jaus M., Comin C.E., Paglierani M., Del Gaudio C., Bianco A., Ribatti D., and Macchiarini P. "Development of Bioengineered Human Larynx." *Biomaterials* 32, no. 19 (2011): 4433-42.

Birchall M.A., Lorenz R.R., Berke G.S., Genden E.M., Haughey B.H., Siemionow M., and Strome M. "Laryngeal Transplantation in 2005: A Review." *American journal of transplantation* 6, no. 1 (2006): 20-26.

Boscolo–Rizzo P. , Maronato F., Marchiori C., Gava A., and Da Mosto M.C. "Long-Term Quality of Life after Total Laryngectomy and Postoperative Radiotherapy Versus Concurrent Chemoradiotherapy for Laryngeal Preservation." *The Laryngoscope* 118, no. 2 (2008): 300-06.

Bosetti C., Scelo G., Chuang S.C., Tonita J. M., Tamaro S., Jonasson J.G., Kliewer E. V., Hemminki K., Weiderpass E., and Pukkala E. "High Constant Incidence Rates of Second Primary Cancers of the Head and Neck: A Pooled Analysis of 13 Cancer Registries." *International journal of cancer* 129, no. 1 (2011): 173-79.

Brian E., Gounant V., Fulgencio J. P., Milleron B., and Bazelly B.. "Tracheal Replacement Using the Abdominal Aorta. Comments on a Case Report." *Revue De Pneumologie Clinique* 63, no. 3 (2007): 224-29.

Bücheler M., and Haisch A. "Tissue Engineering in Otorhinolaryngology." *DNA and cell biology* 22, no. 9 (2003): 549-64.

Budyanto L., Goh Y.Q., and Ooi C.P. "Fabrication of Porous Poly(L-Lactide) (Plla) Scaffolds for Tissue Engineering Using Liquid-Liquid Phase Separation and Freeze Extraction." *Journal of Materials Science-Materials in Medicine* 20, no. 1 (2009): 105-11.

Calasans-Maia M.D., Monteiro, M.L., Ascoli, F.O., and Granjeiro, J.M. (2009). The rabbit as an animal model for experimental surgery. Acta Cir Bras 24, 325-328

Chaubaroux C., Vrana E., Debry C., Schaaf P., Senger B., Voegel J.C., Haikel Y., Ringwald C., Hemmerlé J., and Lavalle P. "Collagen-Based Fibrillar Multilayer Films Cross-Linked by a Natural Agent." *Biomacromolecules* 13, no. 7 (2012): 2128-35.

Colombo B., Longhi R., Marinzi C., Magni F., Cattaneo A., Yoo S. H., Curnis F., and Corti A.. "Cleavage of Chromogranin a N-Terminal Domain by Plasmin Provides a New Mechanism for Regulating Cell Adhesion." *Journal of Biological Chemistry* 277, no. 48 (2002): 45911-19.

Committee for the update of the guide for the care and use of laboratory animals: Institute of Laboratory Animal Resources, National Research Council. Guide for the care and use of laboratory animals. 8th rev. ed. Washington (DC): National Academies Press; 2010

Committee for the update of the guide for the care and use of laboratory animals: Institute of Laboratory Animal Resources, National Research Council. Guide for the care and use of laboratory animals. 9th rev. ed. Washington (DC): National Academies Press; 2011

Coraux C., Hajj R., Lesimple P., and Puchelle E.. "Repair and Regeneration of the Airway Epithelium." *M S-Medecine Sciences* 21, no. 12 (2005): 1063-69.

Coraux, C., Nawrocki-Raby A., Hinnrasky J., Kileztky C., Gaillard D., Dani C., and Puchelle E. "Embryonic Stem Cells Generate Airway Epithelial Tissue." *American Journal of Respiratory Cell and Molecular Biology* 32, no. 2 (2005): 87-92.

Cooper J.S., Pajak T.F., Rubin P., Tupchong L., Brady L.W., Leibel S.A., Laramore G.E., Marcial V.A., Davis L.W., Cox J.D., et al. Second malignancies in patients who have head and neck cancer: incidence, effect on survival and implications based on the RTOG experience. *Int J Radiat Oncol Biol Phys* (1989): 17, 449-456.

Davidson M.B., Mustafa K., and Girdwood R.W.. "Tracheal Replacement with an Aortic Homograft." *Annals of Thoracic Surgery* 88, no. 3 (2009): 1006-08.

Debry C., Xavier C., Frenot M., Gentine A."Intra-Laryngeal Endoprosthesis: An Alternative Therapeutic Approach to Surgical Procedures of Laryngeal Exclusion." *The Journal of Laryngology & Otology* 114, no. 10 (2000): 760-64.

Debry C., Schultz P., and Vautier D. "Biomaterials in Laryngotracheal Surgery: A Solvable Problem in the near Future?" *Journal of laryngology and otology* 117, no. 2 (2003): 113-17.

Delaere P., Vranckx J, Verleden G., De Leyn P., Van Raemdonck D., and Leuven G. Tracheal Transplant. "Tracheal Allotransplantation after Withdrawal of Immunosuppressive Therapy." *New England Journal of Medicine* 362, no. 2 (2010): 138-45.

Dodge-Khatami A., Niessen H.W.M., Koole L.H., Klein M. G., Van Gulik T.M., and De Mol B.A. "Tracheal Replacement in Rabbits with a New Composite Silicone-Metallic Prosthesis." *Asian cardiovascular & thoracic annals* 11, no. 3 (2003): 245-9.

Donath K., and Breuner G. A method for the study of undecalcified bones and teeth with attached soft tissues. The Sage-Schliff (sawing and grinding) technique. *J Oral Pathol* (1982): 11, 318-326.

Dong C.M., Wu X., Caves J., Rele S.S., Thomas B.S., and Chaikof E.L. "Photomediated Crosslinking of C6-Cinnamate Derivatized Type I Collagen." *Biomaterials* 26, no. 18 (2005): 4041-49.

Dupret-Bories A., Schultz P., Vrana N.E., Lavalle P., Vautier D., Debry C.. "Development of Surgical Protocol for Implantation of Tracheal Prostheses in Sheep." *Journal of Rehabilitation Research and Development* 48, no. 7 (2011): 851-63.

Fong E., Tzlil S., and Tirrell D.A. "Boundary Crossing in Epithelial Wound Healing." *Proceedings of the National Academy of Sciences of the United States of America* 107, no. 45 (2010): 19302-07.

Forastiere A.A., Goepfert H., Maor M., Pajak T.F., Weber R., Morrison W., Glisson B., Trotti A., Ridge J.A., and Chao C. "Concurrent Chemotherapy and Radiotherapy for Organ Preservation in Advanced Laryngeal Cancer." *New England Journal of Medicine* 349, no. 22 (2003): 2091-98.

Fuchs J.R, Hannouche D., Terada S., Vacanti J.P., and Fauza D.O. "Fetal Tracheal Augmentation with Cartilage Engineered from Bone Marrow-Derived Mesenchymal Progenitor Cells." *Journal of pediatric surgery* 38, no. 6 (2003): 984-87.

Ganguly A.H.Z., Sharma R., Parsons S., and Patel K.D. "Isolation of Human Umbilical Vein Endothelial Cells and Their Use in the Study of Neutrophil Transmigration under Flow Conditions." *Journal of visualized experiments: JoVE*, (2012): no. 66

Gasnier C., Lugardon K., Ruh O., Strub J. M., Aunis D., and Metz-Boutigue M.H.. "Characterization and Location of Post-Translational Modifications on Chromogranin B from Bovine Adrenal Medullary Chromaffin Granules." *Proteomics* 4, no. 6 (2004): 1789-801.

Go T., Jungebluth P., Baiguero S., Asnaghi A., Martorell J., Ostertag H., Mantero S., Birchall M., Bader A., and Macchiarini P. "Both Epithelial Cells and Mesenchymal Stem Cell-Derived Chondrocytes Contribute to the Survival of Tissue-Engineered Airway Transplants in Pigs." *Journal of Thoracic and Cardiovascular Surgery* 139, no. 2 (2010): 437-43.

Goh Y. Q., and Ooi C.P.. "Fabrication and Characterization of Porous Poly(L-Lactide) Scaffolds Using Solid-Liquid Phase Separation." *Journal of Materials Science-Materials in Medicine* 19, no. 6 (2008): 2445-52.

Gordon S. "Alternative Activation of Macrophages." *Nature Reviews Immunology* 3, no. 1 (2003): 23-35.

Grillo, H.C. "Development of Tracheal Surgery: A Historical Review. Part 1: Techniques of Tracheal Surgery." *Annals of Thoracic Surgery* 75, no. 2 (2003): 610-19.

Grillo, H.C. "Development of Tracheal Surgery: A Historical Review. Part 2: Treatment of Tracheal Diseases." *Annals of Thoracic Surgery* 75, no. 3 (2003): 1039-47.

Grillo, H. C. "Tracheal Replacement: A Critical Review." *Annals of Thoracic Surgery* 73, no. 6 (2002): 1995-2004.

Grossin L., Cortial D., Saulnier B., Félix O., Chassepot A., Decher G., Netter P., Schaaf P., Gillet P., and Mainard D.. "Step‐by‐Step Build‐up of Biologically Active Cell‐Containing Stratified Films Aimed at Tissue Engineering." *Advanced Materials* 21, no. 6 (2009): 650-55.

Guillemot F., Porte M. C., Labrugere C., and. Baquey C. "Ti4+ to Ti3+ Conversion of Tio2 Uppermost Layer by Low-Temperature Vacuum Annealing: Interest for Titanium Biomedical Applications." *Journal of Colloid and Interface Science* 255, no. 1 (2002): 75-78.

Hall A., and Narula A.A. "'Voicing'considerations in Laryngeal Transplantation: A Commentary of the Royal College of Surgeons Working Party Final Report." *Clinical Otolaryngology* 37, no. 1 (2012): 56-57.

Hanson S., Jennifer N., Parker S. T., Shepherd R. F., Gillette M. U.,. Lewis J. A, and. Nuzzo R. G. "3d Microperiodic Hydrogel Scaffolds for Robust Neuronal Cultures." *Advanced Functional Materials* 21, no. 1 (2011): 47-54.

Harunaga J.S., and Yamada K. M. "Cell-Matrix Adhesions in 3d." *Matrix Biology* 30, no. 7–8 (2011): 363-68.

Ho M.H., Kuo P. Y., Hsieh H.J., Hsien T.Y., Hou L.T., Lai J.Y., and Wang D.M.. "Preparation of Porous Scaffolds by Using Freeze-Extraction and Freeze-Gelation Methods." *Biomaterials* 25, no. 1 (2004): 129-38.

Hobson J.C., and Carney A. S. "Post Laryngectomy Speech and Voice Rehabilitation: Past, Present and Future (Re: Anz J. Surg. 2010; 80: 770–1)." *ANZ Journal of Surgery* 81, no. 7-8 (2011): 569-69.

Hofmann A., Ritz U., Verrier S., Eglin D., Alini M., Fuchs S., Kirkpatrick C. J., and Rommens P. M. "The Effect of Human Osteoblasts on Proliferation and Neo-Vessel Formation of Human Umbilical Vein Endothelial Cells in a Long-Term 3d Co-Culture on Polyurethane Scaffolds." *Biomaterials* 29, no. 31 (2008): 4217-26.

Hollister S.J. "Porous Scaffold Design for Tissue Engineering." *Nat Mater* 4, no. 7 (2005): 518-24.

Horuk R., Shurey S., Ng H.P., May K., Bauman J.G., Islam I., Ghannam A., Buckman B., Wei G.P., Xu W., Liang M., Rosser M., Dunning L., Hesselgesser J., Snider R. M., Morrissey M. M., Perez H. D., and Green C.. "Ccr1-Specific Non-Peptide Antagonist: Efficacy in a Rabbit Allograft Rejection Model." *Immunology Letters* 76, no. 3 (2001): 193-201.

Huang Y., Siewe M., and Madihally S.V.. "Effect of Spatial Architecture on Cellular Colonization." *Biotechnology and Bioengineering* 93, no. 1 (2006): 64-75.

Huh D., Matthews B.D., Mammoto A., Montoya-Zavala M., Hsin H.Y., and Ingber D.E."Reconstituting Organ-Level Lung Functions on a Chip." *Science* 328, no. 5986 (2010): 1662-68.

Hwang Y.J., Larsen J., Krasieva T. B., and Lyubovitsky J.G.. "Effect of Genipin Crosslinking on the Optical Spectral Properties and Structures of Collagen Hydrogels." *Acs Applied Materials & Interfaces* 3, no. 7 (2011): 2579-84.

Janssen L.M., Van Osch G.J.V.M., Li J.P., Kops N., De Groot K., Feenstra L., and Hardillo J. A. U.. "Laryngotracheal Reconstruction with Porous Titanium in Rabbits: Are Vascular Carriers and Mucosal Grafts Really Necessary?" *Journal of Tissue Engineering and Regenerative Medicine* 4, no. 5 (2010): 395-403.

Janssen L. M., Van Osch G. J. V. M., Li J. P., Kops N., De Groot K., Von den Hoff J. W., Feenstra L., and Hardillo J.A. U.. "Tracheal Reconstruction Mucosal Survival on Porous Titanium." *Archives of Otolaryngology-Head & Neck Surgery* 135, no. 5 (2009): 472-78.

Jégu J., Binder-Foucard F., Borel C., and Velten M.. "Trends over Three Decades of the Risk of Second Primary Cancer among Patients with Head and Neck Cancer." *Oral Oncology* 49, no. 1 (2013): 9-14.

Kalathur M., Baiguera S., and Macchiarini P.. "Translating Tissue-Engineered Tracheal Replacement from Bench to Bedside." *Cellular and Molecular Life Sciences* 67, no. 24 (2010): 4185-96.

Kanzaki M., Yamato M., Hatakeyama H., Kohno C., Yang J., Umemoto T., Kikuchi A., Okano T., and Onuki T.. "Tissue Engineered Epithelial Cell Sheets for the Creation of a Bioartificial Trachea." *Tissue Engineering* 12, no. 5 (2006): 1275-83.

Karageorgiou V., and Kaplan D.. "Porosity of 3d Biomaterial Scaffolds and Osteogenesis." *Biomaterials* 26, no. 27 (2005): 5474-91.

Karp D.D., Vaughan C.W., Carter R., Willett B., Heeren T., Calarese P., Zeitels S., Strong M. S., and Ki Hong W.. "Larynx Preservation Using Induction Chemotherapy Plus Radiation Therapy as an Alternative to Laryngectomy in Advanced Head and Neck

Cancer a Long-Term Follow-up Report." *American Journal of Clinical Oncology* 14, no. 4 (1991): 273-79.

Karp J.M., and Langer R.. "Development and Therapeutic Applications of Advanced Biomaterials." *Current Opinion in Biotechnology* 18, no. 5 (2007): 454-59.

Keeney M., and Pandit A.. "The Osteochondral Junction and Its Repair Via Bi-Phasic Tissue Engineering Scaffolds." *Tissue Engineering Part B-Reviews* 15, no. 1 (2009): 55-73.

Kim H.J., Huh D., Hamilton G., and Ingber D.E.. "Human Gut-on-a-Chip Inhabited by Microbial Flora That Experiences Intestinal Peristalsis-Like Motions and Flow." *Lab on a Chip* 12, no. 12 (2012): 2165-74.

Kipshidze N., Dangas G., Tsapenko M., Moses J., Leon M. B., Kutryk M., and Serruys P.. "Role of the Endothelium in Modulating Neointimal Formation - Vasculoprotective Approaches to Attenuate Restenosis after Percutaneous Coronary Interventions." *Journal of the American College of Cardiology* 44, no. 4 (2004): 733-39.

Kirkpatrick C. J., Fuchs S., and Unger R. E.. "Co-Culture Systems for Vascularization — Learning from Nature." *Advanced Drug Delivery Reviews* 63, no. 4–5 (2011): 291-99.

Ko P.J., Liu C. Y., Wu Y.C., Chao Y.K., Hsieh M.J., Wu C.Y., Wang C.J., Liu Y.H., and Liu H.P.. "Granulation Formation Following Tracheal Stenosis Stenting: Influence of Stent Position." *Laryngoscope* 119, no. 12 (2009): 2331-36.

Koike Y.A., Itoshi Iwai H., and Morimoto M.. "Restoration of Voice after Laryngeal Surgeries." *The Laryngoscope* 85, no. 4 (1975): 656-65.

Kojima K., Bonassar L.J.,. Roy A.K, Mizuno H., Cortiella J., and Vacanti C.A.. "A Composite Tissue-Engineered Trachea Using Sheep Nasal Chondrocyte and Epithelial Cells." *Faseb Journal* 17, no. 8 (2003): 823-28.

Lavalle P., Voegel J.C., Vautier D., Senger B., Schaaf P., and Ball V.. "Dynamic Aspects of Films Prepared by a Sequential Deposition of Species: Perspectives for Smart and Responsive Materials." *Advanced Materials* 23, no. 10 (2011): 1191-221.

Lefebvre J.L., Pointreau Y., Rolland F., Alfonsi M., Baudoux A., Sire C., de Raucourt D., Malard O., Degardin M., Tuchais C., Blot E., Rives M., Reyt E., Tourani J. M., Geoffrois L., Peyrade F., Guichard F., Chevalier D., Babin E., Lang P., Janot F., Calais G., Garaud P., and Bardet E.. "Induction Chemotherapy Followed by Either Chemoradiotherapy or Bioradiotherapy for Larynx Preservation: The Tremplin Randomized Phase Ii Study." *Journal of Clinical Oncology* 31, no. 7 (2013): 853-59.

Leon X., Pujol A., Lopez,M., Garci, J., Pons G., Sanudo J.R., Masia J., and Quer M.. [Larynx transplant: a therapeutic option for the 21st century? Literature review]. Acta Otorrinolaringol Esp (2008): 59, 127-138.

Leong K.F., Chua C. K., Sudarmadji N., and Yeong W.Y.. "Engineering Functionally Graded Tissue Engineering Scaffolds." *Journal of the Mechanical Behavior of Biomedical Materials* 1, no. 2 (2008): 140-52.

LeSimple P., van Seuningen I., Buisine M.P., Copin M.C., Hinz M., Hoffmann W., Hajj R., Brody S. L., Coraux C., and Puchelle E.. "Trefoil Factor Family 3 Peptide Promotes Human Airway Epithelial Ciliated Cell Differentiation." *American Journal of Respiratory Cell and Molecular Biology* 36, no. 3 (2007): 296-303.

Li J.P., Habibovic P., van den Doel M., Wilson C.E., de Wijn J.R.,. van Blitterswijk C. A, and de Groot K.. "Bone Ingrowth in Porous Titanium Implants Produced by 3d Fiber Deposition." *Biomaterials* 28, no. 18 (2007): 2810-20.

Lobler M., Sass M., Kunze C., Schmitz K.P., and Hopt U.T.. "Biomaterial Implants Induce the Inflammation Marker Crp at the Site of Implantation." *Journal of Biomedical Materials Research* 61, no. 1 (2002): 165-67.

Lorenz R.R., Hicks D. M., Shields R.W., Fritz M. A., and Strome M.. "Laryngeal Nerve Function after Total Laryngeal Transplantation." *Otolaryngology--Head and Neck Surgery* 131, no. 6 (2004): 1016-18.

Lutolf M.P., and Hubbell J.A.. "Synthetic Biomaterials as Instructive Extracellular Microenvironments for Morphogenesis in Tissue Engineering." *Nature Biotechnology* 23, no. 1 (2005): 47-55.

Ma H., Hu J., and Ma P. X.. "Polymer Scaffolds for Small-Diameter Vascular Tissue Engineering." *Advanced Functional Materials* 20, no. 17 (2010): 2833-41.

Macchiarini P., Jungebluth P., Go T., Asnaghi M. A., Rees L. E., Cogan T. A., Dodson A., Martorell J., Bellini S., Parnigotto P. P., Dickinson S. C., Hollander A. P., Mantero S., Conconi M. T., and Birchall M. A. "Clinical Transplantation of a Tissue-Engineered Airway." *Lancet* 372, no. 9655 (2008): 2023-30.

Makris D., Holder-Espinasse M., Wurtz A., Seguin A., Hubert T., Jaillard S., Copin M. C., Jashari R., Duterque-Coquillaud M., Martinod E., and Marquette C.H.. "Tracheal Replacement with Cryopreserved Allogenic Aorta." *Chest* 137, no. 1 (2010): 60-67.

Makris D., and Marquette C.H.. "Tracheobronchial Stenting and Central Airway Replacement." *Current Opinion in Pulmonary Medicine* 13, no. 4 (2007): 278-83.

Martin N., Jaeger D., and Christopher H.. "Optimized Fibrin Gel Bead Assay for the Study of Angiogenesis." *Journal of Visualized Experiments*, no. 3 (2007).

Martinod E. [Tracheal replacement with cryopreserved aortic allograft: a "hot topic" in thoracic surgery]. *Rev Mal Respir*(2012): 29, 939-940.

Martinod E., Azorin J., and Carpentier A.. "Tracheal Replacement: New Perspectives." *Revue Des Maladies Respiratoires* 18, no. 6 (2001): 639-43.

Martinod E., Seguin A., Holder-Espinasse M., Kambouchner M., Duterque-Coquillaud M., Azorin J.F., and Carpentier A.F. Tracheal regeneration following tracheal replacement with an allogenic aorta. *Ann Thorac Surg* (2005) : 79, 942-948; discussion 949.

Martinod E., Zegdi R., Zakine G., Aupecle B., Fornes P., D'Audiffret A., Chachques J.C., Azorin J., and Carpentier A. A novel approach to tracheal replacement: the use of an aortic graft. *J Thorac Cardiovasc Surg* (2001b): 122, 197-198.

Martinod E., Zakine G., Fornes P., Zegdi R., d'Audiffret A., Aupecle B., Goussef N., Azorin J., Chachques J. C., Fabiani J. N., and Carpentier A.. "Metaplastic Transformation of an Aortic Autograft into a Tracheal Tissue. Surgical Implications." *Comptes Rendus De L Academie Des Sciences Serie Iii-Sciences De La Vie-Life Sciences* 323, no. 5 (2000): 455-60.

Mathieu L.M., Mueller T.L., Bourban P.E., Pioletti D.P., Muller R., and Manson J. A. E.. "Architecture and Properties of Anisotropic Polymer Composite Scaffolds for Bone Tissue Engineering." *Biomaterials* 27, no. 6 (2006): 905-16.

Matschegewski C., Staehlke S., Loeffler R., Lange R., Chai F., Kern D.P., Beck U., and Nebe B. J.. "Cell Architecture-Cell Function Dependencies on Titanium Arrays with Regular Geometry." *Biomaterials* 31, no. 22 (2010): 5729-40.

Melchels F.P.W., Barradas C.A.M., van Blitterswijk C.A., de Boer J., Feijen J., and Grijpma D. W.. "Effects of the Architecture of Tissue Engineering Scaffolds on Cell Seeding and Culturing." *Acta Biomaterialia* 6, no. 11 (2010): 4208-17.

Mills R.J., Frith J.E., Hudson J.E., and Cooper-White J.J. "Effect of Geometric Challenges on Cell Migration." *Tissue Engineering Part C-Methods* 17, no. 10 (2011): 999-1010.

Morin K. T., and Tranquillo R. T.. "Guided Sprouting from Endothelial Spheroids in Fibrin Gels Aligned by Magnetic Fields and Cell-Induced Gel Compaction." *Biomaterials* 32, no. 26 (2011): 6111-18.

Moroni L., Curti M., Welti M., Korom S., Weder W., De Wijn J. R., and Van Blitterswijk C. A.. "Anatomical 3d Fiber-Deposited Scaffolds for Tissue Engineering: Designing a Neotrachea." *Tissue Engineering* 13, no. 10 (2007): 2483-93.

Muller S., Koenig G., Charpiot A., Debry C., Voegel J.C., Lavalle P., and Vautier D.. "Vegf-Functionalized Polyelectrolyte Multilayers as Proangiogenic Prosthetic Coatings." *Advanced Functional Materials* 18, no. 12 (2008): 1767-75.

Nakamura T., Sato T., Araki M., Ichihara S., Nakada A., Yoshitani M., Itoi S., Yamashita M., Kanemaru S., Omori K., Hori Y., Endo K., Inada Y., and Hayakawa K.. "In Situ Tissue Engineering for Tracheal Reconstruction Using a Luminar Remodeling Type of Artificial Trachea." *Journal of Thoracic and Cardiovascular Surgery* 138, no. 4 (2009): 811-19.

Narayan D., and Venkatraman S. S.. "Effect of Pore Size and Interpore Distance on Endothelial Cell Growth on Polymers." *Journal of Biomedical Materials Research Part A* 87A, no. 3 (2008): 710-18.

Neville W.E., Bolanowski P.J.P., and Soltanzadeh H.. "Homograft Replacement of Trachea Using Immunosuppression." *Journal of Thoracic and Cardiovascular Surgery* 72, no. 4 (1976): 596-601.

Nicole L., Rozes L., and Sanchez C.. "Integrative Approaches to Hybrid Multifunctional Materials: From Multidisciplinary Research to Applied Technologies." *Advanced Materials* 22, no. 29 (2010): 3208-14.

Noonan B., and Hegarty J. "The Impact of Total Laryngectomy: The Patient's Perspective." *Oncology Nursing Forum* 37, no. 3 (2010): 293-301.

O'Brien F. J., Harley B.A., Yannas I.V., and Gibson L.J.. "The Effect of Pore Size on Cell Adhesion in Collagen-Gag Scaffolds." *Biomaterials* 26, no. 4 (2005): 433-41.

Omori K., Tada Y., Suzuki T., Nomoto Y., Matsuzuka T., Kobayashi K., Nakamura T., Kanemaru S., Yamashita M., and Asato R.. "Clinical Application of in Situ Tissue Engineering Using a Scaffolding Technique for Reconstruction of the Larynx and Trachea." *Annals of Otology Rhinology and Laryngology* 117, no. 9 (2008): 673-78.

Papenburg B.J., Bolhuis-Versteeg L.A.M., Grijpma D.W., Feijen J., Wessling M., and Stamatialis D.. "A Facile Method to Fabricate Poly(L-Lactide) Nano-Fibrous Morphologies by Phase Inversion." *Acta Biomaterialia* 6, no. 7 (2010): 2477-83.

Pavia F.C., La Carrubba V., Piccarolo S., and Brucato V.. "Polymeric Scaffolds Prepared Via Thermally Induced Phase Separation: Tuning of Structure and Morphology." *Journal of Biomedical Materials Research Part A* 86A, no. 2 (2008): 459-66.

Roomans G.M. "Tissue Engineering and the Use of Stem/Progenitor Cells for Airway Epithelium Repair." *European cells & materials* 19 (2010): 284-99.

Rougier S., Galland D., Boucher S., Boussarie D., and Valle M.. "Epidemiology and Susceptibility of Pathogenic Bacteria Responsible for Upper Respiratory Tract Infections in Pet Rabbits." *Veterinary Microbiology* 115, no. 1-3 (2006): 192-98.

Ryan G., Pandit A., and Apatsidis D. P.. "Fabrication Methods of Porous Metals for Use in Orthopaedic Applications." *Biomaterials* 27, no. 13 (2006): 2651-70.

Sargeant T. D., Guler M. O., Oppenheimer S. M., Mata A., Satcher R. L., Dunand D. C., and Stupp S. I. "Hybrid Bone Implants: Self-Assembly of Peptide Amphiphile Nanofibers within Porous Titanium." *Biomaterials* 29, no. 2 (2008): 161-71.

Saigal S., Norris S., Muiesan P., Rela M., Heaton N., and O'Grady J. Evidence of differential risk for posttransplantation malignancy based on pretransplantation cause in patients undergoing liver transplantation. *Liver Transpl* 8 (2002): 482-487.

Sato T., Araki M., Nakajima N., Omori K., and Nakamura T.. "Biodegradable Polymer Coating Promotes the Epithelization of Tissue-Engineered Airway Prostheses." *Journal of Thoracic and Cardiovascular Surgery* 139, no. 1 (2010): 26-31.

Schmidt J.J., Jeong J., and Kong H.. "The Interplay between Cell Adhesion Cues and Curvature of Cell Adherent Alginate Microgels in Multipotent Stem Cell Culture." *Tissue Engineering Part A* 17, no. 21-22 (2011): 2687-94.

Schultz P., Charpiot A., Vautier D., Guilleré F., and Debry C.. "[Research Solutions to Find the Conception of Artificial Larynx]." *Journal of otolaryngology-head & neck surgery= Le Journal d'oto-rhino-laryngologie et de chirurgie cervico-faciale* 39, no. 4 (2010): 410.

Schultz P., Vautier D., Dupret-Bories A., Debry C., and Charpiot A.. "[Replacement of the Trachea Using Surgical Reconstruction: Current State of Research]." Paper presented at the Annales d'oto-laryngologie et de chirurgie cervico faciale: bulletin de la Societe d'oto-laryngologie des hopitaux de Paris, 2009.

Schultz P., Vautier D., Atallah I., Gentine A., and Debry C.. "Reconstruction of the Anterior Mandibule Using a Porous Titanium Implant: A Case Report." *Revue de laryngologie - otologie - rhinologie* 129, no. 3 (2008): 201-5.

Schultz P., Vautier D., Charpiot A., Lavalle P., and Debry C.. "Development of Tracheal Prostheses Made of Porous Titanium: A Study on Sheep." *European Archives of Oto-Rhino-Laryngology* 264, no. 4 (2007): 433-38.

Schultz, P., D. Vautier, J. Chluba, L. Marcellin, and C. Debry. "Survival Analysis of Rats Implanted with Porous Titanium Tracheal Prosthesis." *Annals of Thoracic Surgery* 73, no. 6 (2002): 1747-51.

Schultz P., Vautier D., Egles C., and Debry C.. "Experimental Study of a Porous Rat Tracheal Prosthesis Made of T40: Long-Term Survival Analysis." *European Archives of Oto-Rhino-Laryngology* 261, no. 9 (2004): 484-88.

Schultz P., Vautier D., Richert L., Jessel N., Haikel Y., Schaaf P., Voegel J. C., Ogier J., and Debry C.. "Polyelectrolyte Multilayers Functionalized by a Synthetic Analogue of an Anti-Inflammatory Peptide, Alpha-Msh, for Coating a Tracheal Prosthesis." *Biomaterials* 26, no. 15 (2005): 2621-30.

Seguin A., Martinod E., Kambouchner M., Campo G. O., Dhote P., Bruneval P., Azorin J. F., and Carpentier A.. "Carinal Replacement with an Aortic Allograft." *Annals of Thoracic Surgery* 81, no. 3 (2006): 1068-75.

Seguin A., Radu D., Holder-Espinasse M., Bruneval P., Fialaire-Legendre A., Duterque-Coquillaud M., Carpentier A., and Martinod E.. "Tracheal Replacement with Cryopreserved, Decellularized, or Glutaraldehyde-Treated Aortic Allografts." *Annals of Thoracic Surgery* 87, no. 3 (2009): 861-68.

Shearer H., Ellis M. J., Perera S. P., and Chaudhuri J. B.. "Effects of Common Sterilization Methods on the Structure and Properties of Poly(D,L Lactic-Co-Glycolic Acid) Scaffolds." *Tissue Engineering* 12, no. 10 (2006): 2717-27.

Shooshtarizadeh P., Zhang D., Chich J.F., Gasnier C., Schneider F., Haikel Y., Aunis D., and Metz-Boutigue M.H.. "The Antimicrobial Peptides Derived from Chromogranin/Secretogranin Family, New Actors of Innate Immunity." *Regulatory Peptides* 165, no. 1 (2010): 102-10.

Singer S., Wollbrück D., Dietz A., Schock J., Pabst F., Vogel H.J., Oeken J., Sandner A., Koscielny S., Hormes K., Breitenstein K., Richter H., Deckelmann A., Cook S., Fuchs M., and Meuret S. "Speech Rehabilitation During the First Year after Total Laryngectomy." *Head & Neck* (2012): 20. doi: 10.1002/hed.23183.

Singh M., Berkland C., and Detamore M. S.. "Strategies and Applications for Incorporating Physical and Chemical Signal Gradients in Tissue Engineering." *Tissue Engineering Part B-Reviews* 14, no. 4 (2008): 341-66.

Skowron-zwarg M., Boland S., Caruso N., Coraux C., Marano F., and Tournier F.. "Interleukin-13 Interferes with Cftr and Aqp5 Expression and Localization During

Human Airway Epithelial Cell Differentiation." *Experimental Cell Research* 313, no. 12 (2007): 2695-702.

Stevens M.M., and George J.H.. "Exploring and Engineering the Cell Surface Interface." *Science* 310, no. 5751 (2005): 1135-38.

Strome M., Stein J., Esclamado R., Hicks D., Lorenz R. R., Braun W., Yetman R., Eliachar I., and Mayes J.. "Laryngeal Transplantation and 40-Month Follow-Up." *New England Journal of Medicine* 344, no. 22 (2001): 1676-79.

Sundararaghavan H.G., Monteiro G.A., Lapin N.A., Chabal Y.J., Miksan J.R., and Shreiber D. I.. "Genipin-Induced Changes in Collagen Gels: Correlation of Mechanical Properties to Fluorescence." *Journal of Biomedical Materials Research Part A* 87A, no. 2 (2008): 308-20.

Tatekawa Y., Ikada Y., Komuro H., and Kaneko M.. "Experimental Repair of Tracheal Defect Using a Bioabsorbable Copolymer." *Journal of Surgical Research* 160, no. 1 (2010): 114-21.

Ten Haller E.J.O., Rakhorst G., Marres H. A. M., Jansen J. A., van Kooten T. G., Schutte H. K., van Loon J. P., van der Houwen E. B., and Verkerke G. J.. "Animal Models for Tracheal Research." *Biomaterials* 25, no. 9 (2004): 1533-43.

Tojo T., Niwaya K., Sawabata N., Kushibe K., Nezu K., Taniguchi S., and Kitamura S.. "Tracheal Replacement with Cryopreserved Tracheal Allograft: Experiment in Dogs." *Annals of Thoracic Surgery* 66, no. 1 (1998): 209-13.

Tseng W. C., Cheng G. W., Lee C. F., Wu H. L., and Huang Y. L.. "On-Line Coupling of Microdialysis Sampling with High Performance Liquid Chromatography and Hydride Generation Atomic Absorption Spectrometry for Continuous in Vivo Monitoring of Arsenic Species in the Blood of Living Rabbits." *Analytica Chimica Acta* 543, no. 1-2 (2005): 38-45.

Newsroom U.C. Patient gets successful larynx transplant. Available from Oakland, Ca: University of California, http://www.universityofcalifornia.edu/news/article/24844; (2011) January

Vautier D., Hemmerle J., Vodouhe C., Koenig G., Richert L., Picart C., Voegel J. C., Debry C., Chluba J., and Ogier J.. "3-D Surface Charges Modulate Protrusive and Contractile Contacts of Chondrosarcoma Cells." *Cell Motility and the Cytoskeleton* 56, no. 3 (2003): 147-58.

Vrana E., Builles N., Hindie M., Damour O., Aydinli A., and Hasirci V.. "Contact Guidance Enhances the Quality of a Tissue Engineered Corneal Stroma." *Journal of Biomedical Materials Research Part A* 84A, no. 2 (2008): 454-63.

Vrana N.E., Dupret-Bories A., Chaubaroux C., Rieger E., Debry C., Vautier D., Metz-Boutigue M.H., and Lavalle P.. "Multi-Scale Modification of Metallic Implants with Pore Gradients, Polyelectrolytes and Their Indirect Monitoring in Vivo." *J Vis Exp*. (2013): e50533.

Vrana N.E., Dupret-Bories A., Schultz P., Debry C., Vautier D., Lavalle P.
Titanium Microbead-Based Porous Implants: Bead Size Controls Cell Response and Host Integration. *Adv Healthc Mater*. (2013): 27: 10.1002/adhm.201200369

Vrana N.E., Dupret-Bories A., Bach C., Chaubaroux C., Coraux C., Vautier D., Boulmedais F., Haikel Y., Debry C., Metz-Boutigue M.H., and Lavalle P. "Modification of Macroporous Titanium Tracheal Implants with Biodegradable Structures: Tracking in Vivo Integration for Determination of Optimal in Situ Epithelialization Conditions." *Biotechnology and Bioengineering* 109, no. 8 (2012): 2134-46.

Vrana N.E., Dupret A., Coraux C., Vautier D., Debry C., and Lavalle P.. "Hybrid Titanium/Biodegradable Polymer Implants with an Hierarchical Pore Structure as a Means to Control Selective Cell Movement." *PloS one* 6, no. 5 (2011): e20480.

Wang Y., Subbiahdoss G., Swartjes J., van der Mei H.C., Busscher H. J., and Libera M.. "Length-Scale Mediated Differential Adhesion of Mammalian Cells and Microbes." *Advanced Functional Materials* 21, no. 20 (2011): 3916-23.

Werner S., Huck O., Frisch B., Vautier D., Elkaim R., Voegel J.C., Brunel G., and Tenenbaum H.. "The Effect of Microstructured Surfaces and Laminin-Derived Peptide Coatings on Soft Tissue Interactions with Titanium Dental Implants." *Biomaterials* 30, no. 12 (2009): 2291-301.

Wurtz A., Porte H., Conti M., Dusson C., Desbordes J., Copin M.C., and Marquette C.H.. "Surgical Technique and Results of Tracheal and Carinal Replacement with Aortic Allografts for Salivary Gland-Type Carcinoma." *Journal of Thoracic and Cardiovascular Surgery* 140, no. 2 (2010): 387-U206.

Yang B., Zhou L., Peng B., Dai Y., and Zheng J. Stem cells in a tissue-engineered human airway. *Lancet* (2012): 379, 1487.

Zani Brett G., Kojima K.,. Vacanti C. A, and Edelman E. R.. "Tissue-Engineered Endothelial and Epithelial Implants Differentially and Synergistically Regulate Airway Repair." *Proceedings of the National Academy of Sciences* 105, no. 19 (2008): 7046-51.

Zhang D., Lavaux T., Sapin R., Lavigne T., Castelain V., Aunis D., Metz-Boutigue M.H., and Schneider F. "Serum Concentration of Chromogranin a at Admission: An Early Biomarker of Severity in Critically Ill Patients." *Annals of Medicine* 41, no. 1 (2009): 38-44.

Zhang P., Luo X., and Wang H. Clinical transplantation of a tissue-engineered airway. *Lancet* (2009): 373, 718; author reply 718-719.

Agnès DUPRET-BORIES

# Le larynx artificiel : de l'*in vitro* à la première implantation clinique


## Résumé

**Objectifs :** Ce travail a pour but de développer un larynx artificiel composé de 2 structures : 1) une structure inamovible en titane poreux prolongeant la trachée; 2) une double valve remplissant la fonction de sphincter.
**Matériels et Méthodes :** L'intégration de la prothèse en remplacement trachéal a été testée *in vitro* et *in vivo* sur les modèles animaux rats, lapins et brebis.
Suite à l'ensemble de ces résultats, nous avons réalisé la première application clinique du larynx artificiel.
**Résultats :** 1) L'ajout d'un tube de silicone endoprothétique améliore la survie chez le gros animal; 2) l'intégration tissulaire de la prothèse de trachée associée à un matériel polymérique biodégradable était supérieure à celle des prothèses en titane poreux nu; 3) la vitesse de colonisation des prothèses en titane poreux était accélérée lorsque l'on diminuait la taille des billes.
Un premier patient a été implanté avec une prothèse de larynx artificiel avec des résultats satisfaisants à 9 mois.
**Conclusions :** Nos études concernant l'intégration de prothèses de trachées *in vitro* et *in vivo* ont permis de contribuer à l'aboutissement de la première application clinique de larynx artificiel.

**Mots-clés :** larynx artificiel, laryngectomie totale, prothèse de trachée, titane poreux, épithélium respiratoire.


## Summary

**Background**: The aim of this work is the design of an artificial larynx made of 2 elements: 1) a non-removable bio-integrable structure designed to provide a connection with the remaining trachea; 2) a double valve that fulfills the sphincter function.
**Materials and Methods**: *In vitro* and *in vivo* tests (rat, rabbit and sheep model) were performed to achieve the tracheal prosthesis integration. Following all these results, we carried out the first clinical application of an artificial larynx.
**Results**: i) The long-term survival of the animals was improved when an endoprosthetic silicon calibration tube was used; ii) tissue integration of the prostheses in porous titanium filled with biodegradable polymer was better than the bare porous titanium; iii) prosthesis integration was improved when pore size was decreased.
A first patient was implanted with an artificial functional larynx with satisfactory results after 9 months of implantation.
**Conclusion:** The whole *in vivo* and *in vitro* studies concerning the integration of the tracheal prosthesis has contributed to the success of the first clinical application of the artificial larynx.

**Key words:** artificial larynx, porous titanium, polymer, respiratory epithelium, tracheal prosthesis, total laryngectomy.